A STUDY ON ESTIMATION METHODOLOGY FOR ROUNDABOUT ENTRY CAPACITY CONSIDERING PEDESTRIAN IMPACTS

KANG, Nan

A STUDY ON ESTIMATION METHODOLOGY FOR ROUNDABOUT ENTRY CAPACITY CONSIDERING PEDESTRIAN IMPACTS

Doctoral Dissertation

Submitted in Partial Fulfillment of the
Requirements for the Degree of
Doctor of Engineering

by

KANG, Nan

Academic Advisor:

Prof. Hideki NAKAMURA

Graduate School of Engineering
Nagoya University
May, 2014

Acknowledgements

This dissertation would not have been possible without the guidance and the help of several individuals who in one way or another contributed their valuable assistance in the preparation and completion of this study.

Foremost, I owe deepest and earnest thankfulness to my supervisor, Prof. Hideki Nakamura, whose encouragement, supervision and support from the preliminary to the concluding level enabled me to develop an understanding of truly scientific research and make my PhD experience memorable and productive. His working spirit, insightful guidance and logical ways of thinking have been of great value for me to learn a lifetime.

I would like to express my sincere appreciation to Prof. Toshiyuki Yamamoto, Assoc. Prof. Hirokazu Kato and Assoc. Prof. Koji Suzuki for serving my doctoral committee and for their constructive suggestions that greatly improved the quality of this dissertation.

Many thanks to Dr. Miho Asano, Dr. Wael Alhajyaseen, Dr. Taiki Mabuchi, Dr. Ming Tan Dang, Dr. Meng Li, Dr. Axel Wolfermann, Dr. Kazu Suzuki and Dr. Keshuang Tang for their thought-provoking comments and practical advice at different stages of my research, which helped me focus and enrich my ideas.

I would like to thank all the graduate students and members who used to work or are currently working in this group for their friendly and helpful collaboration, for creating a pleasant working atmosphere and for a nice time full of great memories.

I also would like to express my sincere appreciation to Prof. Hirohisa Morita and Prof. Werner Brilon for giving me significant and helpful advices on my research.

My wholehearted gratitude goes to my family: my parents, my dear aunt in Japan for their continuous and unconditional support, affection, wishes and encouragement. You own all my love and we share all the joys and smile forever.

Abstract

Entry capacity is one of the most important indices for performance evaluation of roundabout. In addition to circulating vehicles, pedestrian flow is another key conflicting stream having significant impact on entry capacity. The pedestrian impact is estimated in the existing method through an adjustment factor f_{ped} (Brilon et al, 1993). This adjustment factor was developed based on the roundabouts which are under the standard design with physical splitter island, crosswalk and distance of one-vehicle length between crosswalk and yield line. However, some of them, e.g. physical splitter cannot be always satisfied due to space limitation, especially in Japan. In addition, it is supposed that pedestrian behavior such as pedestrian approaching side which affects entry driver behavior also have significant impact on entry capacity. Moreover, exiting vehicles blocked by the pedestrians across downstream exits may lead to a queue in circulating roadway, which will prevent entry vehicles from entering roundabout and result in reduction of entry capacity.

Therefore, this study aims to propose an estimation method of roundabout entry capacity which can appropriately reflect the Japanese situations considering pedestrian impact and various influencing factors, i.e. physical splitter island, pedestrian approaching side, far-side pedestrian recognition rate, distance between crosswalk and yield line and queuing exit vehicles blocked by pedestrians across downstream exits. This study is expected to apply for planning and implementing stage regarding the treatment of pedestrians and space issues in future.

In **Chapter 1** the scope of the research is illustrated through providing some background information about performance evaluation for roundabout entry capacity, the estimation of impact of circulating vehicles and pedestrians. In addition, problem statement and objectives of the study are described and the research outline is generally reviewed.

Chapter 2 presents the state-of-the-art review on estimation methods of roundabout entry capacity from two aspects, macroscopic approach and microscopic approach. Macroscopic methods focus on estimating the relationship of entry capacity and circulating flow with various geometry influencing factors, e.g. diameter and angle of legs. Several software

products which were developed based on the macroscopic methodology are introduced. Since this method needs sufficient data to ensure the accuracy of the models, it will be not appropriate to apply on the places where limited number of roundabouts is installed, e.g. Japan. On the other hand, microscopic approach focuses on individual vehicles and is established based on gap acceptance theory. In the microscopic approach, pedestrian impact is also considered commonly through adjustment factor. The models of adjustment factor were developed based on standard roundabout design, e.g. with splitter island at entry/exit which cannot be always satisfied in Japan due to space limitation. Therefore, an appropriate estimation method of roundabout entry capacity considering pedestrian impact is in urgent need to reflect the characteristics of Japanese situation. Moreover, microscopic simulation is popularly utilized for capacity estimation since it can help simulating complicated situations. Therefore, based on the scope of this research, the methodology of estimating entry capacity is developed from two approaches, simulation study and theoretical model.

Since entry capacity is difficult to observe at Japanese roundabouts, a simulation study is conducted for obtaining a reference of entry capacity. In addition, the simulation study is also utilized to identify and examine influencing factors which will be included in theoretical model. In **Chapter 3** the simulation study utilizing VISSIM 5.40 is calibrated based on empirical data which is observed in Japanese roundabouts. Then, a series of simulation experiments are conducted to identify influencing factors. It is found through simulation analysis that, physical splitter island, distance between crosswalk and yield line, pedestrian approaching sides and far-side pedestrian recognition rate have significant impact on entry capacity.

Based on these results, a theoretical model is proposed In **Chapter 4** including the influencing factors which are examined in simulation study. This theoretical model is developed based on a four-leg single-lane roundabout with crosswalk at each entry and left-hand traffic rule is assumed. The capacity of the subject entry is estimated considering two separated situations of circulating flow in front of the subject entry, flowing or queuing. When circulating flow is under the condition of flowing, entry capacity is determined by pedestrians across the subject entry, circulating flow passing in front of subject entry and several influencing factors, i.e., physical splitter island, pedestrian approaching side and distance between crosswalk and yield line. While, if the circulating flow is under the

condition of queuing, the probability of exit vehicles queuing in circulating roadway due to the pedestrians across at downstream exits is considered. Accordingly, the entry capacity is the combination result of these two cases. Through sensitivity analyses it is found that the proposed model can reflect impacts of these influencing factors and the sensitivity of each influencing factor on entry capacity is consistent with the results which have been obtained in simulation analyses.

In **Chapter 5**, a comparison analysis is conducted between the proposed theoretical model and simulation output in order to interpret limitations of each method. It is found that when pedestrian demand is in the low level, both methods give reasonable results comparing to the empirical data. When pedestrian demand is in the high level (200ped/h), the difference is observed. It is implied that this difference is from the limitation of each method, e.g. due to the limited empirical data regarding the high pedestrian demand, pedestrian behavior could not be calibrated in simulation, and in theoretical model the assumption about the impact of queue in circulating roadway is simple without considering discharge time. In Japan, the real situation is that pedestrian demand is lower than 100ped/h in most of intersections. Thus, both methods can be applied in real world with reasonable results. Since simulation analysis performs the safety edge of estimation results, a practical application is conducted based on the simulation output.

Finally, **Chapter 6** summarizes research conclusions and provides some recommendations for future works. The developed methodology provides a new way to estimate roundabout entry capacity considering pedestrian impact through simulation and theoretical model. Besides pedestrians, several influencing factors are considered in this method, i.e., physical splitter island, pedestrian approaching sides, far-side pedestrian recognition rate, distance between crosswalk and yield line and queuing vehicles in circulating roadway due to pedestrians across downstream exits. Both the proposed methods showed reliable results. Accordingly, they are expected to apply at planning and implementing stage regarding the treatment of pedestrians and space issues in future. Although the reasonable estimation results can be proposed by the methods, there are still limitations regarding each method, e.g. calibration of pedestrian behavior in simulation and headway distribution function in theoretical model. In view of that, improvements regarding these limitations will be conducted in future.

.

Table of Contents

List of Tables

List of Figures

1 Chapter 1

INTRODUCTION

1.1 Background

Modern roundabout which is named roundabout thereafter in this research is one type of unsignalized intersection generally with a physical island in the center. Roundabout is different from the circle intersection such as rotary since at roundabout the traffic flow in the circulating roadway is given the priority (Highway Capacity Manual, HCM 2010). It has been proved that roundabouts have advantages on improving operational and safety performance, e.g. lower delay and fewer numbers of accidents are observed after installing roundabouts (Brilon, 2005).

Roundabout Entry capacity which is defined as the maximum number of vehicles can enter roundabout during a certain period in one entry is one of the most important indices for operational performance evaluation of roundabout (HCM 2010). Based on the operating principle and the geometric characteristics of roundabout, users relating to traffic flows at roundabout which is shown in Figure 1.1 and geometric elements at roundabout which is shown in Figure 1.2 are always considered as influencing factors on entry capacity. Besides these, the application environment of roundabout is also considered to have significant impact on entry capacity since entry capacity is the expression of driver behavior and the application environment has influence on the driver behavior.

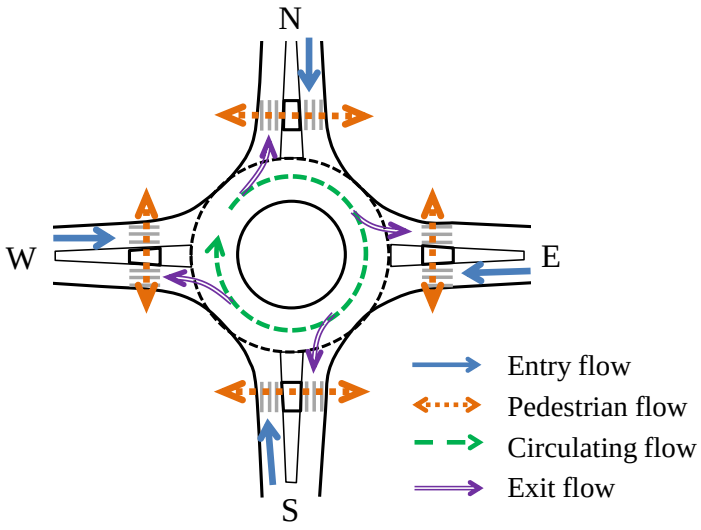

Figure 1.1 Existing flows at roundabouts

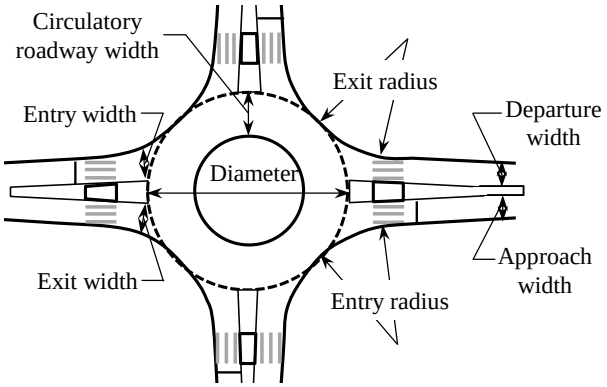

Figure 1.2 Geometry at roundabout

2.1.1 Existing estimation methods of roundabout entry capacity

The existing methods of entry capacity were developed based on these influencing factors considering the typical conditions in various countries. Pedestrian and circulating flows are the main conflict streams to entry flow. Regression models were developed considering circulating flow and geometric elements by U.K. and Germany (Kimber and Semmens, 1977 and Brilon and Stuwe 1991) from the macroscopic approach. On the other hand, microscopic methodology which is based on gap acceptance theory was developed (AustRoads 1993, HBS 2001 and HCM 2010) and widely utilized in the countries which have limited number of roundabouts, e.g. Japan. The impact of pedestrian on entry capacity is considered as an adjustment factor f_{ped} (Brilon et al. 1993, HCM 2010). The details of

estimation methods are described in Chapter 2.

A brief summary of existing estimation methods with influencing factors which are considered in several countries including guidelines and analyses is shown in Table 1.1. The priority of the influencing factors which should be considered in Japan is also marked in this table.

Table 1.1 Brief summary of influencing factors considered in existing estimation methods of entry capacity in several countries

	Influencing factors		Have been considered in other countries			Should be considered in Japan
			U.K. *	Germany **	U.S.A. ***	
Users (traffic flow)	Vehicles	Circulating flow	√	√	√	▲▲
		Exit flow				▲
	Pedestrians			√	√	▲▲
	Bicycles					▲
Geometric elements	Standardize design of roundabout		√	√	√	▲▲
	Diameter		√			▲
	Number of legs					▲
	Number of lanes in entry road			√	√	▲
	Number of lanes in circulating road			√	√	▲
	Width of entry/exit roadway		√			▲
	Width of entry/exit					▲
	Width of circulating roadway					▲
	Entry/exit radius		√			▲
	Angle of legs		√			▲
Application environment	Space issue					▲▲
	Concern about pedestrians					▲▲

▲: Priority of consideration of influencing factors

*Reference: Kimber and Semmens (1977)

**Reference: HBS (2001), Brilon and Stuwe (1991) and Brilon et al (1993)

**Reference: FHWA (2000) and HCM (2010)

2.1.2 Japanese situations

In Japan, about 72% of land is mountainous, so that limited living space is one of the typical characteristics of space issue in Japan. Accordingly, the roundabout standard design, i.e. physical splitter island and space of one-vehicle length cannot be always satisfied at entry/exit roundabouts in Japan. Figure 1.3 shows several roundabouts which have been installed in Japan. It is found that some of entries/exits are designed under the standard design with physical splitter island and one-vehicle space between crosswalk and yield line however they cannot be satisfied at all approaches.

In addition, based on design guideline, four-leg compact single-lane roundabout needs a minimum diameter of 27m. The diameter is requested to be larger when the number of legs increases. However, in Japan, not all roundabouts which the number of legs is more than four can achieve this condition due to the limited space. One example of the roundabout in Karuizawa cho which has six legs and the diameter is 27m is shown in Figure 1.4.

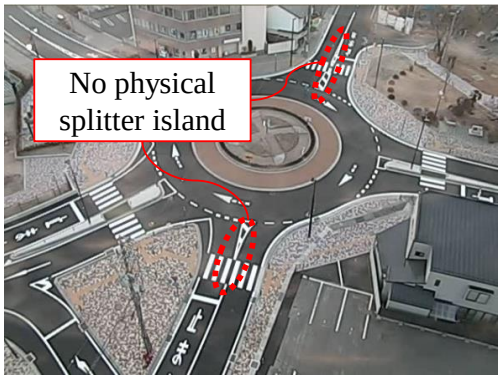

(a) Roundabout in Towa-cho, Iida City

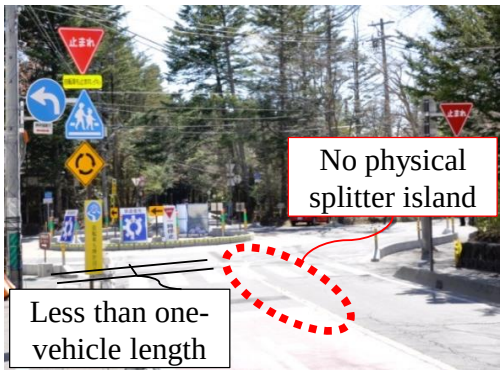

(b) Roundabout in Karuizawa cho

Figure 1.3 roundabouts under the condition without physical splitter island at entry/exit in Japan

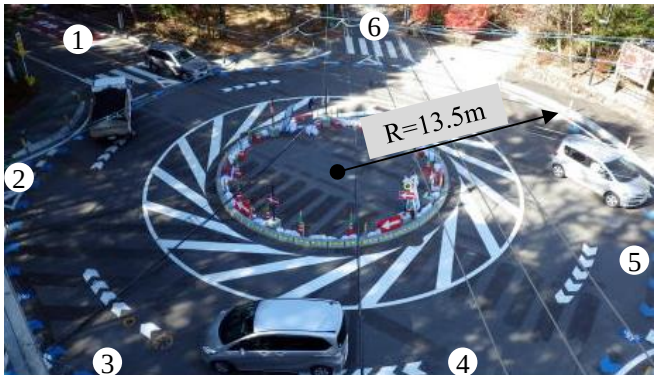

Figure 1.4 The example of roundabout with six legs and the diameter of 27m in Karuizawa Town, Japan

Limited space is a serious issue in Japan and dependent on limited available space, pedestrian density is relatively higher in Japan comparing to other countries, which means roundabouts are likely to be installed at the places with high pedestrian demand in Japan. Therefore, pedestrians have higher priority to be considered as an influencing factor than others. In addition, geometry also will have significant impact on entry capacity which has been proved by existing analyses. Regarding Japanese situation, due to the space limitation, not all roundabouts can be installed by standardized design, e.g. with physical splitter island at entry/exit and one-vehicle length between crosswalk and yield line which will strongly influence entry capacity. Therefore, the consideration on the standardize design has the priority to be considered. Moreover, driver's behavior such as compliance of drivers which can reflect the real situation of application environment also should be considered. Accordingly, pedestrians, several standardize design, i.e. physical splitter island and distance between crosswalk and yield line and driver's compliance have higher priority to be considered as influencing factors on entry capacity.

1.2 Problem statement

In existing estimation method (Brilon et al. 1993), the impact of pedestrian is considered through the adjustment factor f_{ped}. This adjustment factor was developed based on the roundabouts which are under the conditions of single-lane approach with a physical splitter island, crosswalk and space of one-vehicle length between crosswalk and yield line. However, the roundabouts which are installed in Japan have some typical characteristics, i.e. physical splitter islands and space between crosswalk and yield line at entry/exit cannot always be satisfied. Moreover, some influencing factors, i.e. pedestrian approaching sides, far-side pedestrian recognition rate which are directly related to pedestrian behavior are also considered to have impact on entry capacity. Therefore, an estimation methodology of roundabout entry capacity which can reflect these influence factors considering Japanese situations is needed.

1.3 Research objective

The objective of this research is to develop an estimation method of roundabout entry capacity considering pedestrian impact under the Japanese situations. Physical splitter island, distance between crosswalk and yield line, pedestrian approaching sides and far-side pedestrian recognition rate which have impact on pedestrian and driver behavior further influence entry capacity are considered as influencing factors in this methodology. Such an objective is achieved through the following steps:

- Identifying the influencing factors and examining the impact of these influencing factors through microscopic simulation.
- Developing a theoretical model of roundabout entry capacity considering the examined influencing factors.
- Comparing estimated results of entry capacity from simulation and theoretical model to interpret the limitation of these two estimation methods and finally an appropriate estimation method considering Japanese situations is expected.

The proposed methodology in this research would provide a new way to estimate roundabout entry capacity considering pedestrian impact, especially under some

uncommon situations, e.g. without physical splitter island and accordingly enable traffic authorities to evaluate performance of roundabout in planning and implementing stage regarding the treatment of pedestrians and space issues in future.

1.4 Research flow and organization of this dissertation

After clearly defining research objective, a state-of-the-art overview of estimation methodologies of roundabout entry capacity is introduced in **Chapter 2**. Estimation methods are described through macroscopic approach and microscopic approach. Entry capacity is commonly estimated dependent on circulating flow and the impacts of pedestrians and downstream exit flow are considered through the adjustment factors in existing methods. However, these existing methods which are developed based on standard design roundabouts may not be appropriate to apply in Japan since not all standard design can be always satisfied. Thus, in **Chapter 3**, simulation analysis is applied to identify and examine the influencing factors, e.g. physical splitter island and pedestrian approaching sides considering Japanese situations. Then based on the simulation output, a theoretical model considering all these examined influencing factors is proposed in **Chapter 4**. The theoretical model is developed by considering two situations of circulating flow, either flowing or queuing. Influencing factors, i.e. pedestrians demand at subject entry, physical splitter island, distance between crosswalk and yield line, pedestrian approaching sides and far-side pedestrian recognition rate are considered in the condition of flowing circulating flow. And pedestrians across downstream exits and vehicle OD demand are considered as influencing factors when circulating vehicles are queuing. The comparison of simulation output and theoretical model is conducted to interpret the limitation of each method in **Chapter 5**. Also a proposal of estimation method of roundabout entry capacity considering pedestrian impact and Japanese situations is expected in this chapter. Finally, conclusions and some perspectives for future research are provided in **Chapter 6**. The general research outline is presented in Figure 1.5.

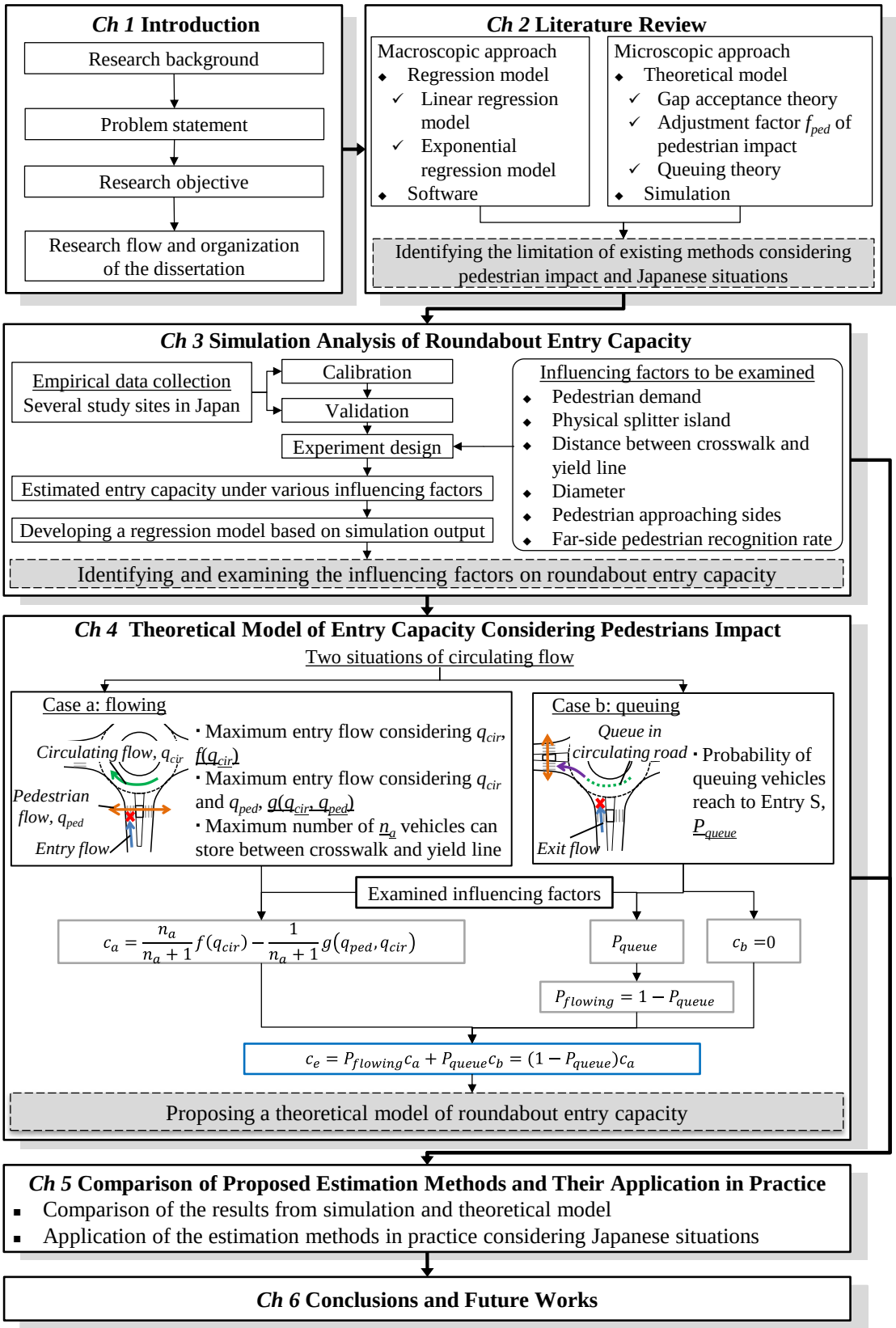

Figure 1.5 Framework of this research

2 Chapter 2

LITERATURE REVIEW OF ESTIMATION METHODS FOR ROUNDABOUT ENTRY CAPAICTY

2.1 Introduction

Roundabout entry capacity is one of the most important indices for evaluating roundabout mobility performance of roundabout. It is defined as the greatest flow that can enter a roundabout from a given approach when the traffic demand is sufficient to cause queuing on that approach. This condition is termed saturation and the flow entering the roundabout is the entry capacity (HCM, 2010). Since roundabout is one kind of unsignalized intersections, a number of fundamental methods applicable to two-way-stop-controlled and two-way-yield-controlled intersection capacity analysis serve as a foundation for roundabout operational performance.

2.1.1 Influencing factors

Traffic flows

At roundabout, two kinds of users vehicles and pedestrians/bicycles (bicycles will not be considered in this research) exist and they can be classified into four categories of flows, i.e. entry flow, pedestrian flow, circulating flow and exit flow as shown in Figure 1.1.

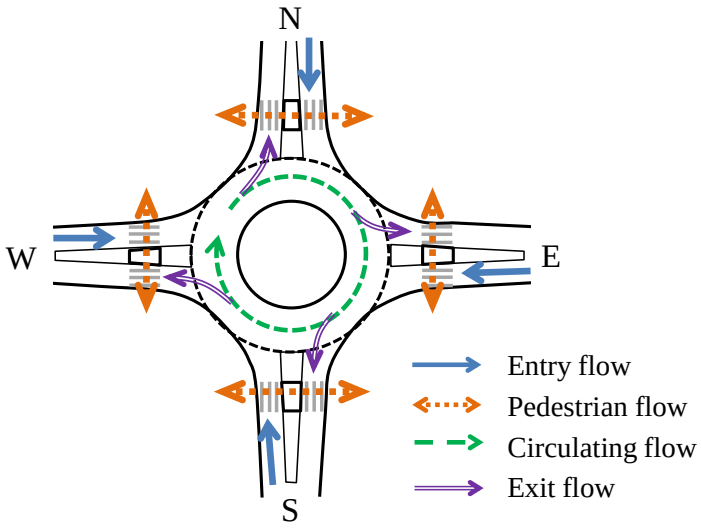

Figure 2.1 Existing flows at roundabouts

Entry S is considered as the subject entry thereafter in this research. Pedestrians across at Entry S and circulating vehicles passing in front of Entry S are given priority at roundabout therefore entry vehicles have to yield to them during entering roundabout as shown in Figure 2.2(a) and Figure 2.2(b). In addition, vehicles exiting to downstream exits may be blocked by pedestrians and probably queue in circulating roadway further will prevent vehicles at upstream entry entering roundabout when the queue reaching up to Entry S as shown in Figure 2.2(c). Moreover, entry drivers may be confused by the offside exit vehicles which are in the upstream circulating flow and do not give any notice to entry drivers and hesitate to enter roundabout as shown in Figure 2.2(d).

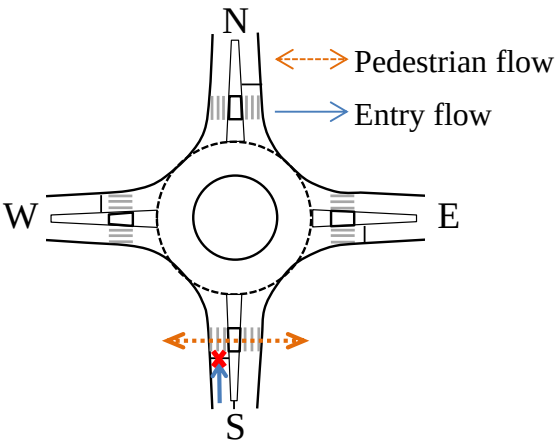

(a) Pedestrian flow

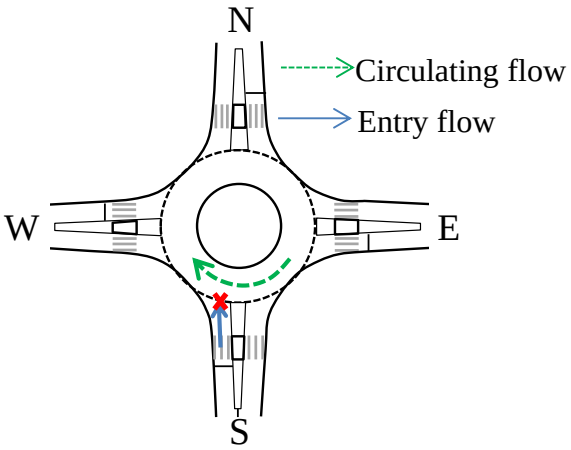

(b) Circulating flow

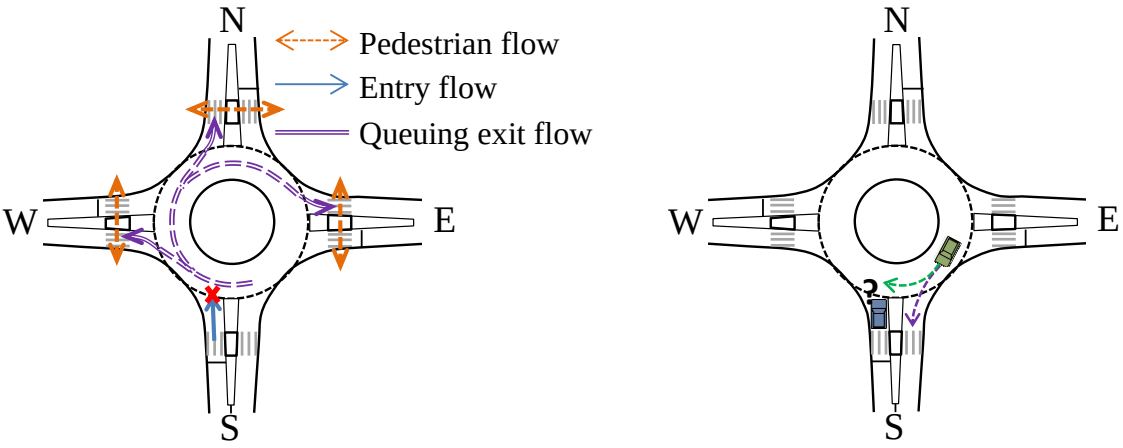

(c) Downstream queuing exit flow (d) Offside exit flow

Figure 2.2 Traffic flows having impact on entry capacity at roundabout

Accordingly, roundabout entry capacity is strongly affected by following traffic flows:

- Circulating vehicles;
- Pedestrians across the subject entry;
- Downstream exit vehicles which are queuing in circulating roadway due to the pedestrians across downstream exits;
- Offside exit vehicles which cannot be classified by entry drivers.

Since pedestrian flow at subject entry and circulating flow have conflict with entry flow, entry capacity is reduced with increase of these two traffic flows. In addition, queuing downstream exit flow will prevent entry vehicle entering roundabout, entry capacity is equal to 0 when the queuing flow reaches up in front of the subject entry. Thus, entry capacity will be reduced when the queuing events occur. And then, since entry drivers may hesitate on the exit vehicles at the same leg and some waiting time is generated, entry capacity will also be reduced by these unrecognized offside exit vehicles.

Entry flow, circulating flow and exit flow are related each other. Circulating flow passing in front of one entry is composed by the entry flows from other entries and exit flows are also generated by entry flows. Accordingly, the entry flow is the basic traffic flow at roundabout and the operation of roundabout is significantly affected by entry flows. This is

also the reason why entry capacity is one of the most important indices for performance evaluation. Since circulating flow and exit flow are related to the entry flow, they are considered as the influencing factors on estimating entry capacity.

Geometry

The geometric elements of the roundabout provide guidance to drivers approaching, entering and travelling through a roundabout. In addition, entry capacity is the performance of driver behavior. Thus, roundabout geometric elements, e.g. number of legs, diameter, circulating roadway width and approach width as shown in Figure 1.2 which are considered to have impact on driver behavior further have influence on entry capacity.

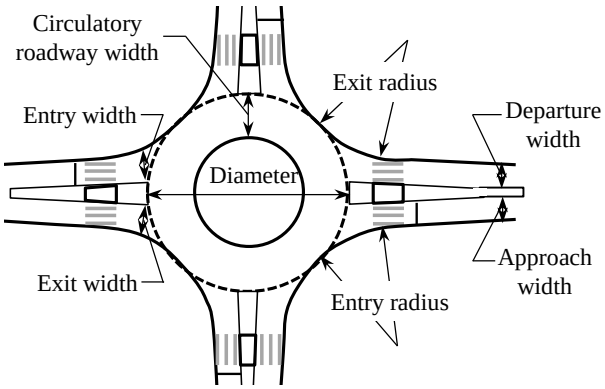

Figure 2.3 Geometry at roundabout

Roundabout with larger diameter can provide better condition for drivers smoothly travelling in circulating roadway which will reduce the probability of congestion in circulating roadway and improve entry capacity. Moreover, when exit vehicles are blocked by pedestrians, larger diameter can provide more storing space for exit and circulating vehicles which will reduce the probability of the queuing vehicles reaching up to the upstream entry and increasing entry capacity. Larger road width including approach, departure and circulating roadway can provide better road conditions to drivers which makes them drive more smoothly and travelling with relatively higher speed. This will also improve entry capacity. In addition, if exit vehicles are blocked at one exit and the queue extends to the circulating roadway, wider circulating roadway provides space for the vehicles to other exits overtaking this queue. Thus, the whole roundabout will still be under

the situation of operation and the performance of entry capacity will be better than the condition of narrow circulating roadway width. Furthermore, entry vehicles and exit vehicles have conflict with circulating vehicles and pedestrians, respectively when entering and exiting roundabout. Based on the gap acceptance behavior, subjects in minor flow cross or merge into major flow by available gaps of major flow. Not all available gaps can be utilized by subjects in minor flow due to limited visibility. Entry capacity is strongly related to the utilization of available gaps. Wider entry/exit width provides more space and better visibility for entry/exit vehicles to flexibly judge circulating vehicles and pedestrians and make decisions. Thus, available gaps can be well utilized and entry capacity is improved.

Accordingly, the existing estimation methods of roundabout entry capacity were developed based on the considerations of these influencing factors and classified into two approaches, macroscopic approach which focuses on modeling the relationship of entry capacity and circulating also considering roundabout geometric elements and microscopic approach which focuses on driver behavior of individual vehicles and considers the impact of pedestrians.

2.2 Macroscopic estimation methods

Regression models are developed in macroscopic estimation methods to reflect the relationship of entry capacity and circulating flow. Besides the circulating flow, the regression model also tries to combine some roundabout geometric elements, e.g. diameter, approaching radius and number of entry lanes in models. Several countries, e.g. U.K. and Germany which have a long history on applying roundabouts with sufficient number of study sites make efforts on this regression model. After that several software, e.g. RODEL, SIDRA and KREISEL are developed based on these regression models.

2.2.1 Regression models

U.K. model

Semmens et al (1980) conducted an experiment at the “4-arm” junction A2/A28, Wincheap, U.K. to estimate the roundabout entry capacity. The observation of entry capacity at a four-leg single lane roundabout is shown in Figure 2.4. From the observation it is found

that entry capacity is reduced when circulating flow increases.

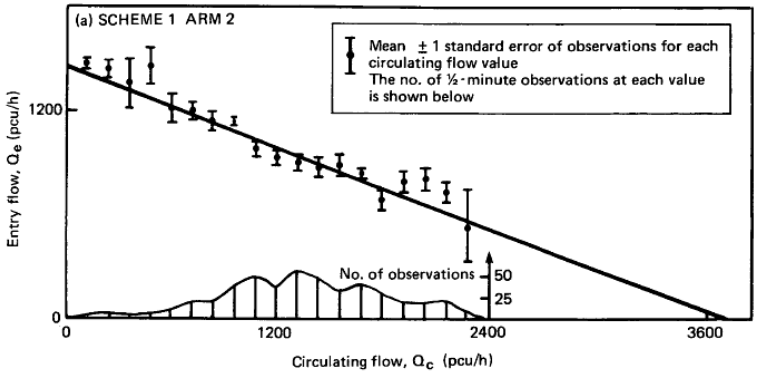

Figure 2.4 Observation of entry capacity changing with circulating flow at a single-lane roundabout on site of Wincheap in U.K. (Semmens et al, 1980)

Based on the observation, Kimber (1977) developed a linear regression model regarding entry capacity (named U.K. model thereafter) as shown in Equation 2.1.

$$c_{cir} = k(F - f_c q_{cir}) \tag{2.1}$$

where c_{cir} = entry capacity considering circulating flow (veh/h)

q_{cir} =circulating flow (veh/h)

k, F and f_c = positive constant determined by the size and shape of the entry

The geometry influencing factors which are considered in this linear regression model and the range of each influencing factor are shown in Table 2.1.

Table 2.1 Geometry influencing factors considered in U.K. model

	Geometry influencing factor	Range
1	narrowest radius of the right edge at the entry, r (m)	[3.4, ∞)
2	width of the lane on the approaching street, v (m)	[1.9, 12.5]
3	width of the entry at the edge of the circulating ring, e (m)	[3.6, 16.5]
4	outer diameter of the roundabout, D_{outer} (m)	[13.5, 71.6]
5	angle between ring and entry, φ (degree)	[0, 77]
6	effective length of the funnel-shaped flare, l' (m)	[1, ∞)

The illustrations of these roundabout geometric elements are shown in Figure 2.5.

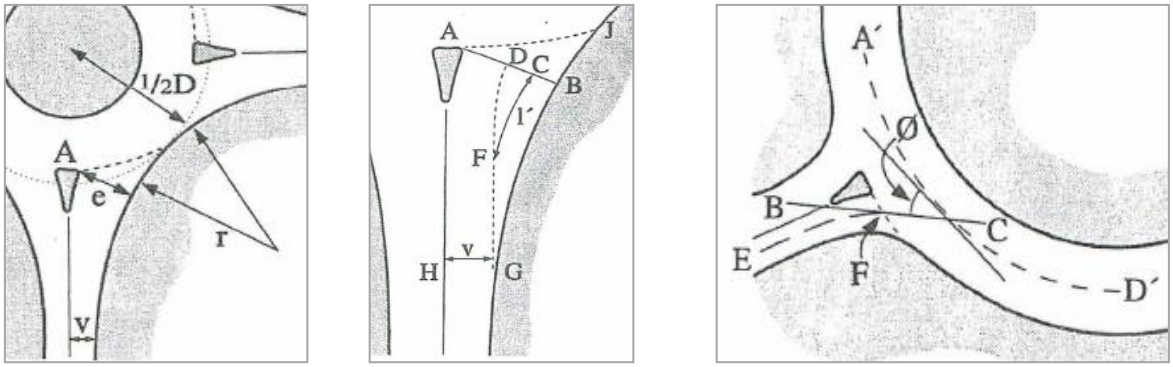

(a) r, v, e and D_{outer} (b) l' (c) φ

Figure 2.5 Illustration of the geometry influencing factors considering in U.K. model (Ourston, 2001)

The calculations of these geometry influencing factors are shown in Equation 2.2~2.7.

$$c_{cir} = k(F - f_c q_{cir}) \quad (2.1)$$

$$k=1-0.00347(\varphi-30)-0.98(1/r-0.05) \quad (2.2)$$

$$F=303x_2 \quad (2.3)$$

$$x_2=v+(e-v)/(1+2S) \quad (2.4)$$

$$S=(e-v)/l' \quad (2.5)$$

$$f_c=0.21TD(1+0.2x_2) \quad (2.6)$$

$$TD=1+0.5/(1+exp((D-60)/10)) \quad (2.7)$$

Based on these formulas, the impact of roundabout geometric elements on entry capacity can be described that entry capacity is reduced more with smaller value of r, v, e, D_{outer}, φ and l'.

Germany model

Similar as U.K. model, Brilon and Stuwe from Germany also developed a linear regression model considering the number of lanes in entry and circulating roadway (1991). The estimation formula is shown in Equation 2.8.

$$c_{cir}=A+Bq_{cir} \quad (2.8)$$

where A, B = constant value which is calibrated by number of lanes in entry and

circulating roadway

The values of *A* and *B* are shown in Table 2.2.

Table 2.2 Values of parameters *A* and *B* in Germany linear regression model

No. of lanes in entry	No. of lanes in circulating road way	A	B
1	1	1218	-0.74
1	2 or 3	1250	-0.53
2	2	1380	-0.50
2	3	1409	-0.42

Besides the linear regression model, Brilon and Grossmann (1991) also developed an exponential model considering the number of lanes in entry and circulating roadways. The exponential formula is described in Equation 2.9.

$$c_{cir} = C\exp(-Dq_{cir}/1000) \tag{2.9}$$

where C, D = constant value which is calibrated by number of lanes in entry and circulating roadway in exponential formula

The values of *C* and *D* are shown in Table 2.3.

Table 2.3 Values of parameters C and D in Germany exponential regression model

No. of lanes in entry	No. of lanes in circulating roadway	*C*	*D*
1	1	1089	7.42
2 or 3	1	1200	7.30
2	2	1553	6.69
3	2	2018	6.68

Although the parameters show different values in linear and exponential models, the relationship of entry capacity and number of lanes can be concluded that entry capacity is increased when the number of lanes either entry road or circulating road increases.

FHWA model

Robinson et al (2000) in U.S.A. developed a regression model based on the formula of U.K. and Germany and this model is adopted in FHWA 2000 (Federal Highway Administration, Roundabouts: An Information Guide, 2000). They selected exponential formula for the model as similar as Germany as shown in Table 2.4.

Table 2.4 Regression model applied in FHWA

		Single-lane roundabout		Multilane roundabout		Urban compact roundabout	
$c_{cir}=E+Fq_{cir}$		E	F	E	F	E	F
		1212	-0.54	2424	-0.71	1218	-0.74
Geometry consideration	r	20m		20m			
	v	4m		8m			
	e	4m		8m			
	D_{outer}	40m		55m			
	φ	30degree		30degree			
	l'	40m		40m			

Three categories of roundabouts, i.e. single-lane roundabout, multilane roundabout and urban compact roundabout are considered in this estimation. Regarding the single-lane and multilane roundabouts, U.K. regression model is applied under the fixed geometry conditions and transferred to exponential formula. The fixed geometric elements are shown in Table 2.4. While regarding the urban compact roundabout, the Germany regression model under the condition of one lane in entry road and circulating road is utilized. The values of parameters *E* and *F* in FHWA model are shown in Table 2.4.

Swiss model

Bovy et al (1991) in Swiss developed a regression model considering the influence of number of lanes at entry and circulating roadway, exiting flow and the width of the splitter island. The estimation formula is shown in Equation 2.10.

$$c_{cir} = (1500 - \frac{8}{9} q_b)\beta \tag{2.10}$$

where $q_b = \gamma q_{cir} + \alpha q_{exit}$

q_{cir} =circulating flow (pcu/h)

q_{exit} =exiting flow (pcu/h)

β = 0.9 to 1.1 for single entry lane (default = 1.00)

= 1.4 to 1.6 for double entry lane (default = 1.50)

= 1.9 to 2.1 for triple entry lane (default = 2.00)

γ = 0.9 to 1.0 for single circulating lane (default = 1.00)

= 0.6 to 0.8 for double circulating lane (default = 0.66)

= 0.5 to 0.6 for triple circulating lane (default =0.55)

b = taken from Figure 2.3 (m)

α = 0.6 for $0< b \leq 9$

= 0.6-0.5/12(b-9) for $9< b \leq 21$

= 0.1 for $21< b \leq 27$

= 0.1-0.1(b-27) for $27 < b \leq 28$

= 0 for $b>28$

In Figure 2.6, C' is the tangent point of supposing trajectory (middle line of the road)in entry road and circulating roadway and C is the tangent point of supposing trajectory in exit road and circulating roadway. And b is calculated as the length of curve between C and C'.

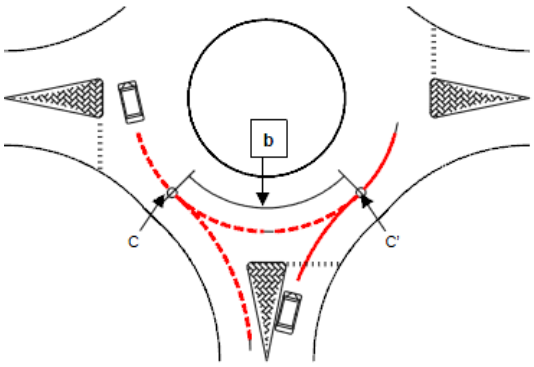

Figure 2.6 Swiss measure of the parameter "b"(Bovy, 1991)

French model

Louah (1993) proposed an exponential regression model to estimate entry capacity considering exiting flow and geometry influencing factors, i.e. radius of central island, entry width, circulating width and width of splitter island. The model is currently utilized

in software implementation GIRABASE. The formula of the model is expressed in Equation 2.11.

$$c_{cir} = C_F \exp(-D_F q_g) \tag{2.11}$$

where $q_g = q_{exit} k_{exit} (1 - \frac{q_{exit}}{q_{cir} + q_{exit}}) + q_{ci} k_{ti} + q_{co} k_{to}$

$C_F = \frac{3600}{t_f} (\frac{L_e}{3.5})^{0.8}$

q_c =total conflicting flow (pcu/h)

q_{ci} =conflicting flow on inner lane (default = 0.4*qc) (pcu/h)

q_{co} =conflicting flow on outer lane (default = 0.6*qc) (pcu/h)

q_{exit} =exiting flow (pcu/h)

D_F =3.525 for urban area

=3.625 for rural area

t_f =follow-up time of entry vehicles =2.05s

L_e =entry width (m)

k_{exit} $= \frac{R}{R + L_{cir}} - \frac{L_s}{L_{s,\max}}$ For $L_i < L_{i,max}$

=0 else

R =radius of the central island (m)

L_{cir} =circulating width (m)

L_s =width of the splitter island (m)

$L_{s,max} = 4.55\sqrt{R + \frac{L_{cir}}{2}}$

k_{ti} $= \min\left\{ \begin{array}{l} \frac{160}{L_{cir}(R + L_{cir})} \\ 1 \end{array} \right.$

k_{to} $= \min\left\{ \begin{array}{l} 1 - \frac{(L_{cir} - 8)}{L_{cir}} (\frac{R}{R + L_{cir}})^2 \\ 1 \end{array} \right.$

The entry capacity is calculated by each formula based on the fixed conditions which are shown in Table 2.5.

Table 2.5 Assumed conditions for estimating entry capacity by regression models

(a) Geometry input conditions

Geometric elements	Value	Geometric elements	Value	Geometric elements	Value
Number of legs	4	Number of lanes in entry road	1	Number of lanes in circulating roadway	1
Diameter (m)	40	Width of entry road (m)	3.5	Width of circulating roadway (m)	5
Narrowest radius of the right edge at the entry (m)	20	Width of the lane on the approaching street (m)	4	Radius of central island (m)	6
Width of the entry at the edge of the circulating ring (m)	4	Angle between ring and entry (degree)	30	Effective length of the funnel-shaped flare (m)	40
Width of splitter island (m)	10				

(b) Other input conditions

Parameters	Value	Parameters	Value
Follow-up time (sec)	2.05	Exit flow (veh/h)	100

Table 2.5(a) shows the geometry input conditions and Table 2.5(b) shows the other conditions, i.e. follow-up time and exit flow which are included in Swiss and French models. And the estimated results are shown in Figure 2.7.

It is found that the performance of entry capacity in exponential model is different from that in linear model. The estimated entry capacity in exponential model is reduced sharply when circulating flow is in the level of low demand whereas it slightly changes when circulating flow is in the high level. On the other hand, the reduction of estimated entry capacity in linear model is uniform due to the selection of form of models. In linear models, since U.K. model is directly utilized in the FHWA model (for single-lane roundabout), the estimated entry capacity shows the same performance. Either in linear model or exponential model, Germany model shows the lowest result of entry capacity.

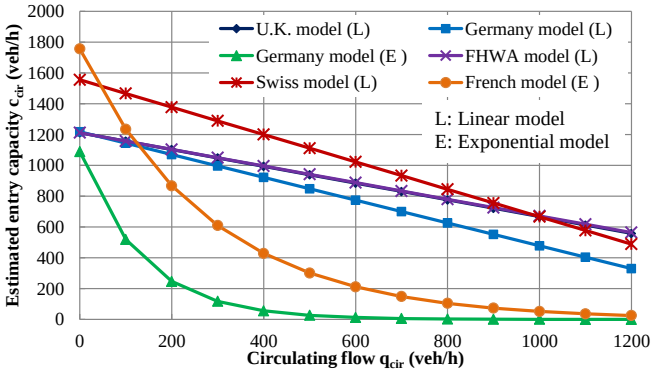

Figure 2.7 Estimated results of entry capacity by applying regression models

The characteristics of regression method are described as follows.

Regression models are developed based on empirical data, thus they represent characteristics of local drivers which may makes the models have poor transferability to other countries or at other times, e.g. inexperienced US drivers versus experienced UK drivers.

Then, in order to develop regression models, the observation of entry capacity under the oversaturated conditions is necessary which requests sites with continuous queuing. This cannot be satisfied at any country, thus limiting the application of regression model.

Regression method tries to consider roundabout geometric elements in the estimation entry capacity. However, since each situation (traffic volume pattern and/or geometric conditions) must be observed in order to develop an appropriate model, this requires a large data collection effort. The situations cannot be satisfied in the countries which few roundabouts are installed, e.g. Japan.

Furthermore, regression method too much focuses on the specific combination of parameters so that provides no real understanding of the underlying traffic flow theory of determining and accepting gaps upon entering the intersection.

2.2.2 Macroscopic software

Several countries developed software, e.g. ARCADY and RODEL based on the regression models which are introduced in the previous sections. The applications of these software products are described as follows.

ARCADY: This software is produced by the Transport Research Laboratory in U.K. and based on U.K. model. This software is utilized to estimate traffic capacity, queuing and delay at roundabouts. A prime attribute is that the capacities it predicts have been measured.

RODEL: This software is also produced by U.K. and based on U.K. regression model. It includes both an evaluation mode (geometric parameters specified) and a design mode (performance targets specified). Comparing to ARCADY, it includes a crash prediction model and can be applied for evaluation and design at multiple roundabouts.

GIRABASE: This software is developed by French based on French regression model which is utilized to estimate capacity, delay and queuing. The estimated entry capacity from this software production is the average value and sensitive to geometric elements.

2.3 Microscopic estimation method

As mentioned previously, regression method needs sufficient data to calibrate parameters which cannot be satisfied in the countries having limited roundabouts, e.g. Japan. In order to overcome this limitation, microscopic method which focuses on individual vehicle is developed. Since roundabout is one type of unsignalized intersections, the concept of capacity estimation at unsignalized intersection, i.e. gap acceptance theory is also applied on roundabout. Besides circulating vehicles, pedestrians are also considered from several ways, e.g. adjustment factor and queue theory. Similar as macroscopic method, several software products and simulations are developed based on microscopic theoretical models.

2.3.1 Theoretical models

Gap acceptance theory

At unsignalized intersections, since subjects in major flow are given priority, subjects in minor flow have to yield to major flow. As shown in Figure 2.8, gap is defined as the headway between two subjects.

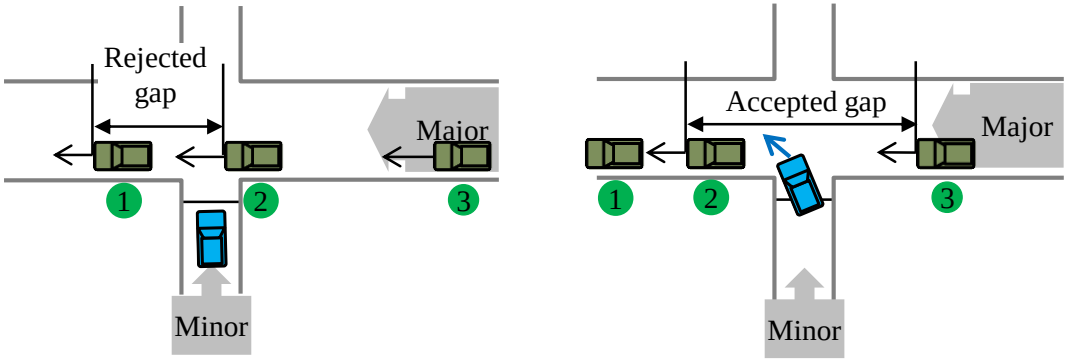

(a) Rejected gap (b) Accepted gap

Figure 2.8 Illustration of accepted gap and rejected gap

Subjects in minor flow judge the gaps in major flow to decide crossing or merging into major flow. This gap judging behavior is the gap acceptance behavior. During the judging procedure, accepted gap is defined as the gap in major flow which is utilized by subjects in minor flow to cross or merge into major flow while rejected gap is defined as the gap in major flow which is neglected by subjects in minor flow.

Accordingly, the capacity of minor flow is determined by the situations of accepted gaps, i.e. the length of the accepted gap which decides how many vehicles can cross or merge in one accepted gap and how the accepted gaps appear in major flow which is dependent on arrival patter of subjects in major flow. At roundabout, entry flow and circulating flow is the minor and major flow, respectively. Thus, entry capacity is determined by how many vehicles can enter in one accepted gap of circulating flow and how the accepted gaps are provided by circulating vehicles which is related to headway distribution of circulating vehicles. $E(t)$ is defined as the maximum number of vehicles can enter in one available gap at gap size of t sec and $h(t)$ is defined as the density function of headway distribution. Therefore, entry capacity c_{cir} is calculated as the cumulative result of product of $h(t)$ and $E(t)$ at all levels of circulating flow q_{cir} during certain period as shown in Equation 2.12.

$$c_{cir} = q_{cir} \int_0^{\infty} h(t)E(t)dt \tag{2.12}$$

Headway distribution model $h(t)$ and the model of maximum entering vehicles $E(t)$ are developed under various situations which are introduced as follows.

Density function of headway distribution $h(t)$

M1 model

Headway distribution is related to arrival pattern of vehicles. Breiman (1963), Thedeen (1964), Weiss and Hermann (1962) and Brown (1972) have demonstrated that on a road with unrestricted overtaking, the headway process at some reasonably large distance from the entry point will be a Poisson process. And the headway of vehicles follows exponential distribution. For a flow of q (veh/s), headway distribution under this assumption which is named M1 model is shown in Equation 2.13.

$$h_1(t) = e^{-\lambda_1 t},\ t \geq 0 \tag{2.13}$$

where λ_1 =arrival rate (veh/s) and under the condition of random arrival pattern λ_1 is equal to q

M2 model

Through observing the empirical data in real world, it is found that the headway of vehicles will not reduce to 0 due the length of vehicle and the consideration of safety. Breiman et al (1968) and Cox and Lewis (1966) showed the empirical evidence of this behavior. Thus, a parameter of minimum headway τ is defined and added in the M1 model. Due to this τ, M1 model is shifted to the new M2 model and the headway distribution is described in Equation 2.14.

$$h_2(t) = e^{-\lambda_2 (t-\tau)},\ t \geq \tau \tag{2.14}$$

Since τ is the lost time between two vehicles, assuming the flow is Q (veh/h), in one hour the total lost time is τQ (sec) and "free time" is equal to 3600-τQ (sec). Thus, the arrival rate λ_2 (veh/s) in free time is calculated as shown in Equation 2.15.

$$\lambda_2 = \frac{q}{1 - \tau q} \tag{2.15}$$

M3 model

Free flow actually does not commonly happen in real world. In most situations, traffic flow includes two types of vehicles, bunched vehicles which are closely following preceding vehicles and free vehicles which are travelling without interacting with the vehicles ahead. Many headway distribution models regarding this situation have been developed. Schuhl (1955) and Buckley (1962, 1968) considered both headways of bunched vehicles and free vehicles while Cowan (1975) developed a model which did not consider headways between the bunched vehicles since they are usually not accepted but rather models the larger gaps. Headway distribution under this condition is named M3 model and is shown in Equation 2.16.

$$h_3(t) = \alpha e^{-\lambda_3(t-\tau)} \tag{2.16}$$

where α =the proportion of free vehicle in total flow

And the arrival rate λ_3 under this situation is calculated as Equation 2.17.

$$\lambda_3 = \frac{\alpha q}{1-\tau q} \tag{2.17}$$

It is obvious that when α=1, the M3 model turns to the M2 model and when α=1 with τ=0, this M3 model turns to the M1 model. Several analyses were conducted to estimate α. Tanner (1962) set α to (1-τq), however the distribution of the number of vehicles in platoons is not the same. Brilon (1988) developed a model for α which showed a good fit to data as shown in Equation 2.18.

$$\alpha = e^{-Aq} \tag{2.18}$$

where A =a value which can be related to categories of lanes (median lane or other) and width of the lane.

Sullivan and Troutbeck (1993) estimated the value of A which ranged from 6 to 9.

Expected number of entering vehicles $E(t)$ in one accepted gap in size t

For a queue waiting in minor road, the number of vehicles in queue can cross or merge into major flow is determined by following two conditions:

1. How many seconds of the accepted gap in major flow which is chosen by the first vehicle in the queue;

2. How many seconds of headway which is kept by following vehicles in the queue to the preceding vehicle if the accepted gap in major flow is large enough to allow more than one vehicle to cross or merge into.

Two parameters are utilized to describe these two conditions, critical gap t_c and follow-up time t_f for condition 1 and 2, respectively. In FHWA (Chapter 8: Theory flow of unsignalized intersection, 2000) critical gap is defined as the minimum gap that all drivers in the minor stream are assumed to accept at all similar locations while follow-up time is defined as the headway of queuing vehicles in minor road successively crossing or merging into major flow in one accepted gap.

Based on this, under the assumption of discrete departure of minor flow, Tanner (1962), Harders (1976), Troutbeck (1986) and others developed a step model of $E(t)$. The formula of $E_1(t)$ is described in Equation 2.19 and the result of $E_1(t)$ is shown in Figure 2.9.

$$E_1(t)=\begin{cases} \text{int}\left(\dfrac{t-t_c}{t_f}\right),\ t\geq t_c & \text{(2.19-a)} \\ 0,\ t<t_c & \text{(2.19-b)} \end{cases}$$

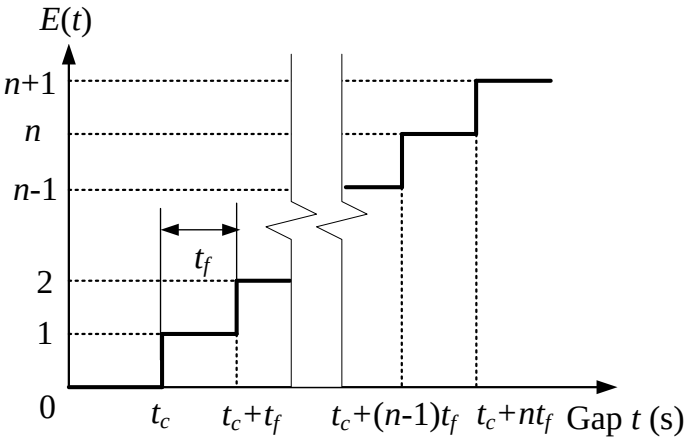

Figure 2.9 Step model of $E_1(t)$

While under the assumption of continuous departure of minor flow, Siegloch (1973) and McDonald and Armitage (1978) developed a continuous model for $E(t)$. In Siegloch's

model, based on the observation which is shown in Figure 2.10, for each of the gap which is accepted by only *n* vehicles, the average gap size is calculated.

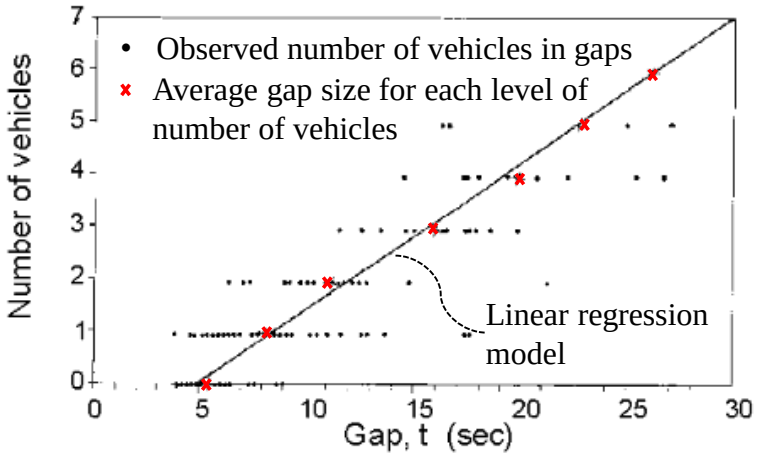

Figure 2.10 Observation of number of vehicles in various gaps (Siegloch, 1973)

Then, the linear regression model of $E_2(t)$ is developed with the slope of t_f and the formula is described in Equation 2.20.

$$E_2(t)=\begin{cases} \dfrac{t-t_0}{t_f}, & t\geq t_0 \qquad (2.20\text{-a}) \\ 0, & t<t_0 \qquad (2.20\text{-b}) \end{cases}$$

where t_0 =the intercept of the gap size at X axis and can be calculated by tc and tf as shown in Equation 2.21.

$$t_0 = t_c - \frac{t_f}{2} \qquad (2.21)$$

The result of $E_2(t)$ is shown in Figure 2.11.

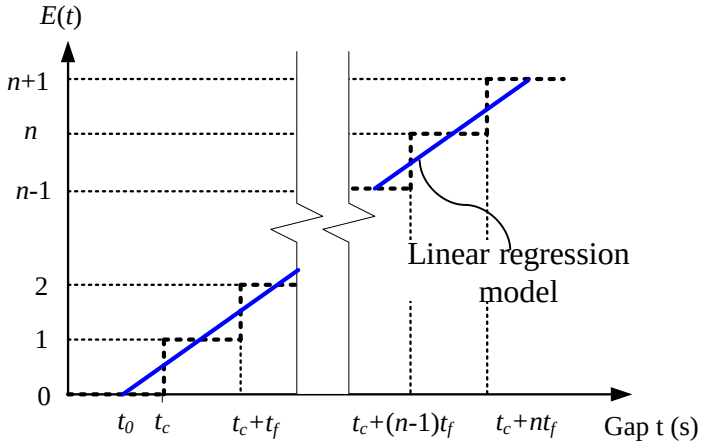

Figure 2.11 Linear regression model of $E_2(t)$

Applications of microscopic methods in different countries

The microscopic method is widely utilized in many countries and adopted by many guidelines and manuals. There are three types of $h(t)$ models, i.e. $h_1(t)$, $h_2(t)$ and $h_3(t)$ and two types of $E(t)$ models, i.e. $E_1(t)$ and $E_2(t)$. Each country selects different types of $h(t)$ and $E(t)$ models based on their situations and these applications are introduced as follows.

High Capacity Manual, HCM (*1997, U.S.*)

HCM 1997 considered h_1(t) and $E_1(t)$ models for single-lane roundabouts based on the background provided by Troutbeck (1986) and Siegloch (1973). The estimation formula is shown in Equation 2.22.

$$c_{cir} = \frac{q_{cir} e^{-q_{cir} t_c / 3600}}{1 - e^{-q_{cir} t_f / 3600}} \tag{2.22}$$

Based on empirical data, the critical gap t_c has an upper and lower bound of 4.1 sec and 4.6 sec, respectively while the follow-up time t_f has an upper and lower bounds of 2.6 sec and 3.1 sec, respectively.

National Cooperative Highway Research Program, NCHRP Report 572 (*2007, U.S.*)

NCHRP model considers $h_1(t)$ and $E_2(t)$ models and the estimation formula is shown in Equation 2.23.

$$c_{cir} = \frac{3600}{t_f} \exp(-\frac{t_c - t_f / 2}{3600} q_{cir}) \quad (2.23)$$

The selection of t_c and t_f is the same as HCM 1997.

HCM 2010 (*2010, U.S.*)

The entry capacity model for single-lane roundabout which is applied in HCM 2010 is based on the model in NCHRP 2007 which was developed by Harders (1968) and giving the constant value of t_c and t_f, i.e. t_c=5.1sec, t_f=3.2sec. Thus, the estimation formula in HCM 2010 is shown in Equation 2.24.

$$c_{cir} = 1130 \exp(-0.0010 q_{cir}) \quad (2.24)$$

Handbuch für die Bemessung von Straßenverkehrsanlagen, HBS (*2001, Germnay*)

In German guideline HBS, $h_3(t)$ and $E_2(t)$ models are considered. Moreover, number of lanes at entry and circulating roadway n_e and n_c is considered in the estimation formula. The German model which is adopted in HBS 2001 is shown in Equation 2.25.

$$c_{cir} = n_e \frac{3600}{t_f} \left(1 - \frac{\tau \frac{q_c}{3600}}{n_c} \right)^{n_c} \exp\left[-\frac{q_{cir}}{3600} \left(t_c - \frac{t_f}{2} - \tau \right) \right] \quad (2.25)$$

Guide to Traffic Engineering Practice Part 6-Roundabout, AustRoads (*1993, Australia*)

The estimation method which is adopted in Australian guideline includes $h_3(t)$ and $E_1(t)$ models and has been incorporated into the software *aaSIDRA* (1996). This method considers geometric influencing factors, e.g. number of lanes in entry and circulating roadway and diameter. In addition, impact of OD traffic at roundabout is also considered in this estimation. The formulas of entry capacity in AustRoads are shown in Equation 2.26.

$$c_{cir} = \max(f_{od} q_g, q_m) \quad (2.26)$$

$$q_g = \frac{3600}{t_f}\left(1-\tau_{cir}\frac{q_{cir}}{3600}+0.5t_f\varphi_{cir}\frac{q_{cir}}{3600}\right)\exp\left(-\lambda\left(t_c-\tau_{cir}\right)\right)$$

$$q_m = \min(q_e, 60n_m)$$

$$f_{od} = 1-f_{qcir}\left(p_{qd}p_{cd}\right)$$

where q_g =minimum entry flow (veh/h)

q_e =entry arrival flow (veh/h)

f_{od} =o-d adjustment factor

$q_{qd}q_{cd}$ ≈0.5 to 0.8 (0.6 used)

n_m =minimum entry flow (veh/min)

n_c =number of lanes in conflicting flow

τ_{cir} =minimum headway in circulating traffic (sec)

=2.0 for n_c=1

=1.2 for n_c=2

φ_{cir} =proportion of unbunched conflicting vehicles

$$= \exp\left(\frac{-5.0q_{cir}}{3600}\right) \text{ for } n_c=1$$

$$= \exp\left(\frac{-3.0q_{cir}}{3600}\right) \text{ for } n_c=2$$

λ =arrival headway distribution factor (veh/s)

$$= \frac{\varphi_{cir}q_{cir}/3600}{1-\tau_{cir}q_{cir}/3600} \text{ for } q_{cir}/3600 \le 0.98/\tau_{cir}$$

$$= \frac{49\varphi_{cir}}{\tau_{cir}} \text{ else}$$

For n_c =1

$$f_{qcir}\begin{cases} = 0.04+0.00015q_{cir} & \text{for } q_{cir}<600 \\ = 0.0007q_{cir}-0.29 & \text{for } 600\le q_{cir}\le 1200 \\ =0.55 & \text{for } q_{cir}>1200 \end{cases}$$

For n_c =2

$$f_{qcir}\begin{cases} =0.04+0.00015q_{cir} & \text{for } q_{cir}<600 \\ =0.0035q_{cir}-0.29 & \text{for } 600\le q_{cir}\le 1800 \\ =0.55 & \text{for } q_{cir}>1800 \end{cases}$$

Australia model is the only model which considers geometric factors in estimation of t_c and t_f. The details are introduced as follows.

For the dominant entry lane (lane at a multi-lane roundabout with the largest entry flow), the formula of t_f is shown in Equation 2.27.

$$t_f = t_{fd} = t_{f0} - 3.94*10^{-4} q_{cir}, \text{ subject to } t_{fmin} \le t_f < t_{fmax} \quad (2.27)$$

where $t_{f0} = 3.37 - 0.0208 D_i + 0.889*10^{-4} D_i^2 - 0.395 n_e + 0.388 n_c$

subject to $20 \le D_i \le 80$

D_i =inscribed diameter (m)

n_e =number of entry lanes

t_{fmin} =1.2sec

t_{fmax} =4.0sec

While for the subdominant entry lane (lane at a multi-lane roundabout with the smallest entry flow), the formula of t_f is shown in Equation 2.28.

$$t_f = t_{fs} = 2.149 + (0.5135 t_{fd} - 0.8735) r_{ds}, \text{ subject to } t_{fd} \le t_{fs} \le t_{fmax} \quad (2.28)$$

where r_{ds} = q_d/q_s , ratio of dominant flow q_d and subdominant flow q_s in the entry

The formula of critical gap tc is shown in Equation 2.29.

$$t_c = \begin{cases} (3.6135 - 3.137*10^{-4} q_{cir} - 0.339 w_L - 0.2775 n_c) t_f & \text{for } q_{cir} \le 1200 \quad (2.29\text{-a}) \\ (3.2371 - 0.339 w_L - 0.2775 n_c) t_f & \text{else} \quad (2.29\text{-b}) \end{cases}$$

Subject to $1 \le t_c/t_f \le 3.0$ and $t_{cmin} \le t_c \le t_{cmax}$

where t_{cmin} =2.2sec

t_{cmax} =8.0sec

w_L =average entry width (m)

Roundabout entry capacity is estimated by these microscopic formulas under the

conditions which are shown in Table 2.6 and the estimated results are shown in Figure 2.12.

Table 2.6 Assumed conditions for estimating entry capacity by microscopic method

(a) Geometry input conditions

Geometric elements	Value	Geometric elements	Value	Geometric elements	Value
Number of legs	4	Number of lanes in entry road	1	Number of lanes in circulating roadway	1
Diameter (m)	40	Width of entry road (m)	3.5		

(b) Other input conditions

Parameters	Value	Parameters	Value
Follow-up time in other models except Australia model (sec)	3.2	Critical gap in other models except Australia model (sec)	5.1
Minimum headway in circulating flow (sec)	2		

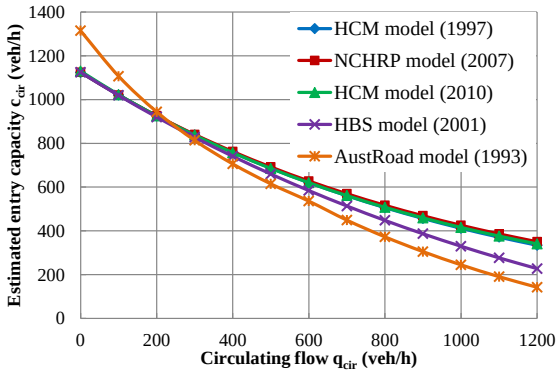

Figure 2.12 Estimated entry capacity through several microscopic formulas

It is found that although the same values of t_c, t_f and τ are input, the estimated entry capacity shows different results by models. The results from the U.S. formulas are almost the same and when circulating flow is in the low level (q_{cir}≤400veh/h), they are similar to the result from HBS formula. When q_{cir} increases, the result from HBS model shows lower

performance on entry capacity than that from U.S. models. This can be contributed that regarding the headway distribution, HBS model applies M3 model whereas U.S. models applies M1 model. When q_{cir} is in the high level, circulating vehicles arrived as bunching pattern which reduces the probability of available gaps ($t>t_c$) comparing to the assumption of Poisson arrival pattern in M1 model. This difference can also be observed through comparing the results from U.S. models to AustRoad model. And the difference between the result from AustRoad model and others is supposed to cause by the consideration of geometric influence factors in AustRoad model.

Regarding the microscopic method, the estimation procedures exist for critical gap do not require sites with oversaturated conditions. And the follow-up time can be directly measured in the field without utilizing complicated mathematical equations.

The gap acceptance theory is applied based on several assumptions, i.e. (a) constant t_c and t_f values; (b) exponential distribution for priority stream gaps and (c) constant traffic volumes for each traffic stream. These idealized assumptions are considered somewhat unrealistic; however, various evaluations have suggested that more realistic headway distributions are not significantly more accurate. Furthermore, the resulting generalized solutions are not easy to apply in practice. In addition to the concern related to realistic distributions of headways and other gap acceptance parameters, there are a number of other theoretical limitations. These are described below:

Inconsistent gap acceptance occurs in practice and has not been accounted for in theory. These include (a) rejecting a large gap before accepting a smaller gap, (b) driver on the roundabout giving up the right of way, (c) forced right of way when the traffic is congested, and (d) different vehicle types accepting different gaps.

Geometric factors are not directly taken into account. Although the geometric elements of diameter and average of entry width are considered in Australia model, it is more complicated to apply this model than others.

Adjustment factor considering pedestrian impact

Pedestrian flow is another key stream to influence entry capacity besides circulating flow. Pedestrian impact on entry capacity in current methods is commonly estimated by

adjustment factor f_{ped}. Then, the entry capacity c_{RAB} considering pedestrian impact is calculated by the maximum entry flow under the impact of circulating flow c_{cir} which is introduced in the previous section multiplying this adjustment factor as shown in Equation 2.30.

$$c_{RAB} = c_{cir} * f_{ped} \tag{2.30}$$

Marlow and Maycock (1982) developed a model of f_{pedM} based on queue theory considering pedestrian demand at subject entry, width of crosswalk and pedestrian crossing speed. This method is a little complicated on application. Stuwe and Brilon (1992) estimated f_{pedSB} based on circulating flow and pedestrians across subject entry with better applicability. Suzuki et al (2013) developed a model of f_{pedS} considering the impact of pedestrian on entry vehicles based on gap acceptance behavior and the impact of pedestrian on offside exit vehicles further influencing arrival pattern of circulating flow. Besides the impact of pedestrian across subject entry, pedestrians at other entries are also considered. The adjustment factor f_{pedR} which is developed by Rodegerdts and Blackwelder (2011) was estimated through considering the impact of block events at adjacent downstream exit due to pedestrians on entry capacity by queue theory.

Estimation of f_{pedM}

Marlow and Maycock (1982) developed the adjustment factor f_{pedM} based on queue theory. They treat the crosswalk and the roundabout entry as two queuing systems in secession. First of all, the capacity of the two queuing systems (crosswalk and entry) is calculated. Following that the total capacity which is the roundabout entry capacity under the impact of pedestrian and circulating flow is calculated.

Under the assumption that pedestrians have priority on crosswalk, the capacity of the crosswalk is first calculated based on the formula by Griffiths in Equation 2.31 (1981).

$$c_{cs} = \frac{\mu}{\mu\beta + (e^{\mu\alpha} - 1)(1 - e^{-\mu\beta})} 3600 \tag{2.31}$$

where c_{cs} =capacity of the crosswalk for vehicles (veh/h)

μ =volume of pedestrians (ped/s)

β =minimum time gap between two vehicles (sec) when driving across the crosswalk=$1/c_0$, c_0 is capacity of one lane of the entry, at an empty

roundabout (veh/s)

α = B/v_{FG}, time needed to cross the crosswalk by the pedestrians (sec)

B =width of road at crosswalk (m)

v_{FG} =walking speed of pedestrians at the crosswalk (m/s)

The pedestrian walking speed v_{FG} is about 0.5 to 2.0 m/s. If there is no information available, a value of 1.4 m/s will be used. The parameter B can be set individually according to the given situation in every single entry. Thus, the total capacity of the crosswalk-entry system, a relation of R is significant as described in Equation 2.32.

$$R = \frac{c_{cs}}{c_{cir}} \tag{2.32}$$

And f_{pedM} in this method is calculated by this R as shown in Equation 2.33.

$$f_{pedM} = \frac{R^{N+2} - R}{R^{N+2} - 1} \tag{2.33}$$

where N =Number of vehicles that can queue between the area between crosswalk and entry

N also can be set for every single entry as the same as the width of crosswalk B.

Maylow and Maycock's model considered more geometric factors than Stuwe's model, i.e. the width of crosswalk and distance between crosswalk and entry.

Estimation of f_{pedSB}

Brilon et al (1993) developed an adjustment factors f_{pedSB} for one-lane and two-lane roundabout based on observation at three roundabouts in Germany with heavy pedestrian flow. All these study sites were installed under the standard design, i.e. physical splitter island and crosswalk existing at each entry/exit and the space of one-vehicle length between crosswalk and yield line is satisfied. Based on the observations, f_{pedSB} is estimated considering pedestrian flow and circulating flow. The formulas for one-lane roundabout are shown in Equation 2.34~2.36 dependent on different levels of pedestrian and circulating flows.

$$f_{pedSB} = 1 \qquad \text{For } q_{cir}>881\text{pcu/h} \qquad (2.34)$$

$$f_{pedSB} = 1 - 0.000137 q_{ped} \qquad \text{For } q_{cir}\leq 881\text{pcu/h and } q_{ped}<101\text{ped/h} \qquad (2.35)$$

$$f_{pedSB} = \frac{1119.5 - 0.715 q_{cir} - 0.644 q_{ped} + 0.00073 q_{cir} q_{ped}}{1068.6 - 0.654 q_{cir}} \qquad \text{For } q_{cir}\leq 881\text{pcu/h and } q_{ped}\geq 101\text{ped/h} \qquad (2.36)$$

The results of f_{pedSB} changing with pedestrian and circulating flows are shown in Figure 2.13.

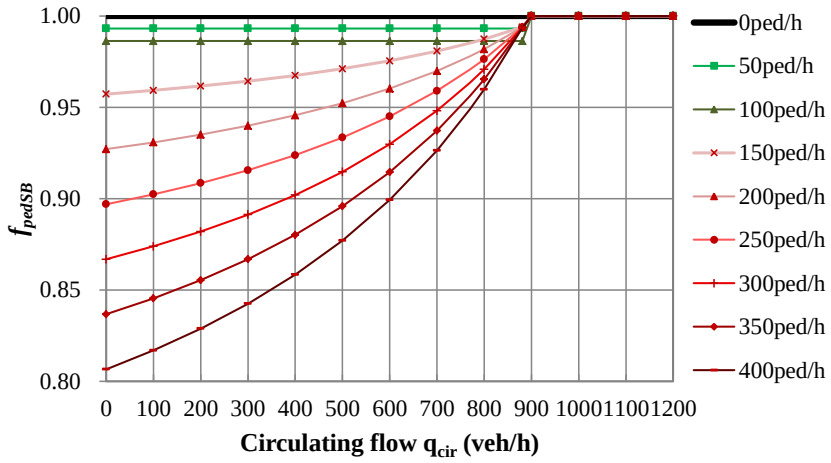

Figure 2.13 Result of f_{pedSB} changing with pedestrian and circulating flows

For one-lane roundabout, if the circulating traffic is 900pcu/h or higher, pedestrians do not have any more influence on the capacity of the entry. This seems to be logical since when there is a queue the pedestrians can use the crosswalk without interfering with traffic.

Estimation of f_{pedS}

Suzuki et al (2013) estimated pedestrian impact mainly from the consideration of arrival pattern of circulating vehicles. Offside exit vehicles departing from the subject entry may be blocked by pedestrians and have impact on arrival pattern of circulating vehicle further influencing entry capacity.

Thus, the arrival pattern of circulating vehicles will be divided into three classifications. W is defined as the time from the exit vehicles are blocked by pedestrians until an accepted gap of pedestrians appears for the queuing vehicles. These queuing vehicles will depart

from the approach exit as saturation flow during this accepted gap and T is defined as the duration of arriving time of circulating vehicles under saturation flow. And S is the left time without W and T. In time W, since circulating vehicles are blocked in circulating roadway, only pedestrians have conflict with entry vehicles while in time S, both pedestrians and circulating vehicles have conflict with entry vehicles. In time T, since circulating vehicles passing in front of the subject entry as saturation flow, entry vehicles cannot find accepted gaps of circulating vehicles further cannot enter roundabout. The illustrations of W and T are shown in Figure 2.14.

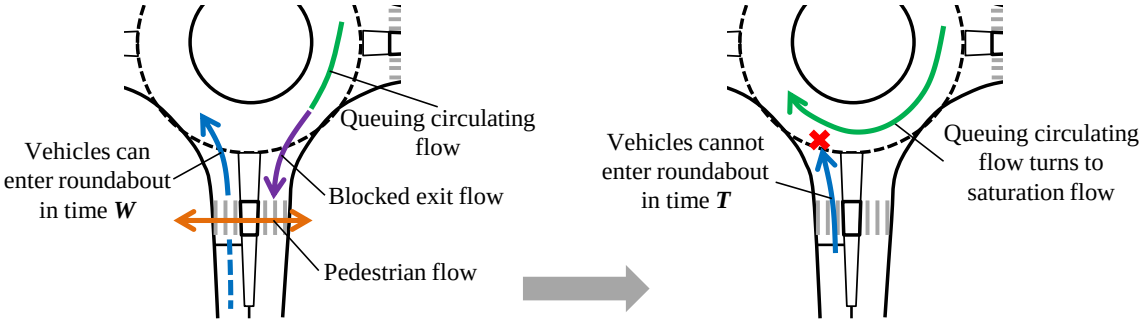

Figure 2.14 Illustration of time W and T

Thus, roundabout entry capacity is counted during time W and S as shown in Equation 2.37.

$$c_{RAB} = T_{cap}\frac{3600}{t_f} \tag{2.37}$$

where T_{cap} =the time duration of vehicles can enter roundabout

The adjustment factor f_{pedS} in this analysis is actually equal to the parameter of T_{cap} and is calculated by Equation 2.38.

$$f_{pedS} = T_{cap} = E(W)\frac{\int_{t_c}^{\infty}(x-t_c)f_p(x)dx}{\int_0^{\infty}xf_p(x)dx} + E(S)\frac{\int_{t_c}^{\infty}(x-t_c)f_{Super}(x)dx}{\int_0^{\infty}xf_{Super}(x)dx} \tag{2.38}$$

where $E(W)$ =expected value of W

$E(S)$ =expected value of S

$f_p(x)$ =density function of gaps of pedestrians

$f_{Super}(s)$ =density function of overlap gaps of pedestrians and circulating vehicles

Estimation of f_{pedR}

Vehicles exiting downstream exits will be blocked by pedestrians across downstream exits and a queue may be generated at exits even extending into circulating roadway. When the queuing vehicles reach in front of subject entry, the vehicles at upstream entry cannot enter roundabout therefore capacity of the entry is reduced. The illustration of this case is shown in Figure 2.15.

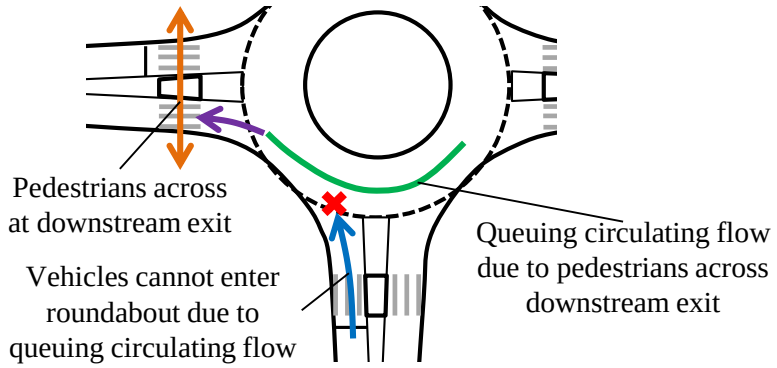

Figure 2.15 Illustration of the impact of pedestrians from downstream exits

Rodegerdts and Blackwelder (2008) developed a model to estimate the pedestrian impact at downstream exits through focusing on the time duration of blocking events. Two scenarios of conflict pedestrians and vehicles are analyzed, pedestrians yielding to vehicles and vehicles yielding to pedestrians. As mentioned at the beginning of section 2.2, the scenario pedestrian yielding to vehicles does not have impact on entry capacity. For the other scenario, the block duration is calculated based on queue theory. The impact of the queue at downstream exit can be calculated based on following assumptions.

- Vehicle arrivals at downstream exit are approximately Poisson distributed.
- Vehicles queue whenever a pedestrian is in the crosswalk.

The time over which the queue accumulates is constant, i.e. pedestrian speed is constant and the time it takes the queue to clear is constant.

When a queue enters the circulating roadway, it blocks all entries to the roundabout.

The probability of the queue with a length of n vehicles under the condition of Poisson distribution of exit vehicles is calculated by the Equation 2.39.

$$P_{queue}(n) = \frac{e^{-q_{exit}\left(T_b + \frac{3600\overline{Q_e}}{S_{exit}}\right)}\left[q_{exit}\left(T_b + \frac{3600\overline{Q_e}}{S_{exit}}\right)\right]^n}{n!} \tag{2.39}$$

where $P_{queue}(n)$ =the probability that a queue with n vehicles will occur during blocking event

q =queue length (used in estimating probabilities of specific queue lengths (number of vehicles)

$\overline{Q_e}$ =average expected queue (number of vehicles)

q_{exit} =vehicle flow rate on the exit being studied (veh/h)

T_b =duration of blocking event (sec)

S_{exit} =saturation flow rate of exiting vehicles upon release from blocking event (veh/h)

Then, average duration of queue blocking on a per event basis t_{avg} is calculated by Equation 2.40.

$$t_{avg} = \sum_{n=0}^{n=\infty} P_{queue}(n) t_{queue}(n) \tag{2.40}$$

where $t_{queue}(n)$ =duration over which a queue of length n exceeds queue length Q_{max}

Q_{max} =the maximum number of vehicles from crosswalk to the exit which does not block circulating roadway

$t_{queue}(n)$ is calculated by the queue-time curve which is shown in Figure 2.16 and is described in Equation 2.41.

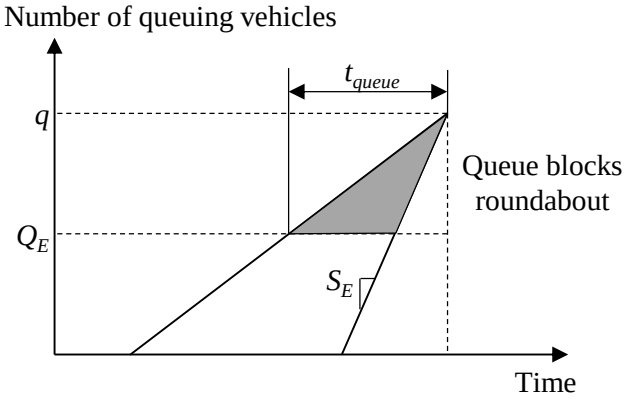

Figure 2.16 Calculation of $t_{queue}(n)$

$$t_{queue}(n) = \frac{(t_b + n/S_{exit})(n - Q_{\max})}{n} \tag{2.41}$$

Accordingly, the total time t_{block} during the study time period that the circulatory roadway is blocked is calculated by the t_{avg} and the number of blocking events n_{event} occurring during the study time period which is shown in Equation 2.42.

$$t_{block} = n_{event} t_{avg} \tag{2.42}$$

During this blocking time, entry capacity is lost since circulating roadway is block. Thus, fpedR under this situation is calculated by Equation 2.43.

$$f_{pedR} = 1 - \frac{t_{block}}{3600} \tag{2.43}$$

The adjustment factors f_{pedM} and f_{pedSB} considered the situation on subject entry only. These adjustment factors were developed based on the empirical roundabouts with standard design, i.e. physical splitter island and crosswalk at entry/exit and the space of one-vehicle length between yield line and crosswalk. In Japan, these conditions cannot always be satisfied due to space limitation. In addition, several influencing factors, i.e. pedestrian approaching sides, far-side pedestrian recognition rate which have impact on pedestrian behavior further influencing entry capacity are not considered. On the other hand, adjustment factors f_{pedS} and f_{pedR} estimated pedestrian impact from other exits but complicated to apply and difficult to calibrate parameters in empirical data. Therefore, a method estimating entry capacity considering component impact of pedestrians and

circulating vehicles and which can appropriately reflect Japanese situations is needed.

2.3.2 Microscopic software and simulation

Similar as macroscopic approach, there are also many software products and simulations which were developed based on microscopic method.

Microscopic software

SIDRA: This software is developed in Australia and based on the model proposed by Alcelik, R. (1997). It can evaluate capacity, delay, queue, fuel and environmental measures and also can be utilized to conduct evaluation at two-way stop controlled, all-way stop controlled and signalized intersections. This product also gives roundabout capacities from U.S. HCM 1997 and German procedures. It utilizes field data for the gap acceptance parameters to calibrate the model. An important attribute of SIDRA is that the user can alter parameters to easily reflect local driving.

HCS-3: This product is developed by U.S. and based on HCM 1997 method. It is limited to capacity estimation. The data used to calibrate the models were recorded in the U.S. and the two curves are given to reflect the uncertainty from the results. The upper bound average capacities are anticipated at most roundabouts. The lower bound results reflect the operation that might be expected until roundabouts become more common.

KREISEL: This product is developed by Germany and based on German gap acceptance estimation formula. It offers many user-specified options to implement the full range of procedures which are found in the literature from U.S., Europe, Britain and Australia. KREISEL gives the average capacity from a number of different procedures. It provides a means to compare these procedures. Moreover, the f_{pedSB} model is also included in KREISEL so that pedestrian impact can be reflected by this product.

Microscopic simulation

Comparing to software products, simulation has advantages on providing visual procedure and more flexibility on setting facility and geometric elements. Capacity can only be observed under the condition of oversaturation, however, oversaturation or queuing cannot be easily satisfied in real world which have limitation on estimation of capacity and

identification of influencing factors. By utilizing simulation, various situations and phenomenon can be realized, e.g. oversaturation, queuing and gap acceptance behavior. AIMSUN 6.1 (2010) and VISSIM 5.40 (2012) are two microscopic simulations which is developed by Spain and Germany, respectively. They are not only utilized for roundabout analysis, but also can be applied for other type of intersections or network analysis. VISSIM has better functions on simulating pedestrian behavior thus it is more utilized in the studies which is related to pedestrian analyses.

Tollazzi et al (2011) established a program in simulator to estimate roundabout entry capacity considering pedestrian and cyclist impact. The parameters in program are based on empirical data. Entry capacity was found to be reduced when motorized vehicles are disturbed by pedestrian and cyclist flow.

Lu et al (2011) quantitatively assessed the performance of four pedestrian signals at modern roundabouts under a spectrum of crosswalk layouts, signal installations, and operational conditions, aimed to provide access management community with an objective basis for identifying treatments to improve the roundabout accessibility. The study results suggested a non-monotonic relationship between the signalization effects and all levels of vehicle volumes.

Regarding the pedestrian impact, not only pedestrian flow has impact on entry capacity, other geometric factors, e.g. distance of crosswalk and yield line also have impact on entry capacity through changing the reaction of drivers to pedestrians.

Duran and Cheu (2011) identified the influence of crosswalk position on entry capacity at two-lane roundabout and found that entry capacity was reduced with decreasing the distance between downstream edge of crosswalk and yield line.

2.4 Summary

Considering limited number of roundabouts in Japan, microscopic approach is selected in this research. Based on the objective of this research, i.e. to develop a methodology on estimating roundabout entry capacity considering pedestrian impact and Japanese situation, both microscopic simulation study and theoretical model are conducted. Microscopic simulation study utilizing VISSIM 5.40 is first conducted to identify influencing factors.

The impacts of physical splitter island, distance between crosswalk and yield line, pedestrian approaching sides and far-side pedestrian recognition rate on entry capacity are examined. Since simulation is calculated by empirical data, the results from simulation can also be considered as reference. Then, based on the results from simulation study, a theoretical model is proposed including these identified influencing factors. Finally, a comparison analysis is conducted between the proposed theoretical model and simulation study for interpreting limitations of two methods and an appropriate method is expected for implementation in design and planning stage.

3 Chapter 3

SIMULATION ANALYSIS OF ROUNDABOUT ENTRY CAPACITY

3.1 Introduction of simulation

In this chapter, the impact of influencing factors, i.e. physical splitter island, distance between crosswalk and yield line, pedestrian approaching sides and far-side pedestrian recognition rate on entry capacity will be examined through simulation analysis. Before conducting the analysis, parameters in simulation are calibrated by empirical data which is observed at real roundabouts in Japan. After identifying the influencing factors, a regression model of entry capacity based on simulation output is developed including these influencing factors.

3.1.1 Building roundabout in VISSIM 5.40

VISSIM 5.40 utilizes “link” and “connection” to build facilities, e.g. road and intersection. A roundabout is drawn in simulation based on the real site which is located in Japan, i.e. Towa-cho roundabout in Iida City, Nagano Prefecture (details of this roundabout is introduced later in the section of “Data collection” in this chapter). Figure 3.1 shows the 2D and 3D vision of the two study sites drawing in simulation.

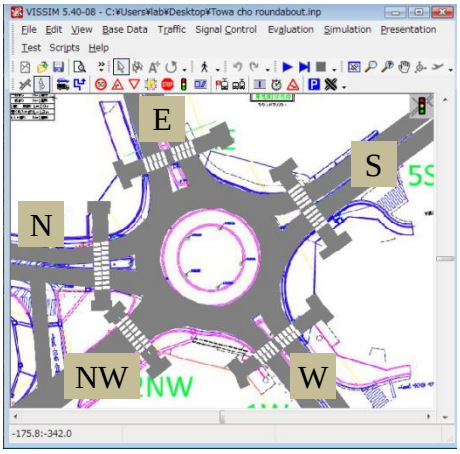

(a) 2D vision in simulation

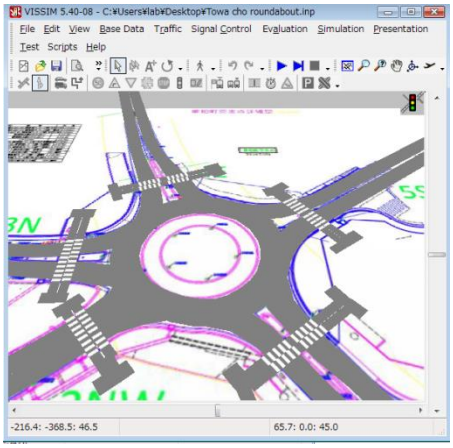

(b) 3D vision in simulation

Figure 3.1 Configuration of Towa-cho roundabout in VISSIM 5.40

3.1.2 Setting up vehicle and pedestrian traffic in VISSIM 5.40

Two categories of traffic are considered in this research, vehicle traffic and pedestrian traffic. The basic procedure of setting the vehicle/pedestrian traffic is described as follows.

- Set up the basic information for each category, e.g. vehicle/pedestrian type, vehicle/pedestrian size and vehicle/pedestrian speed.
- Select the model of car-following behavior.
- Set up traffic volume and traffic route.
- Define conflict behavior between vehicle & vehicle and vehicle & pedestrian

Setting up basic information for vehicles/pedestrians

Vehicles

For vehicles, basic information such as vehicle type, size and color is set up by the functions of “vehicle types” and “vehicle classes”. In the function of “vehicle types”, six types of vehicle are included, car, HGV, bus, tram, pedestrian and bike. For each type, the length of one type of vehicles is given a range while the width of one type of vehicles is an input parameter. For one type of vehicles, various classes can be identified for different objectives, e.g. the cars from East and West Approach can be defined as two classes.

Vehicle speed is set in the function of “desired speed”. A distribution is needed to input in the function of “desired speed”. Stochastic distributions of desired speeds are defined for each vehicle type within each vehicle composition. If not hindered by other vehicles, a driver will travel at his desired speed.

In order to complete other travelling behavior, e.g. overtaking and stopping behavior, an acceleration or deceleration is needed. VISSIM 5.40 does not use a single value to set acceleration and deceleration but use distributions. Four functions, i.e. maximum acceleration, desired acceleration, maximum deceleration and desired deceleration need to be set in VISSIM 5.40. Maximum acceleration is defined as the maximum technically feasible acceleration, regarded only if an acceleration exceeding the desired acceleration is required to keep the speed on slopes while desired acceleration is used for any other situation. Maximum deceleration is defined as the maximum technically feasible deceleration which is adjusted on slopes by 0.1(m/s^2) for each percent of positive gradient and -0.1(m/s^2) for each percent of negative gradient. Regarding desired deceleration, if it is lower than the maximum deceleration, the desired deceleration is used as the maximum for the deceleration. As the same as the function of “desired speed”, a distribution needs to be set in these functions. Desired speed is selected in the function of “vehicle compositions” and the functions of acceleration/deceleration are selected in the function of “vehicle types” for each type and class of vehicle.

Pedestrians

Similar as the setting of vehicles, basic information including pedestrian types (male and female), size (length, width and height) and pedestrian classes is set up in the function of “pedestrian types” and “pedestrian classes”. The procedures of setting speed and acceleration/deceleration of pedestrians are as the same as the setting of vehicles while in the function of “pedestrian compositions” and “pedestrian types”.

Selecting the model in car-following model

Two models are included in the function of car-following behavior in VISSIM 5.40, i.e. Wiedemann 74 model and Wiedemann 99 model. VISSIM 5.40 gives five default road situations, i.e. urban (motorized), right-side rule (motorized), freeway (free lane selection), footpath (no interaction) and cycle-track (free overtaking). Based on the concept of models,

Wiedemann 74 model is more suitable for urban road and merging/weaving areas while Wiedemann 99 model is more appropriate for interurban (motorway) traffic except merging/weaving areas. In this research, the roundabout is assumed to locate in the cross of urban roads. Therefore, only the parameters in Wiedemann 74 model are introduced.

Regarding following behavior, three general input parameters, i.e. “look ahead distance” (minimum, maximum and number of observed vehicles), “look back distance” (minimum and maximum) and “temporary lack of attention” (duration and probability) are included regardless the model types. The “look ahead distance” defines the distance that a vehicle can see forward in order to react to other vehicles either in front or to the side of it (within the same link). The “look back distance” defines the distance that a vehicle can see backwards in order to react to other vehicles behind (within the same link). The “temporary lack of attention” is related to the situation that vehicles will not react to a preceding vehicle (except for emergency braking) for a certain amount of time. The “duration” defines how long this lack of attention lasts and the “probability” defines how often this lack of attention occurs.

In Wiedemann 74 model, three parameters, i.e. “average standstill distance”, “additive part of desired safety distance” and “maltipic part of safety distance” are needed to calibrate. The “average standstill distance” defines the average desired distance between stopped cars. It has a variation between -1.0(m) and +1.0(m) which is normal distributed around 0(m) with a standard deviation of 0.3(m) while the other two parameters affect the computation of the safety distance. By these, the distance d between two vehicles is computed using Equation 3.1 and 3.2.

$$d = ax + bx \tag{3.1}$$

$$bx = (bx\_add + bx\_mult * z)\sqrt{v} \tag{3.2}$$

where ax =average standstill distance (m)

bx_add =additive part of desired safety distance (m)

bx_mult =multiplic part of desired safety distance

z =a value of range [0,1] which is normal distributed around 0.5 with a standard deviation of 0.15

v =vehicle speed (km/h)

Setting up traffic volume and traffic route for vehicle traffic/pedestrian traffic

Vehicle traffic can be created in any link in network. The volume and the route of vehicle flow is set in the function of "vehicle input" and "routing decisions and routes", respectively. VISSIM 5.40 has a sub-simulator which is named as VISWALK to control pedestrian behavior. Through this VISWALK, the volume and route of pedestrian flow is set. First, "pedestrian area" is built and then pedestrian volume and route are set in the function of "pedestrian input" and "routing decisions and routes", respectively.

Defining conflict behavior for vehicle & vehicle and vehicle & pedestrian

Conflict area is defined as the overlap area of two roads. VISSIM 5.40 applies two functions "priority rules" and "conflict areas" to control the travelling behavior approaching to the conflict area from different directions. These two functions have the same mechanisms on judging behavior that subjects in minor flow should yield to subject in major flow and apply gap acceptance behavior to cross or merge into major flow. Since the function of "conflict area" has better applicability and is recommended by VISSIM 5.40, it is selected in this research. In Figure 3.2, the overlap of the cross part in roads with green color and red color is the conflict area which is built by the function of "conflict area" in VISSIM 5.40. The green color represents that the road is major road having priority while the red color means that the road is the minor road without priority.

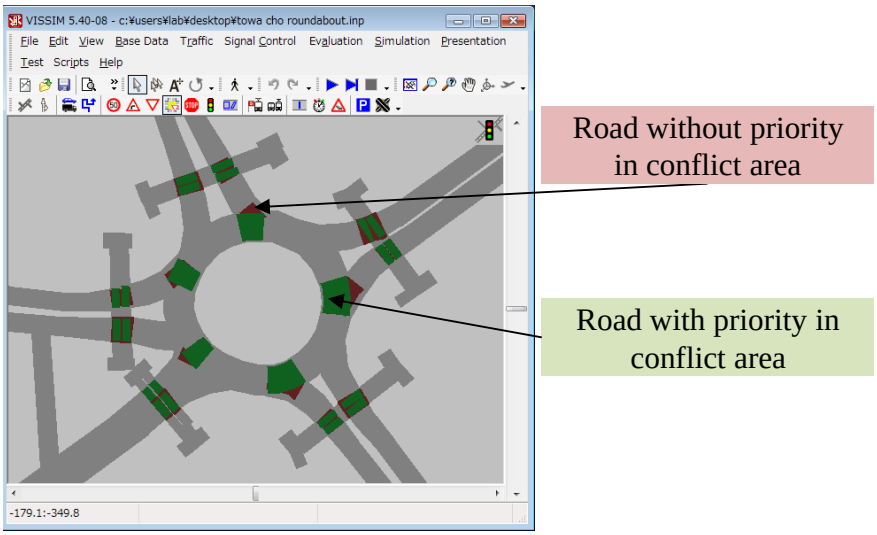

Figure 3.2 Conflict area at roundabout in simulation

In order to simply explain the mechanism of judging behavior, the illustration of conflict area is drawn at a T intersection as shown in Figure 3.3. Figure 3.3(a) shows the case at

time t and (b) shows the case at the time t_{edge} when minor flow subject arrives at the upstream edge B of the conflict area.

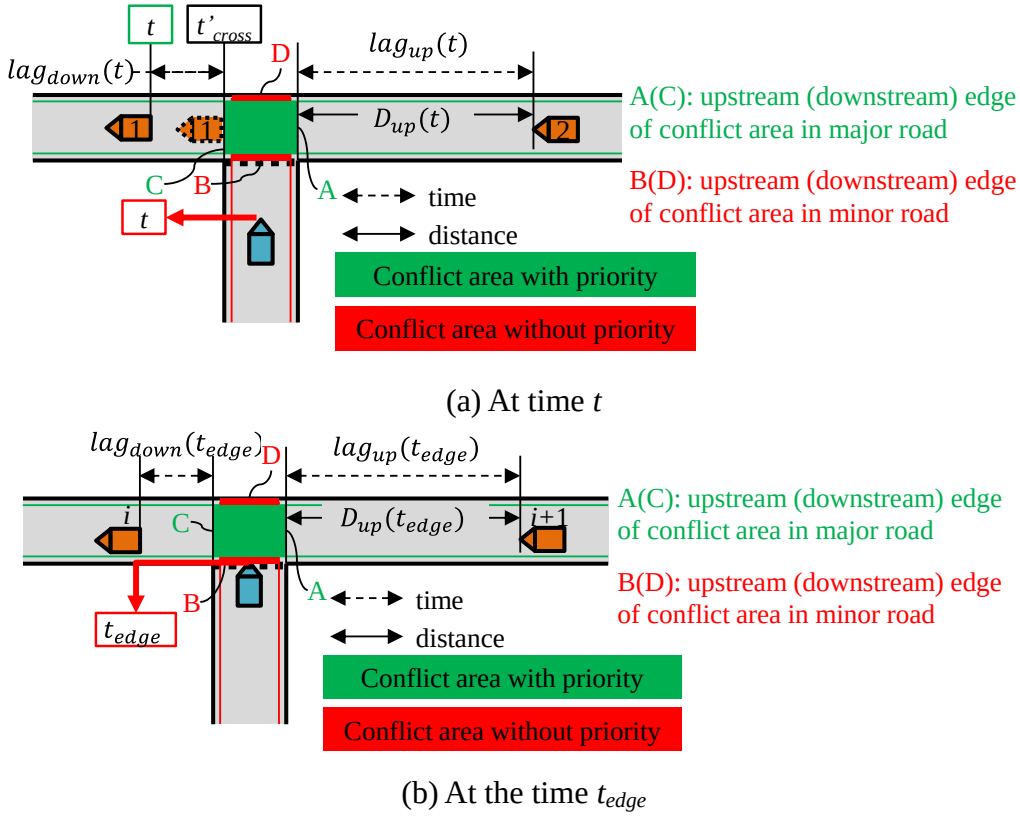

Figure 3.3 Example of conflict area at T intersection

In Figure 3.3(a), S2 is the subjects having passed conflict area in major road and the closest one from the downstream edge C of the conflict area. S1 is the subjects approaching to conflict area in major road and the closest one which has the minimum distance to the upstream edge A of conflict area.

The basic procedure is that at time t, subject in minor road first judges whether there is subject of major flow in the conflict area, if no, then continuing to judge the closest approaching subject (S2). And if "go" decision is satisfied, finally judging the closest passed subject (S1). In both "approaching group" and "passed group", the subjects are judged one by one from the closest one.

Regarding the procedure of judging the "approaching group", an expected time $lag_{up}(t)$ of S2 from the current time and the time crossing the upstream edge of the conflict area is calculated by the distance $D_{up}(t)$ between the current position and the upstream edge of

conflict area the current speed of S2. This $lag_{up}(t)$ is compared to the input time value "rear gap" in the function of "conflict area" and dependent on the result of comparison, subject in minor flow makes the decision stop/go regarding the closet vehicle. This procedure repeats until the minor flow subject makes "go" decision. Then, regarding the judging procedure to the "passed group", a passed time $lag_{down}(t)$ of S1 from the current time to the time S1 leaving the downstream edge of conflict area is calculated and compared to another input value "front gap" in the function of "conflict area". This procedure will also be repeated under the condition the "go" decision for "approaching group" is available. When "go" decisions are made for both "approaching group" and "passed group", the minor flow subject will cross or merge into major flow. The judging procedure at the time when the minor flow subject arrives at the upstream edge B of the conflict area is shown as a flowchart in Figure 3.4.

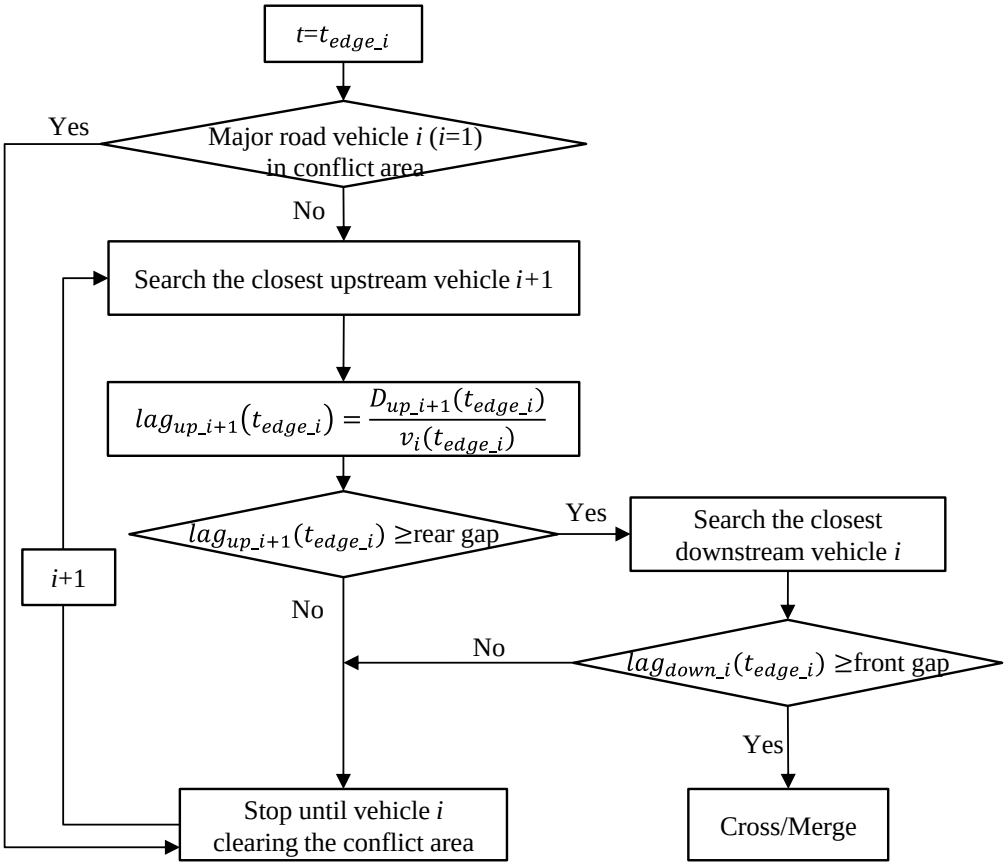

Figure 3.4 Flowchart of judgment procedure of subject in minor flow

In the function of "conflict area", five parameters are needed to calibrate, i.e. "visibility", "front gap", "rear gap", "safety distance factor" and "additional stop distance". The

“visibility” is defined as the maximum distance from where an approaching vehicle can see vehicles on the other link. The “front gap” is defined as the minimum gap in seconds between the rear end of a vehicle on the main road and the front end of a vehicle on the minor road. The “rear gap” is defined as the minimum gap in seconds between the rear end of a vehicle on the minor road and the front end of a vehicle on the major road, i.e. the time that a yielding vehicle must provide after it has left the conflict area before a vehicle with right of way enters the conflict area. The “safety distance factor” is multiplied with the normal desired safety distance of a vehicle on the major road to determine the minimum headway which a vehicle from the minor road must provide at the moment when it is completely inside the merging conflict area. The “additional stop distance” is defined as the distance that moves the stop line upstream of the conflict area. As a result, yielding vehicles stop further away from the conflict and thus also need to travel a longer distance until they pass the conflict area.

3.2 Application of simulation

Parameters in simulations are needed to calibrate for ensuring that simulation output can reflect real situations. A study site, i.e. Towa-cho roundabout in Iida City, Nagano Prefecture, Japan is selected for this simulation calibration. Since it is difficult to observe entry capacity at this study site, the headway distribution from simulation output is compared to empirical results for validating the simulation after parameter calibration.

3.2.1 Parameters to be calibrated

The input parameters which are needed to calibrate are shown in Table 3.1. Among these parameters, some of them are set by default values, e.g. look ahead distance in the function of “car-following model”. And others, e.g. distribution of desired acceleration are calibrated by empirical data. The parameters which are given default values are shown in Table 3.2.

Table 3.1 Parameters to be calibrated in VISSIM 5.40

	Functions	Vehicles/Pedestrians		Parameters to be calibrated
1	Functions of acceleration(acc) /deceleration(dec)	Vehicles/Pedestrians	a	Distribution of desired acc
			b	Distribution of maximum acc
			c	Distribution of desired dec
			d	Distribution of maximum dec
2	Desired speed	Vehicles/Pedestrians	a	Distribution of desired speed
3	Car-following model (Wiedemann 74 models)	Vehicles	a*	Look ahead distance (m)
			b*	Look back distance (m)
			c*	Temporary lack of attention
			d	Average standstill distance (m)
			e	Additive part of safety distance (m)
			f	Multiplic. part of safety distance
4	Conflict area	Vehicles/Pedestrians	a*	Visibility (m)
			b*	Front gap (sec)
			c	Rear gap (sec)
			d	Safety distance factor
			e	Additional stop distance (m)

*: Parameters to be set by default values

Table 3.2 Parameters which are set by default values

	Parameters	Default values		Parameters	Default values
3.a	Look ahead distance (m)	100	3.b	Look back distance (m)	100
3.c	Temporary lack of attention	0	4.a	Visibility (m)	100
4.d	Safety distance factor	1.5			

3.2.2 Data collection

In order to calibrate parameters, empirical data, e.g. speed, acceleration and gap of vehicles and pedestrians and headway is collected at two study sites in Japan. Video surveys were

conducted at these two sites in 2010 and 2013. Raw trajectory data is first collected from the videos and then, the necessary data, e.g. speed is obtained by the analyzing software "TrafficAnalyzer" (Suzuki and Nakamura, 2006). After inputting the empirical data in simulation, headway distribution of vehicles is output to compare to empirical results for validation.

Study sites

Towa-cho roundabout is the first case which was converted from a signalized intersection to a roundabout in 2013 in Japan. The layout of Towa-cho roundabout is shown in Figure 3.5.

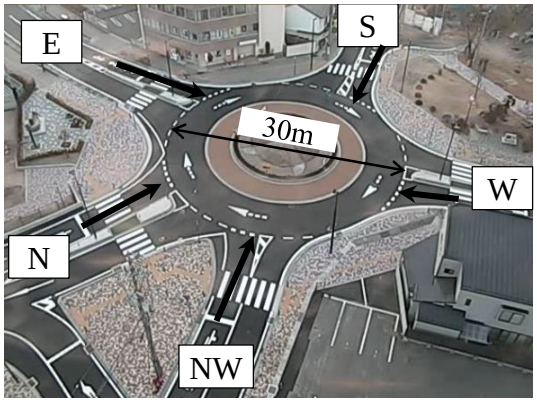

Figure 3.5 Layout of Towa-cho roundabout

Towa-cho roundabout is a five-leg roundabout with diameter of 30m. Physical splitter islands exist at Entries N, E and W. geometric elements of crosswalk and the space of one-vehicle length are satisfied at each entry/exit.

A video survey was conducted at Towa-cho roundabout on 9th May 2013 (Thu), from 7:00 to 19:00. Table 3.3 shows the O/D matrices of vehicle and pedestrian demand in 12 h. For pedestrians, near-side is defined as the left curb side of the crosswalk according to left-hand traffic in Japan whereas far-side is the right curb side of the crosswalk.

Table 3.3 Traffic Demand of Towa-cho roundabout in 12 hours (6:00~18:00)

(a) Vehicle Demand: 12 hours

Origin \ Destination	N	E	S	W	NW
N		161	797	404	14
E	85		160	1163	152
S	666	203		494	459
W	481	1226	338		332
NW	2	116	378	90	

(b) Pedestrian Demand: 12 hours

	N	E	S	W	NW
From near side	32	65	59	57	50
From far side	158	45	29	54	36

In the period of the observation, it was also under the unsaturated traffic condition. In 12 hours, 1,226 vehicles entered into roundabout from Entry West, which was the highest in all approaches. Regarding circulating flow, number of vehicles passing in front of Entry NW was the highest with the number of 3,391 vehicles. Considering both entry and circulating flows, Entry West was selected as the subject approach for collecting data with the circulating demand of 1,753 vehicles/12 hours.

Data processing

Vehicle and Pedestrian maneuvers which include the positions and timings are extracted from video data by using video image processing system *TrafficAnalyzer* (Suzuki and Nakamura, 2006). The position of each vehicle and pedestrian is extracted every 0.5 second, then their video coordinates are converted to the global coordinates by projective transformation. The point where the right-rear wheel is touching the ground is the reference observation point for all vehicles. All video observations were done from high buildings around the intersections, thus for all video tapes, the observation angle is large. This allows us to track the right rear wheel of all turning vehicles without facing any problems. By assuming the dimension of turning vehicles, the observed trajectory based on

the right-rear wheel is transformed to the trajectory which corresponds to the center-front of the vehicle. The assumed vehicle size for passenger cars is 4.7m*1.8m (length*width), while for the heavy vehicles is 6m*2.2m (length*width). The transformed trajectories are smoothened by Kalman smoothing method. Figure 3.6 shows the data processing procedure using *TrafficAnalyzer*.

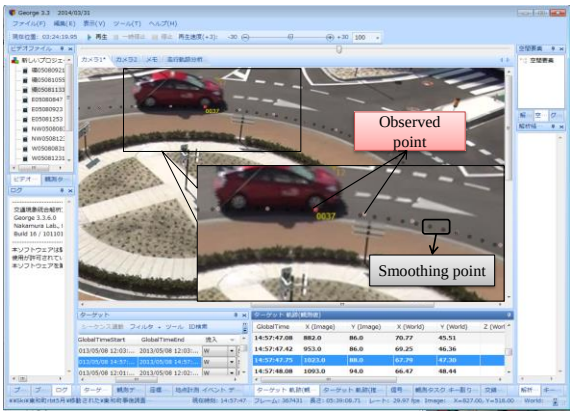

Figure 3.6 Points used in data collection and processing (at Towa-cho Roundabout)

A series of information of observed subjects, e.g. time, coordination, acceleration/deceleration, speed and space can be obtained by this software.

Collection acceleration/deceleration and speed

Collection of acceleration/deceleration regarding vehicles

Acceleration and deceleration are collected on the free flow vehicles which are defined as the vehicle not influenced by others. The free flow vehicles are observed between the section A which is 40m upstream from the stop line before entering roundabout and the section B which is 5m after exiting downstream crosswalk. The illustration of the observation area for vehicles from West to East is shown at Towa-cho roundabout as an example in Figure 3.7.

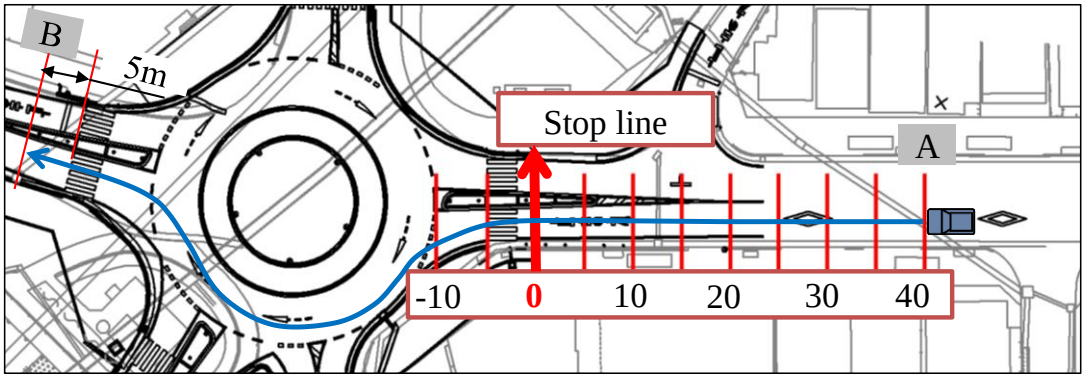

Figure 3.7 The illustration of observation area (W→E as an example)

Thus, Figure 3.8 shows an example of acceleration/deceleration procedure of a free flow vehicle between section A and section B at Towa-cho roundabout.

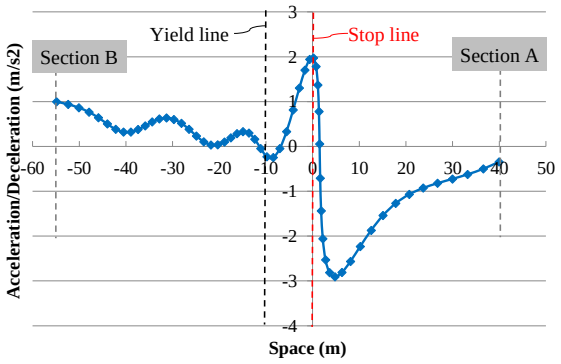

Figure 3.8 An example of acceleration/deceleration procedure of a free flow vehicle at Towa-cho roundabout (W→E)

It is found that the acceleration is reduced during approaching to roundabout and the maximum deceleration appears near the stop line ("0" in the space axis). The vehicle accelerates after passing the stop line, and decelerates again during approaching to the yield line. After passing the yield line, the vehicle accelerates under a low value until leaving roundabout.

The observation of free flow vehicles is conducted from 14:30 to 16:30 at all entries. In these 2 hours, 135 vehicles are observed. The maximum acceleration and absolute value of deceleration of each observed vehicle is collected and the distributions of the maximum values are shown in Figure 3.9.

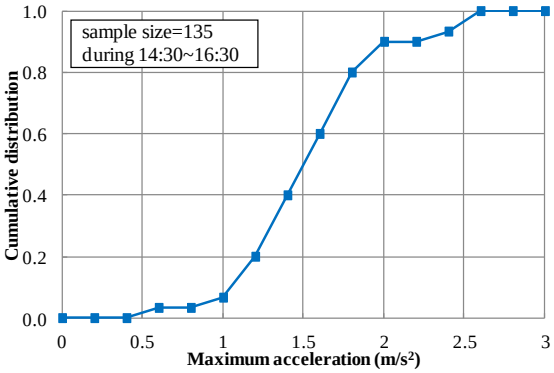

(a) Distribution of maximum acceleration

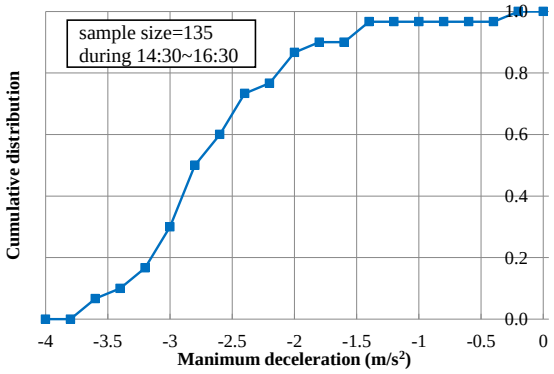

(b) Distribution of maximum deceleration

Figure 3.9 Distributions of maximum acceleration and deceleration

There is no clearly The definition of "desired acceleration/deceleration" is not clearly described in the VISSIM 5.40 manual.

The definition of "desired acceleration/deceleration" is not clearly described in the VISSIM 5.40 manual. Dependent on the description in the manual, the "desired acceleration/deceleration" is the value commonly utilized in most cases, thus, the average value is selected to represent the "desired acceleration/deceleration". The average acceleration and deceleration of a vehicle are calculated to represent the desired values. The distribution of average acceleration and deceleration is shown in Figure 3.10.

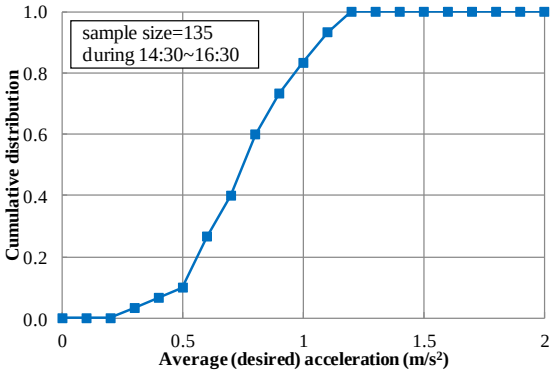

(a) Distribution of desired acceleration

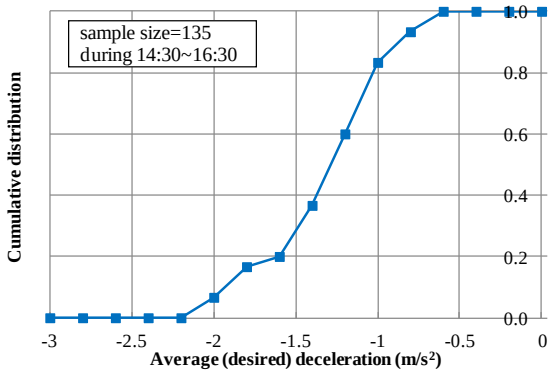

(b) Distribution of average deceleration

Figure 3.10 Distributions of average acceleration and deceleration

Collection of speed

Speed is also collected on the free flow vehicles and in the same observation area as the acceleration/deceleration collection. Figure 3.11 shows an example of whole speed profile of a vehicle from the section A to the section B at Towa-cho roundabout.

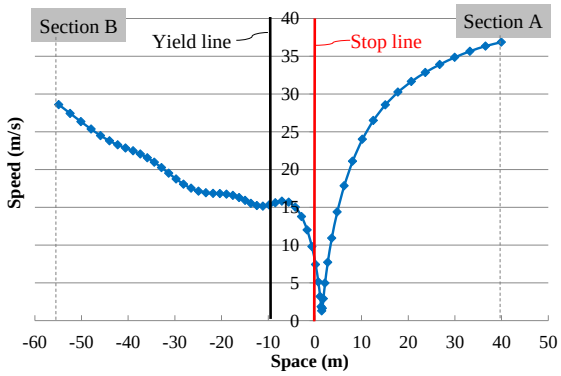

Figure 3.11 An example of whole speed profile of a vehicle in observation area

At roundabout, vehicles are requested to decelerate and stop twice near the stop line and yield line for giving priorities to pedestrians and circulating vehicles, respectively, no matter pedestrians and circulating vehicles existing or not. This can be observed through speed profile which is shown in Figure 3.11. It can also be found that vehicles travelling in circulating roadway with a lower speed than that in entry road due to the geometric characteristic of circle road. Only the function of "desired speed" cannot realize the decelerating behavior in circulating roadway. Thus, the function of "speed reduction" is utilized. The input parameter of the function of "speed reduction" is similar as the function of "desired speed" which a distribution of speed is necessary to input. Accordingly, the average entry speed v_{avge} between the section A and the upstream yield line in the observation area is calculated to input in the function of "desired speed" and the average circulating speed v_{avgc} between the upstream yield line and the downstream yield line is calculated to input in the function of "speed reduction". The distribution of the average (desired) entering and circulating speed is shown in Figure 3.12(a) and (b), respectively.

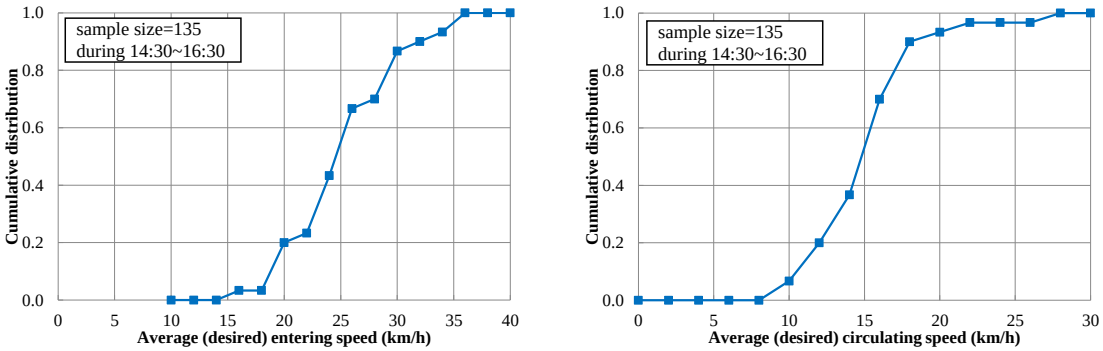

(a) Entering speed (b) Circulating speed

Figure 3.12 Distribution of average (desired) speed before reaching the stop line

Collection regarding pedestrians

The procedure of collecting acceleration/deceleration and speed is similar as the collection for vehicles. Pedestrian trajectory is observed between section C and section D. Sections C and D are 5m from the curbs of crosswalk along the pedestrian trajectory before and after crossing, respectively. The illustration of the observation area for one example of pedestrian is shown in Figure 3.13.

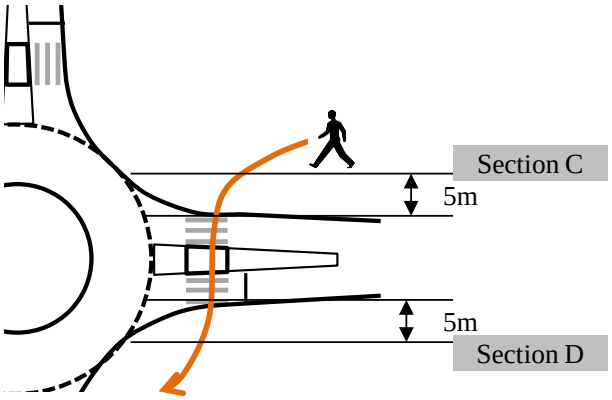

Figure 3.13 Illustration of pedestrian observation area of an example

Figure 3.14 shows travelling behavior of a pedestrian in observation area at Towa-cho roundabout. Figure 3.14(a) is an example of acceleration/deceleration profile of a pedestrian and (b) shows an example of speed profile of this pedestrian.

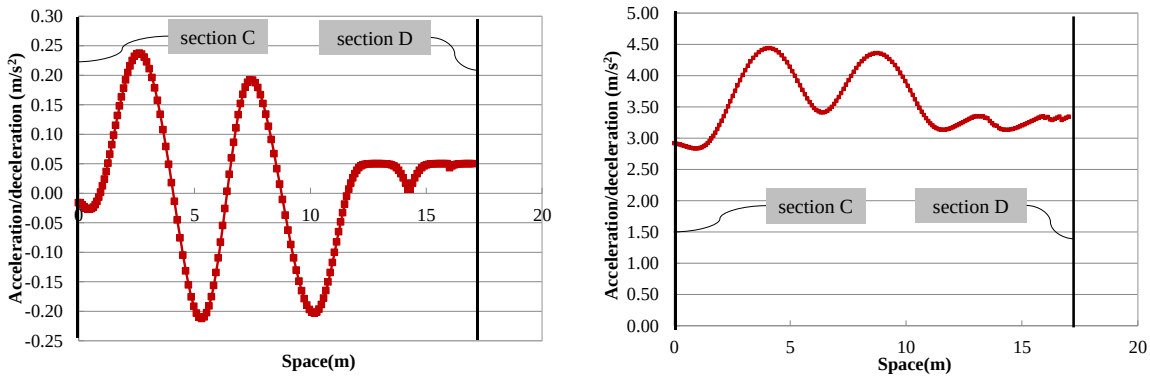

(a) Acceleration/Deceleration (b) Speed profile

Figure 3.14 Example of changing of acceleration/deceleration and speed of a pedestrian in observation area at Towa-cho roundabout

Based on this example, it is found that the acceleration/deceleration and speed of pedestrian is relatively stable comparing to that of vehicles.

The maximum acceleration and deceleration of each observed pedestrian is collected during the period of 7:00~10:00 and 15:00~17:00. The distributions of the maximum values are shown in Figure 3.15.

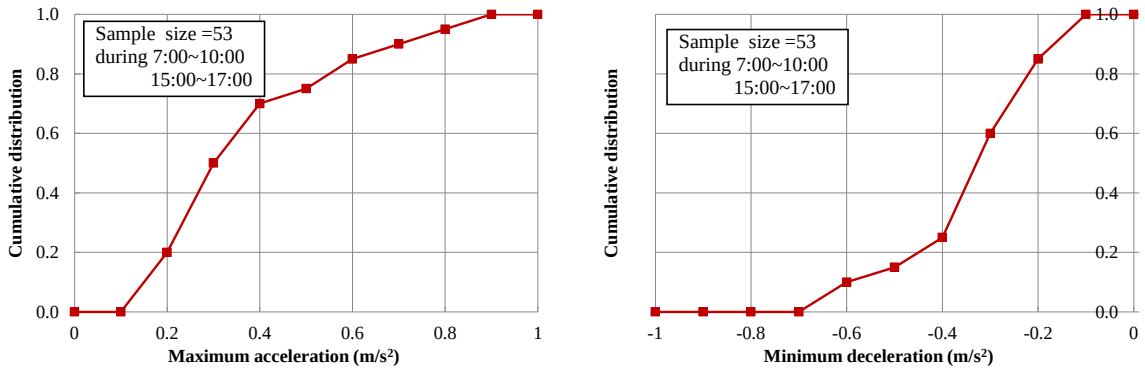

(a) Maximum acceleration (b) Minimum deceleration

Figure 3.15 Distributions of maximum acceleration and deceleration

The average acceleration and deceleration of a vehicle are calculated to represent the desired values. The distribution of average (desired) acceleration and deceleration is shown in Figure 3.16.

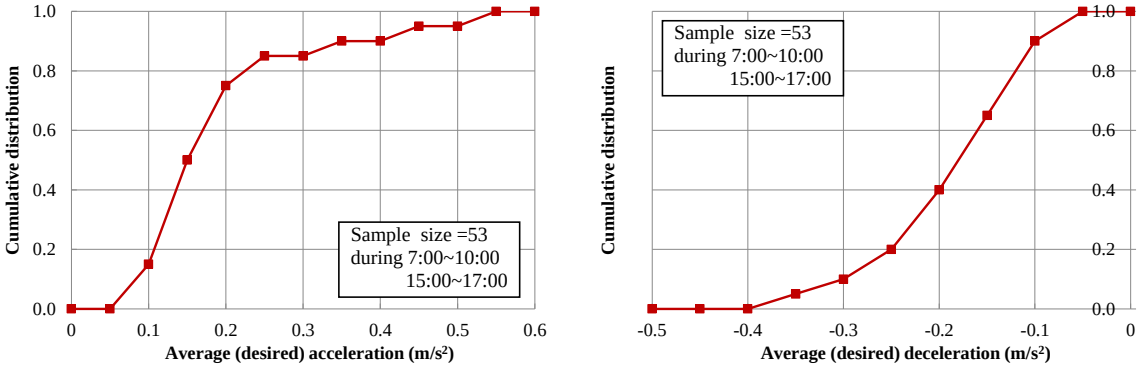

(a) Distribution of average acceleration (b) Distribution of average deceleration

Figure 3.16 Distributions of average acceleration and deceleration

And the distribution of the average crossing speed of pedestrians is shown in Figure 3.17.

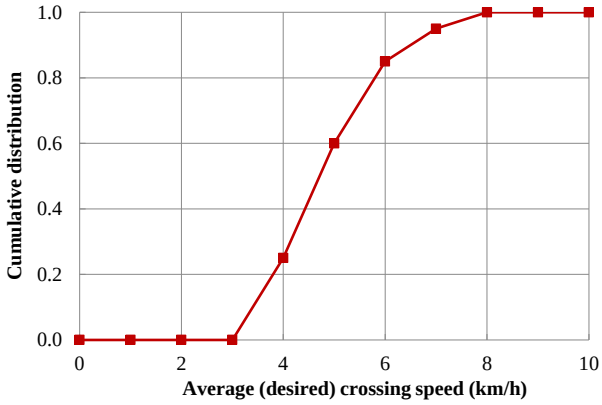

Figure 3.17 Distribution of average crossing speed

Collection of parameters in "car-following model"

In gap acceptance theory, three headway parameters are included, i.e. critical gap t_c in circulating flow, follow-up time t_f of entry vehicles and minimum headways of circulating vehicles. Among these parameters, t_c is the value which needs to be calculated dependent on gaps of circulating vehicles whereas t_f and τ are the values directly from observation. The values of t_f and τ are actually related to the minimum headway and realized by the function of "car-following model" in simulation. In "Wiedemann 74 model" which is selected in this research, headway is described as distance *d* between vehicles and three parameters are necessary to be calibrated, i.e. "average standstill distance" *ax*, "additive part of safety distance" *bx_add* and "multiplic. part of safety distance" *bx_mult* (Based on the Equations 3.1 and 3.2).

$$d = ax + bx \tag{3.1}$$

$$bx = (bx\_add + bx\_mult * z)\sqrt{v} \tag{3.2}$$

where ax =average standstill distance (m)

bx_add =additive part of desired safety distance (m)

bx_mult =multiplic part of desired safety distance

z =a value of range [0,1] which is normal distributed around 0.5 with a standard deviation of 0.15

v =vehicle speed (km/h)

Dependent on the empirical data, t_f/τ and speed v of vehicles is collected for the calibration of d. The parameter ax is collected by the average distance between two queuing vehicles from empirical data. Then, the parameters of bx_add and bx_mult are adjusted to obtain the value of d based on Equations 3.1 and 3.2.

Collection of t_f and τ

As shown in Figure 3.18, the time of the front edge of vehicle passing the section E and F is collected. The section E is near the yield line and the section F is the connection of central point of roundabout and middle point of the yield line at the subject entry. Time t_i, $i \in n$ and t_j, $j \in n$ is defined as the passing time for entry vehicles and circulating vehicles, respectively. Based on the passing time, the headway of two successive vehicles is calculated as t_{i+1}-t_i and t_{j+1}-t_j.

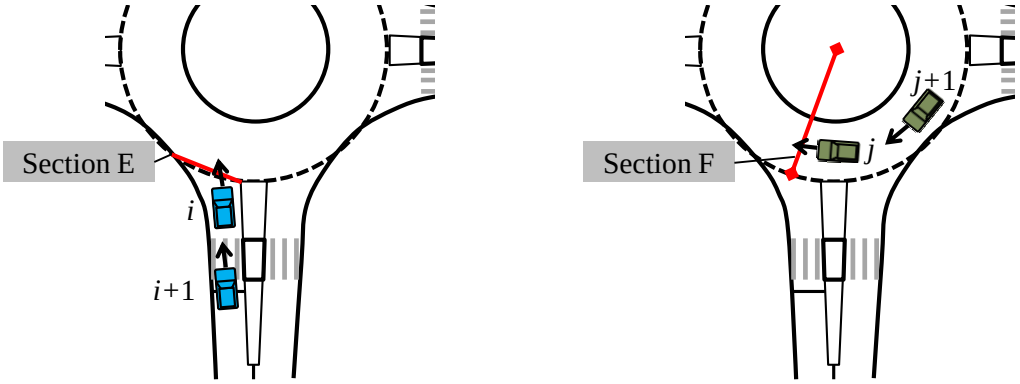

(a) Collection of headway of entry vehicles

(b) Collection of headway of circulating vehicles

Figure 3.18 Illustration of calculation of headway of entry and circulating vehicles

The headway of entry vehicles is collected at Entry W and the headway of circulating

vehicles is collected for the vehicles passing in front of Entry W during the period of 7:00~9:00. Then, the distribution of headway of entry vehicles circulating vehicles is calculated for the values smaller than 5sec (t<5sec). The results are shown in Figure 3.19. The average value of each distribution is selected as the input value of t_f and τ, i.e. t_f =3.1sec and τ=2.6sec.

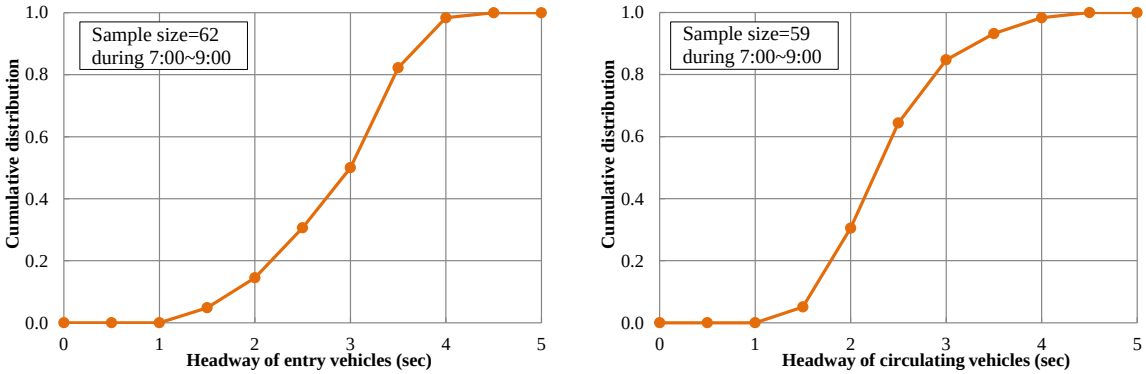

(a) Headway distribution of entry vehicles

(b) Headway distribution of circulating vehicles

Figure 3.19 Distribution of headway of vehicles

In addition, *ax* is collected by the distance between two queuing entry vehicles, from the rear edge of vehicle *i* and the front edge of vehicle *i*+1, during the period of 7:00~9:00. Since circulating vehicles did not queue in the observation, the value of *ax* which is calculated from entry vehicles is also applied for setting car-following behavior of circulating vehicles. The result of distribution of *ax* is shown in Figure 3.20. The average value is selected as the input value, *ax*=2.1m.

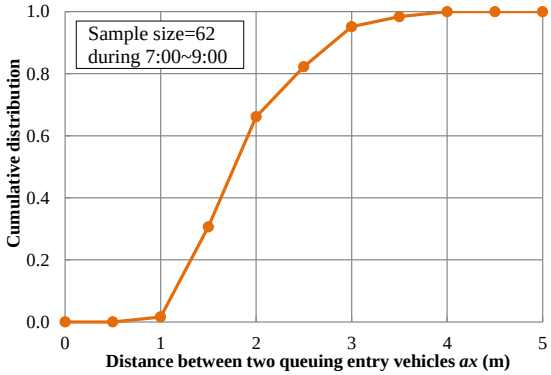

Figure 3.20 Distribution of *ax* between two queuing entry vehicles

After adjusting the values of *bx_add* and *bx_mult*, the input values of parameters in

"Wiedemann 74 model" are shown in Table 3.4.

Table 3.4 Values of parameters for inputting in "Wiedemann 74 model"

Parameters and variables	Regarding entry vehicles (t_f=3.10sec)	Regarding circulating vehicles (τ=2.60sec)
$d=t\cdot v-L_v$ (m)	16.5	5.83
ax (m)	2.10	2.10
v (km/h)	25.0	15.0
z	0.50	0.50
bx_add	3.12	1.04
bx_mult	4.68	1.56

L_v: the average length of vehicles=4.5m, *v*=25km/h and 15km/h (average value of desired speed) for entry and circulating vehicles, respectively

Collection of parameters in the function of "conflict area"

The function of "conflict area" is utilized to realize conflict behavior in simulation and three parameters, i.e. front gap, rear gap and additional stop distance. In gap acceptance theory, the conflict behavior is reflected by the parameter of critical gap t_c. However, the parameter of t_c cannot be directly input in simulation. Based on the definition and function of "front gap" and "rear gap", "front gap" can be calculated as the minimum time which can be used for a vehicle in minor flow to cross or enter into the major flow lag after a vehicle in major flow leaving the conflict area, while "rear gap" can be calculated as the minimum time lag of vehicles in major road entering into conflict area for a vehicle of minor flow crossing or entering into the major flow. Based on this, "front gap" and "rear gap" can be related to t_c and the relationship of these headway parameters is shown in Figure 3.21.

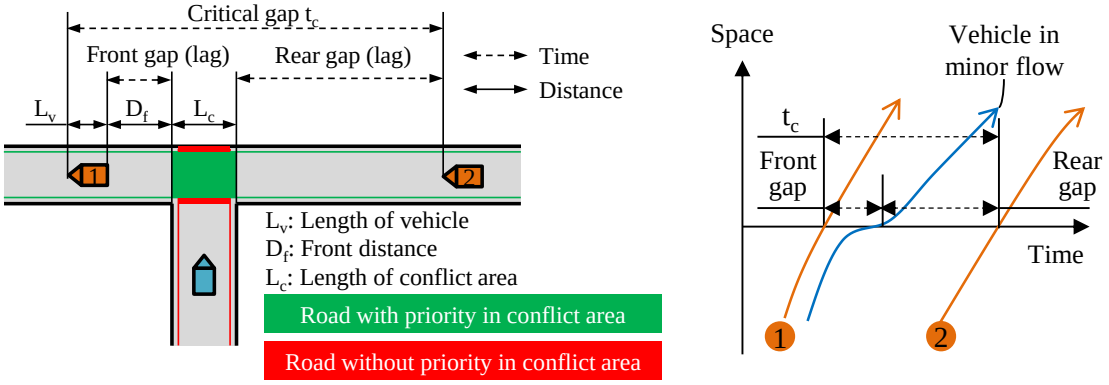

Figure 3.21 The relationship of t_c and "front/rear gap"

Considering the utilization of t_c in the later chapter regarding a theoretical model, the value of t_c is calculated from empirical data and transferring to front/rear gap based on the relationship between them. The parameter of D_f in Figure 3.21 is defined as the minimum distance between the subject in major road which has crossed conflict area and the downstream edge of conflict area in major road. This D_f is utilized to calculate the value of "front gap". Dependent on relationship of headway parameters and the value of t_c and "front gap", the value of "rear gap" is calculated.

Collection of t_c

Aggregating gaps by the interval of 1 sec, the value of t_c is commonly calculated by two methods based on the observed gaps, "probability method" and "cumulative distribution method". In "probability method", the probability of accepted gap of t sec is calculated by the number of accepted gap of t sec in the total number of accepted and rejected gaps of t sec as shown in Equation 3.3. And the illustration of this method is shown in Figure 3.22(a).

$$\textit{Probability of accepted gap} = \frac{n_{accepted(t)}}{n_{accepted(t)} + n_{rejected(t)}} \quad (t=1, 2, \ldots n \text{ sec}) \qquad 3.3$$

where $n_{accepted(t)}$= Number of accepted gaps of t sec

$n_{rejected(t)}$= Number of rejected gaps of t sec

The critical gap in this method is calculated as the value which the probability is equal to 0.5. The accuracy of calculation by this method cannot be sure under the condition of limited number of samples and the position of "0.5 probability" is significantly influenced

by the value of n which represents the range of observed gaps.

The other one "cumulative distribution method" is not limited by the number of samples and widely applied in guidelines and manuals, e.g. NCHRP (2009). In this method, the cumulative distributions of accepted gaps and rejected gaps are calculated by Equation 3.4.

$$\textit{Cumulative distribution of accepted(rejected) gap}=\frac{n_{accepted/\,rejected(<t)}}{N_{accepted/\,rejected}} \quad (t=1, 2, \ldots n \text{ sec}) \qquad 3.4$$

where $n_{accepted/rejected(<t)}$= Number of accepted/rejected gaps which are shorter than t sec

$N_{accepted/rejected}$= Total number of accepted/rejected gaps in the observation

The illustration of this method is shown in Figure 3.22(b). Two distributions have a crossing point in the procedure of gap changing and the value of t_c is calculated as the gap size at this crossing point.

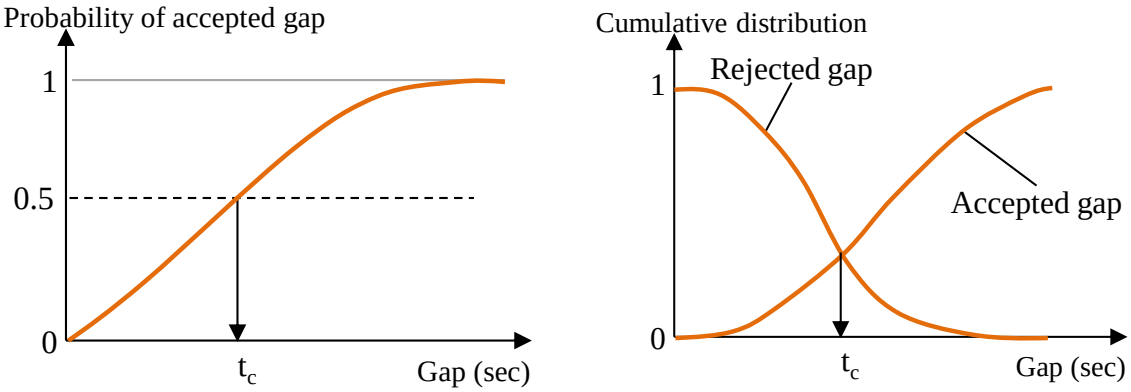

(a) Probability method **(b) Cumulative distribution method**

Figure 3.22 Calculation of t_c

In this research, the "cumulative distribution method" is applied since the number of samples is not sufficient to ensure the accuracy of the result from the "probability method".

Either accepted gap or rejected gap is the headway of circulating vehicles, which is collected as the time difference of two successive circulating vehicles passing one section F in circulating roadway. The accepted gap and rejected gap is collected for the circulating vehicles passing in front of Entry W during the period of 7:00~9:00 (peak hour). The gaps shorter than 10sec are selected for the calculation of accepted gap and rejected gap. The result is shown in Figure 3.23 and the value of t_c is calculated to be 4.6sec.

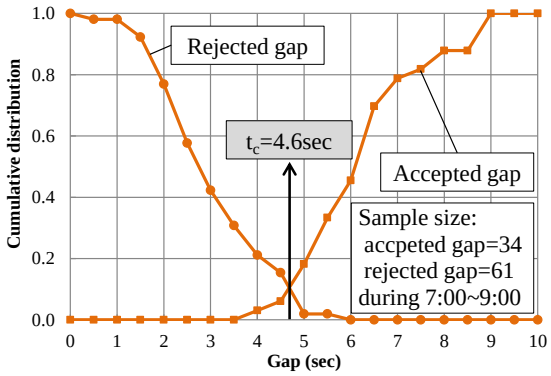

Figure 3.23 Results of t_c in front of Entry W

Calculation of front gap and rear gap in simulation

The value of "front gap" is calculated by D_f and speed of major flow subjects, i.e. circulating vehicles and pedestrians. The value of D_f is assumed to be 2.5m and 1.5m for circulating vehicles and pedestrians, respectively. Based on the speed from empirical data, the value of "front gap" is calculated to 0.5sec for circulating vehicles and 1.35s for pedestrians. Then, the value of "rear gap" can be calculated also which is equal to 2.18sec. Regarding the pedestrians, since the pedestrian volume in this site is in the low level, the critical gap for pedestrians cannot be collected by empirical data. Thus, the "rear gap" for pedestrians is input by the default value which is equal to 3.1sec. By applying the default value of rear gap (3.1sec), pedestrians will be reacted before crossing the conflict area which is defined as the overlap of crosswalk and entry/exit roadway. The input values of parameters regarding the function of "conflict area" are shown in Table 3.5.

Table 3.5 Input values of parameters in the function of "conflict area"

Parameters	The conflict between entry and circulating vehicles	The conflict between entry/exit vehicles and pedestrians
Visibility (m)	100	100
Front gap (sec)	0.500	1.35
Rear gap (sec)	2.18	3.10
Safety distance factor	1.50	1.50
Additional stop distance (m)	0	5.00

3.2.3 Validation

Since the Towa-cho roundabout is operated under the unsaturated situation, entry capacity cannot be observed and utilized for validation. Based on gap acceptance theory, entry capacity is decided by headway distribution $h(t)$ of major flow and two parameters in model of E(t), i.e. t_c and t_f. Thus, distributions of these variables are utilized for validation. Regarding circulating vehicles, the distribution of headway of circulating vehicles and entry vehicles and the distribution of accepted/rejected are examined under the condition without pedestrians. For pedestrians, since accepted/rejected gap cannot be observed in study sites, only the distribution of headway of pedestrians under the condition without circulating vehicles is examined.

The vehicles during morning peak, i.e. 8:00~9:00 and the pedestrians during the period of 8:00~9:00 at the study site are observed for validation. Table 3.6 shows the O/D matrix of vehicle and pedestrian traffic during each period.

Table 3.6 Traffic Demand of vehicles and pedestrians in 1 hour

(a) Vehicle OD demand in 1 hour of morning peak (8:00~9:00)

Origin \ Destination	N	E	S	W	NW
N		10	81	48	0
E	9		9	175	14
S	56	13		41	27
W	63	76	28		6
NW	0	2	24	2	

(B) pedestrian demand in 1 hour of morning peak (7:00~8:00)

	N	E	S	W	NW
From near-side	2	10	9	8	3
From far-side	10	9	8	10	4

The validation was conducted through comparing the simulated result to the observed result. The entry vehicles from Entry W and circulating vehicles passing in front of Entry W in empirical data and simulation are selected for calculating the distributions. The

"two-sample Kolmogorov-Smirnov statistic test" (K-S test) is calculated for verifying the goodness of fit between simulation output and observation. In K-S test, D_i which represents the absolute value of the difference of two distributions at each aggregation level *i* is first calculated by Equation 3.5.

$$D_{n,n'} = \left| F_{1,n}(sim) - F_{2,n'}(obs) \right| \tag{3.5}$$

where $F_{1,n}(sim)$= The empirical distribution function of simulation

$F_{2,n'}(obs)$= The empirical distribution function of observation

n= Number of samples in simulation

n'= Number of samples in observation

The value $maxD_{n.n'}$ is defined as the maximum value of $D_{n,n'}$. The hypothesis in "two-sample K-S test" is that if $maxD_{n,n'}$<critical value, two distributions have good fitness; else, null hypothesis. In this research, the K-S test value at 95% confidence interval is selected as the critical value. The critical value varies dependent on the number of samples and is calculated by Equation 3.6 when number of samples is larger than 12 (Kolmogorov, A., 1933, Smirnov, N., 1948 and Justel, A. et al, 1997)

$$D_{95\%} = 1.36\sqrt{\frac{n+n'}{nn'}} \tag{3.6}$$

where $D_{95\%}$= The critical value at the 95% confidence interval

1.36= The coefficient at the 95% confidence interval

The estimated and observed results regarding the headway distribution of circulating/entry vehicles are shown in Figure 3.24. And the results of distributions of headway of pedestrians are shown in Figure 3.25.

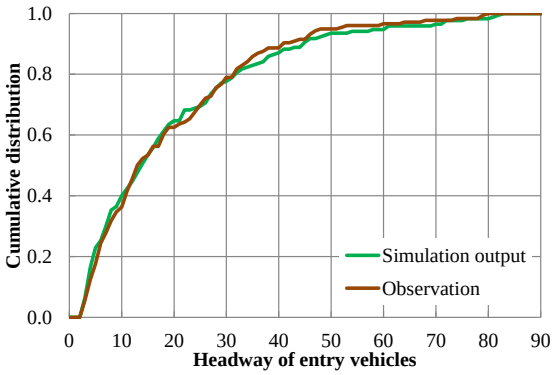

Number of samples	
Observation	Simulation
172	172
$D_{95\%}$=0.147	
$maxD_{n,n'}$=0.0342	

(a) Headway distributions of entry vehicles from Entry W

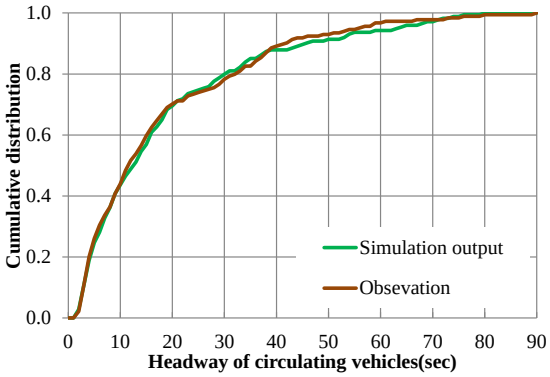

Number of samples	
Observation	Simulation
119	119
$D_{95\%}$=0.176	
$maxD_{n,n'}$=0.0563	

(b) Headway distributions of circulating vehicles passing in front of Entry W

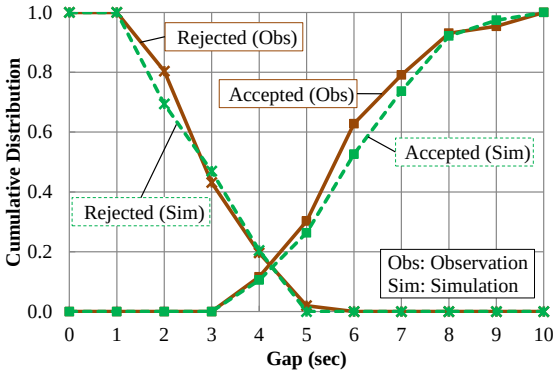

Number of samples			
Accepted gap		Rejected gap	
Obs	Sim	Obs	Sim
27	20	27	25
$D_{95\%}$=0.401		$D_{95\%}$=0.377	
$maxD_{n,n'}$=0.101		$maxD_{n,n'}$=0.0648	

(c) Distributions of accepted gap and rejected gap

Figure 3.24 Validation of simulation regarding vehicle traffic

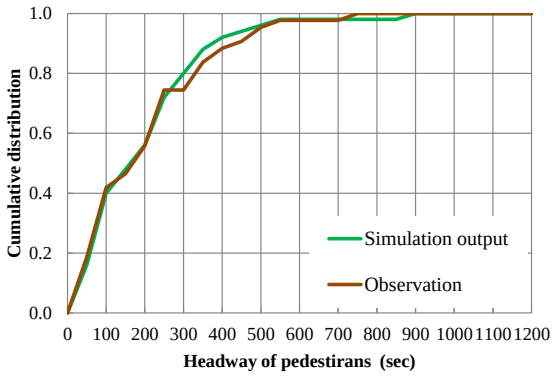

Number of samples	
Observation	Simulation
81	81
$D_{95\%}$=0.214	
$maxD_{n,n'}$=0.0493	

Figure 3.25 Validation of simulation regarding headway of pedestrians

It is found that headway distributions of vehicles and pedestrians follow the negative exponential distribution in simulation. For each result, the hypothesis $maxD_{n,n'} < D_{95\%}$ is satisfied, thus, it can be concluded that there is no significant difference between the results of observation and simulation and it is implied that all parameters are well calibrated.

3.3 Hypothesis and simulation design

The analysis on examining the impact of influencing factors is conducted at a four-leg roundabout with diameter of 27m. Geometry layout of this roundabout is shown in Figure 3.26.

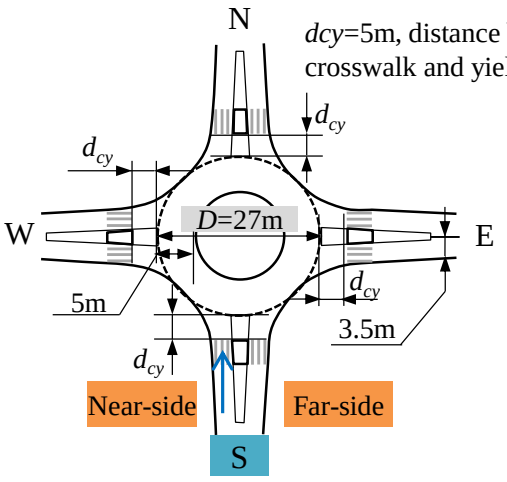

Figure 3.26 Layout of roundabout to be analyzed in this research

The angle of two adjacent approaches is set to be 90 degree. Crosswalk with width of 3m is set at each entry/exit and space between downstream crosswalk and yield line is set to 5m. The width of entry and exit roads at approach is set to 3.5m and width of circulating

roadway is set to 5m. According to these geometry information, roundabout is built in VISSIM by the functions of “links” and “connections”. Figure 3.27 shows the configuration of this roundabout which is drawn in simulation. Blue lines and pink lines represent link and connection, respectively. The length of link of entry/exit road is set to 100m.

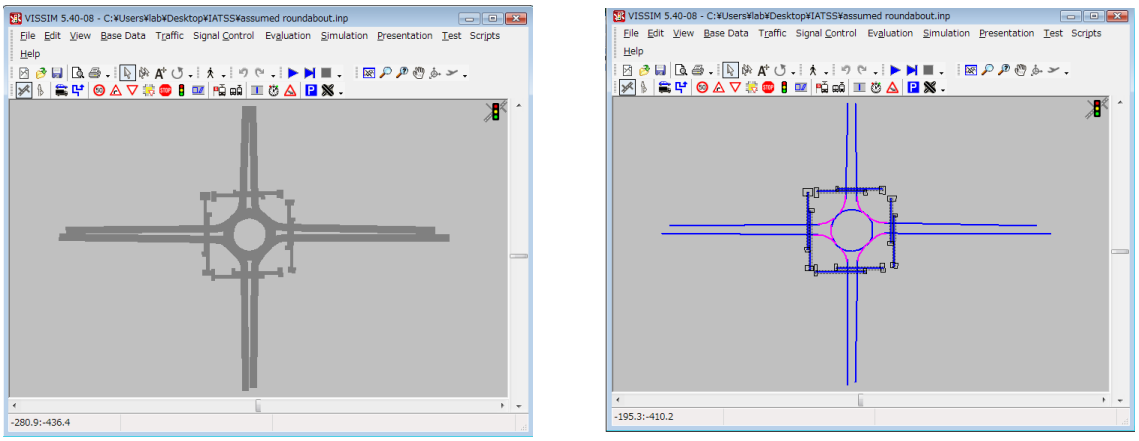

(a) 2D vision in simulation (b) Links and connections of roundabout

Figure 3.27 Configuration of roundabout in VISSIM 5.40

3.3.1 Hypothesis of influencing factors regarding pedestrians

Pedestrian approaching sides

Pedestrian approaching side is classified into near-side and far-side. Near-side is the left curb side of the crosswalk according to left-hand traffic in Japan whereas far-side is the right curb side of the crosswalk as illustrated in Figure 3.28. Far-side directional ratio r_{far} is defined as the proportion of far-side pedestrians in total pedestrian demand regarding one entry. At Entry S, three ratios are examined, 0, 0.5, 1. The far ratio at other entries is assumed to be identical and the value of 0.5 is given. Pedestrians from different directions are set in simulation to walk in separate lines in crosswalk as shown in Figure 3.28.

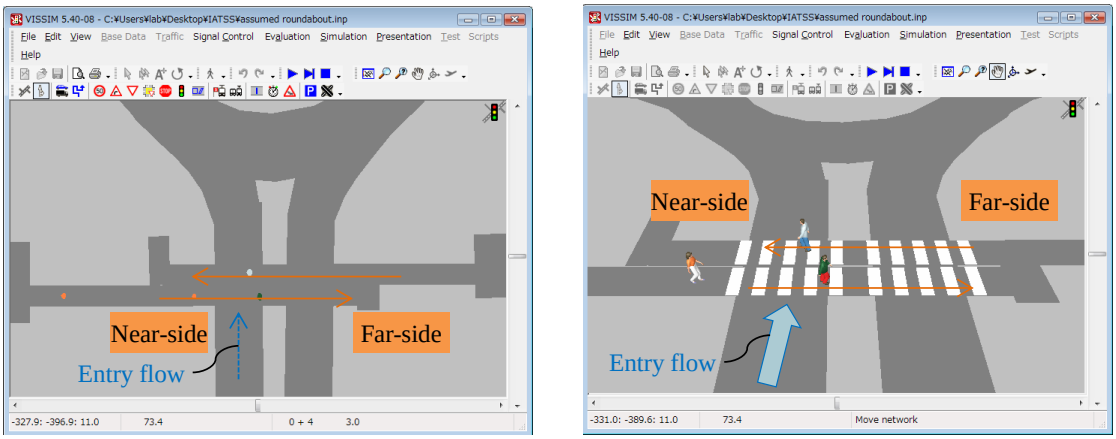

(a) 2D vision (b) 3D vision

Figure 3.28 Screenshot of pedestrians from different directions walking in different lines in simulation

With/without physical splitter island

Under the condition without physical splitter island, an assumption is given in this research, i.e. entry drivers have to stop when pedestrians are about to cross the curb regardless pedestrian approaching sides due to pedestrians having on crosswalk, then restart after pedestrians finish crossing the conflict area shown in Figure 3.29(a). Waiting time is defined as the time duration from the vehicle stopping to restarting. Thus, the waiting time of a pedestrian from far-side is longer than that from near-side due to longer crossing distance. Entry capacity will be affected by the different waiting time, which is caused by pedestrian approaching side. From the view point of mobility, physical splitter islands provide waiting space to crossing pedestrians. Regarding entry vehicles, it also provides opportunities to pass crosswalk before far-side pedestrians arriving at the physical splitter island as illustrated in Figure 3.29(b). Thus, after installing physical splitter island, the waiting time of a pedestrian from far-side will become shorter comparing to before and equal to that of near-side pedestrians. As a result, entry capacity is expected to relatively increase due to existence of physical splitter island.

The situation without physical splitter island is assumed only at Entry S and other entries are assumed to install physical splitter island. The reactions to pedestrians are realized by inputting different rear gaps for near-side and far-side pedestrians.

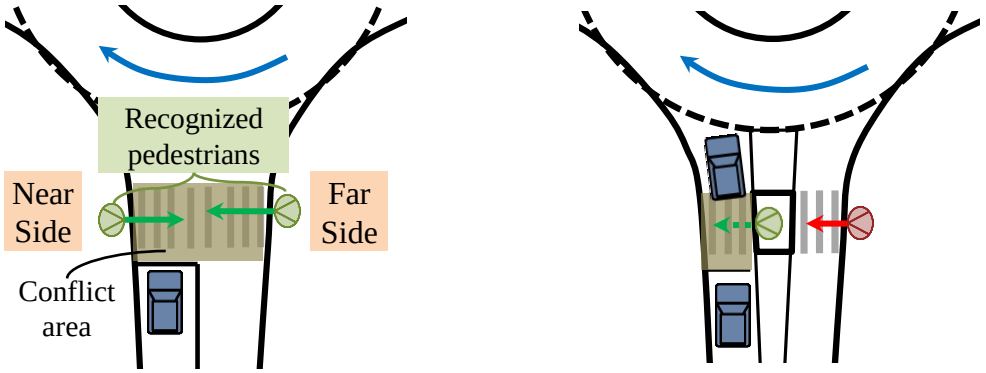

(a) Without physical splitter island (b) With physical splitter island

Figure 3.29 Reactions to pedestrians under the condition with/without physical splitter island

***Far-side Pedestrian Recognition Rate* (*FPRR*)**

Through observing the real situation in Japan, it is found that not all drivers follow the traffic rule on giving priority to crossing pedestrians under the condition without physical splitter island. Some of drivers yield to a pedestrian although he/she has been in crosswalk as illustrated in Figure 3.30(b).

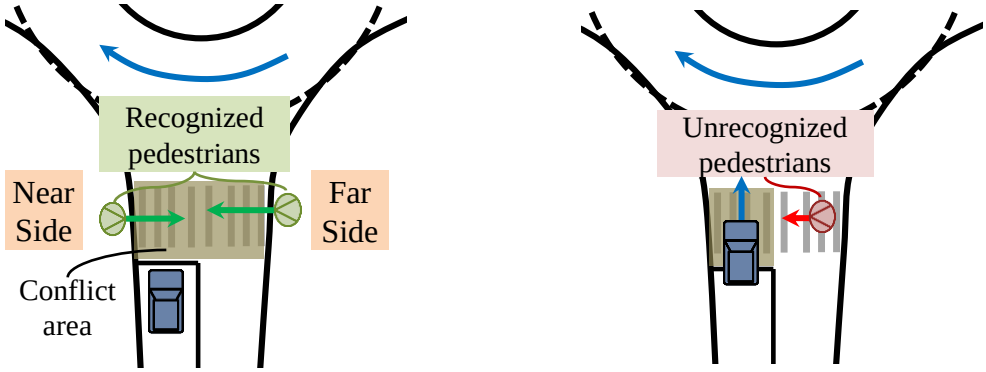

(a) Without physical splitter island and FPRR=100%

(b) Without Physical Splitter Island and 0<FPRR<100%

Figure 3.30 Illustration of recognition of pedestrians by entry vehicle driver

The waiting time due to an unrecognized pedestrian will be shorter than that due to a recognized pedestrian. Far-side pedestrians are more frequently unrecognized by entry drivers under the condition without physical splitter island. Thus, far-side pedestrian recognition rate (FPRR) is defined to represent the percentage of pedestrians recognized by

entry vehicles at the curb of crosswalk. Higher value of FPRR represents that more entry drivers strictly follow the traffic rule so that longer waiting time is generated. Thus, entry capacity will be reduced more significantly with higher value of FPRR. In this research, it is assumed that for the recognized far-side pedestrians entry drivers stop at the moment when they are about to cross the curb of crosswalk while for the unrecognized far-side pedestrians entry vehicles stop at the moment when they leave the middle line of the crosswalk as if the edge of physical splitter island. And the three values of FPRR, i.e. 0, 0.5 and 1 are examined in this research.

Recognized far-side pedestrians and unrecognized far-side pedestrians are assigned in separate lines with different values of rear gap.

In reality, FPRR is related to the yield rate in practice. This yield rate can be calculated to the number of cases that vehicle yielding to pedestrian in all conflict events. Salamati, K. (2014) calculated this yield rate for analyzing the driver yielding behaviors to pedestrians in U.S.

Distance between crosswalk and yield line at the subject approach

Before vehicles entering roundabout, crossing pedestrians and passing circulating vehicles are two continuous blocks regarding entry flow. The space between these two blocks will have significant impact on entry capacity. This space provides opportunities for entry vehicles to separately judge pedestrians and circulating vehicles. When the space can accommodate at least one vehicle as shown in Figure 3.31, entry vehicles can wait in this space to search available gaps of circulating vehicles independently after crossing pedestrian flow. Under this situation, the utilization of available gaps of circulating vehicles will be relatively increased comparing to the condition the space is smaller than one-vehicle length, since entry vehicles have to simultaneously judge pedestrians and circulating vehicles when the space cannot accommodate one vehicle and the available gaps of circulating vehicles may be neglected. Thus, entry capacity will be reduced more under the condition the distance between crosswalk and yield line is shorter than one-vehicle length. On the other hand, this space also provides opportunities to exit vehicles for waiting pedestrians and plays a role of storing exit vehicles. The probability of exit vehicles queuing in the circulating roadway will be reduced when this distance

between crosswalk and yield line is given to store more exit vehicles. Thus, the capacity of upstream entry will be relatively improved.

Since the range of length of vehicle in simulation is set to be [4.1m, 4.7], two cases of distance at the subject entry are examined, i.e. 1m which represents the situation no vehicle can be stored in this space and 5m which one vehicle can be accommodated in this space. While at other entries, only 5m is set in simulation.

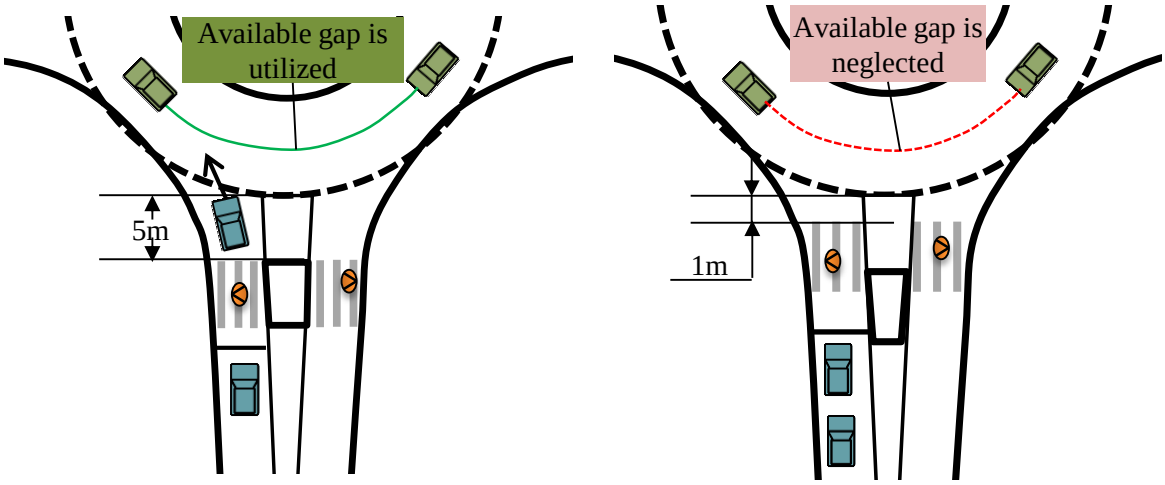

(a) Accommodating one vehicle (5m) (b) No more than one vehicle (1m)

Figure 3.31 Illustration of distance between crosswalk and yield line

3.3.2 Simulation design

Input of traffic flows

Vehicle flow

Entry S is assumed to be the subject entry to estimate entry capacity. In order to observe entry capacity, saturated condition of entry flow, 1600veh/h is created at Entry S. Based on gap acceptance theory, the headway distribution $h(t)$ of circulating vehicles has significant impact on entry capacity. Since circulating flow is composed of entry vehicles from each entry, the priority of entry(in major/minor road) and turning ratio at each entry affect the composition of circulating flow further influence arrival rate of circulating vehicles passing the subject entry. Thus, in this research, the roundabout is assumed to locate under the

condition that the ratio of traffic demand between major road and minor road is equal to 8:2. Entries E and W are in the major road and Entries N and S are in the minor road. For each major and minor road, a fixed turning ratio is given. The turning ratio at Entries E and W q_L:q_{Th}:q_R=1:8:1 whereas at Entries N and S, q_L:q_{Th}:q_R=4:2:4. Circulating flow is composed of flow E→W, E→N and N→W. The illustration of vehicle flow is shown in Figure 3.32.

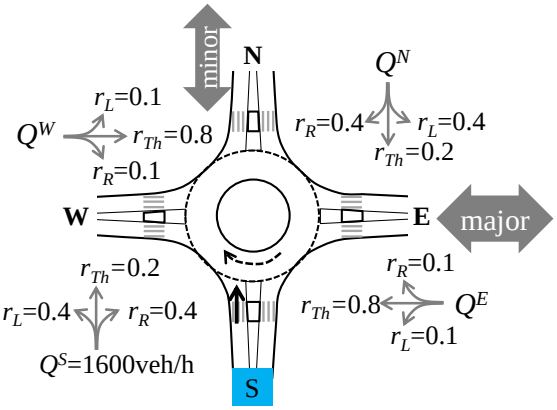

Figure 3.32 Setting of vehicles flow in simulation

Pedestrian flow

Pedestrian demand is referred to the observation in Japan which is provided by *Ministry of Land, Infrastructure, Transport and Tourism* (国土道路交通省, 2014). Figure 3.33 shows this record in this report and it is found that based on the census data, pedestrian demand is lower than 200ped/h/approach at most roads (more than 99%).

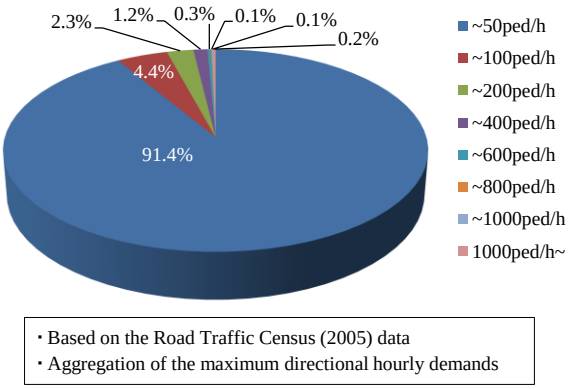

(Report of “ラウンドアバウトの計画・設計に必要な知見に関する検討”)

Figure 3.33 Pedestrian demand based on the census data in H17

Accordingly, at any entry, the maximum pedestrian demand of one entry is set to be

200ped/h in order to include the case of high pedestrian demand and with the interval of 50ped/h when pedestrian demand is lower than 200ped/h. Moreover, pedestrian demand at Entries N, W and E is set to satisfy the condition $Q_{ped}^{N} = Q_{ped}^{W} = Q_{ped}^{E}$.

Near-side pedestrians to approach exit vehicles under the condition without physical splitter island under the condition without physical splitter island, since regarding exit vehicles, near-side is actually far from the exit vehicles as shown in Figure 3.34, near-side pedestrians have impact on exit vehicles as the same as that of far-side pedestrians on entry vehicles.

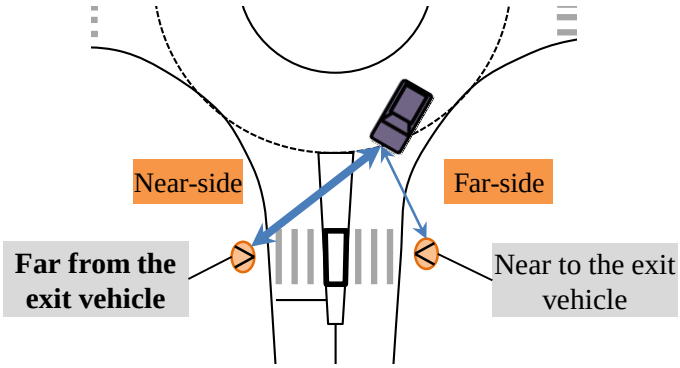

Figure 3.34 Pedestrians to exit vehicles

Thus, for exit vehicles, the setting of FPRR to near-side pedestrians is the same as that of far-side pedestrians.

Selection of parameters

The parameters regarding acceleration/deceleration and speed are input by the empirical data from Towa-cho roundabout which are introduced in the Section 3.2.2 “Data collection”. While, the gap parameters, i.e. critical gap t_c, follow-up time t_f and minimum headway of circulating vehicle τ are selected from several roundabouts in Japan in order to reflect the Japanese situation. The geometry layout and observed gap parameters of these study sites are shown in Table 3.7.

Table 3.7 Basic geometric information and observed gap parameters

Study sites	Layout	Number of legs	Diameter (m)	t_c (sec)	t_f (sec)	τ (sec)
Assumed roundabout	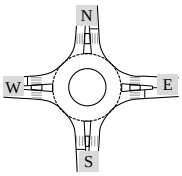	4	27	4.5	3.2	2.2
Azuma-cho roundabout		5	40	4.2	3.1	2.5
Towa-cho roundabout		5	30	4.7	3.7	2.6
Ropontsuji roundabout		6	27	4.9	3.3	2.8
Hitachitaga roundabout		4	30	5.0	3.2	2.2

In existing analysis, it is found that geometry of roundabout, e.g. number of legs and diameter has impact on gap parameters, especially t_c (Kang et al, 2012). Thus, the selection of gap parameters is based on the geometry of proposed study sites. The roundabout which is built in simulation is assumed to be 4-lag single line roundabout with the diameter of 27m. Regarding the proposed study sites, only the roundabout which is located in Hitachitaga, Ibaraki Prefecture Japan has the closest geometry conditions to the assumed one, i.e. 4-leg single line roundabout with the diameter of 30m. The diameter of the Hitachitaga roundabout is littler larger than the assumed roundabout in simulation. It is supposed that the value of t_c will be reduced when the diameter becomes smaller since entry drivers can see more area of the roundabout and more easily make decision to the

approaching upstream circulating vehicles. While diameter is not supposed to have impact on the values of t_f and τ. Thus, t_c, t_f and τ are assumed to be the value of 4.5sec, 3.2sec and 2.2sec, respectively considering the geometry of the assumed roundabout in simulation. Based on these values, a series of setting of parameters can be confirmed.

Dependent on the value of t_c, "rear gap" of vehicles in the function of "conflict area" is calculated which is equal to 2.8 sec. For the conflict of entry vehicles and pedestrians, in this research, it is assumed that when FPRR is in the range [0,1), for the unrecognized far-side pedestrians, all entry vehicles stop at the moment when the pedestrians are about to leave the middle line of the crosswalk as the same as the situation that physical splitter island is installed. While, when FPRR is equal to 1, the assumption is that that all entry vehicles stop at the moment when pedestrians are about to cross the edge of crosswalk regardless pedestrian approaching sides under the condition without physical splitter island. These assumptions are also applied on the case of exiting vehicle and near-side pedestrians. In order to realize these assumptions, the "rear gap" for near-side and far-side pedestrians under the condition without physical splitter island is necessary to be given the value of 1.7sec and 6.00sec. If the value of "rear gap" is smaller than these input values, entry vehicles will cross the crosswalk even pedestrians already enters the crosswalk. The setting of parameters in the function of "conflict area" regarding entry vehicles is shown in Table 3.8. For exit vehicles, the values for near-side pedestrians and far-side pedestrians are mutually exchanged.

Table 3.8 Input values of parameters in the function of "conflict area" based on Japanese situations (the case for the entry vehicles)

Category	Vehicle-Vehicle	Vehicle-Pedestrian			
		With physical splitter island		Without physical splitter island	
		Near-side	Far-far	Near-side	Far-far
Rear gap (sec)	2.80	1.70			6.00
Front gap (sec)	0.500	1.35			

Then, based on the value of t_f and τ, the value of parameters in the function "Wiedemann 74 model" is recalculated. The input values of these parameters are shown in Table 3.9.

Table 3.9 Input values of parameters in the function of "Wiedemann 74 model" based on Japanese situations

Parameters and variables	Regarding entry vehicles (t_f=3.20sec)	Regarding circulating vehicles (τ=2.20sec)
$d=t \cdot v-L_v$ (m)	17.2	4.17
ax (m)	2.10	2.10
v (km/h)	25.0	15.0
z	0.50	0.50
bx_add	3.28	0.58
bx_mult	4.92	0.87

L_v: the average length of vehicles=4.5m, *v*=25km/h and 15km/h (average value of desired speed) for entry and circulating vehicles, respectively

Running simulation

After calibrating and validating parameters, the simulation environment has been adjusted to represent the situation of study site. The entry capacity was examined under the various conditions, i.e., with/without splitter island, near/far pedestrian approaching sides and far-side pedestrian recognition rate (FPRR). All scenarios from five aspects tested in this study are shown as follows.

- Circulating flow: 7 levels
- Pedestrian flow: 0 to 200ped/h in increment of 50ped/h
- Existence of splitter island: with, without
- Far-side directional ratio r_{far}: 0, 0.5 and 1
- FPRR: 0, 0.5 and 1
- Distance between crosswalk and yield line: 1m and 5m

For every combination of input conditions, the VISSIM model was run for 10 times with a unique random number seed. Thus, in total 6,300 combinations were computed and each of them was run for 1h15min simulation time with 15min warm-up time. The data in first

15min of warm-up time was not included in results. Performance statistics were measured at 15min intervals. The measured entry flow (veh/h) was averaged based on 10 simulation runs. Figure 3.35 shows a screenshot of the VISSIM model during a simulation run.

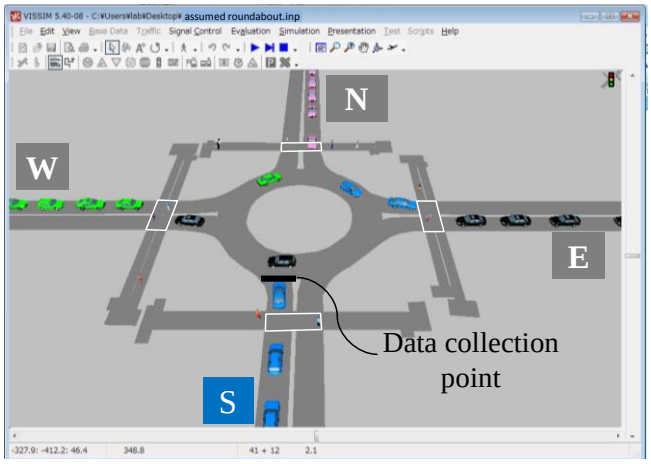

Figure 3.35 Screenshot of simulation

3.4 Results and discussions

3.4.1 Maximum entry flow without pedestrians

Figure 3.36 shows the entry capacity from simulation under the condition without pedestrians at any entry.

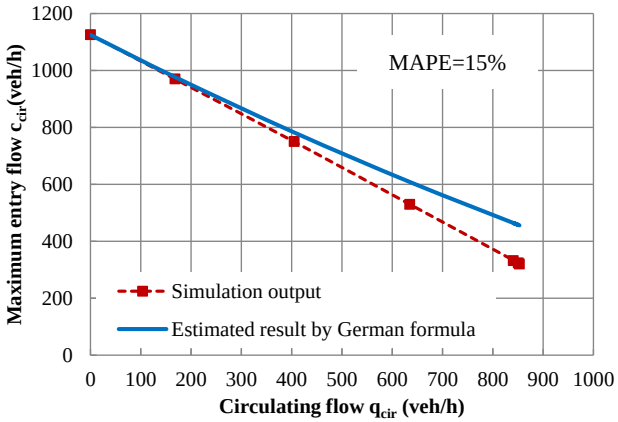

Figure 3.36 Estimated Maximum entry flow without pedestrians

The simulation output is compared to the estimated result by German formula which is shown in Equation 2.25 to examine the accuracy of simulation output. The parameter t_c, t_f and τ is input by the value of 4.5sec, 3.2sec and 2.2sec. The statistic *Mean Absolute Percentage Error* (*MAPE*) is applied to evaluate the relative margin of estimation errors.

MAPE returns the absolute percentage difference in both values which is calculated by Equation 3.7.

$$MAPE_i = \left(\frac{1}{N} \sum_{i=1}^{N} \frac{| x_i - \hat{x}_i |}{x_i} \right) \cdot 100\% \tag{3.7}$$

where x_i = the estimated results by applying German formula

$\hat{x}_i$ = the estimate results from simulation analysis

It is found that when circulating flow is in low level simulation output matched well with estimated result and when circulating flow is increased the simulation output is lower than the estimated result. Generally, it can be concluded that the simulation output is reasonable according to the MAPE value (<15%) comparing to the estimated result. Moreover, the simulation output shows that under the condition without pedestrians, circulating flow is no more than 850veh/h. This is because when entry flows from other entries are increased, circulating flows passing in front of these entries are increased as well. Thus, the vehicles which form the circulating flow passing in front of Entry S may be prevented entering roundabout so that the circulating flow cannot reach a high level.

3.4.2 Pedestrian demand at subject entry

Figure 3.37 shows the result of estimated entry capacity under the conditions (1) with physical splitter island; (2) no pedestrians across other entries; (3) r_{far}=0.5 and (4) FPRR=1. It was found that at the same level of circulating flow, entry capacity is reduced when pedestrian demand increases.

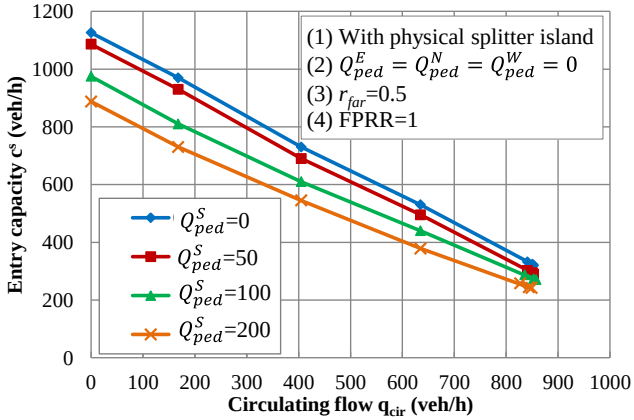

Figure 3.37 Estimated entry capacity changing with pedestrian demand at subject entry (Entry S)

3.4.3 Pedestrian approaching side

Figure 3.38 plots the estimated entry capacity considering pedestrian approaching side under the conditions (1) without physical splitter island; (2) no pedestrians across other entries and (3) FPRR=1. The results under the pedestrian demands of 50ped/h, 100ped/h and 200ped/h were selected as the examples shown in Figure 3.40 (a), (b) and (c), respectively.

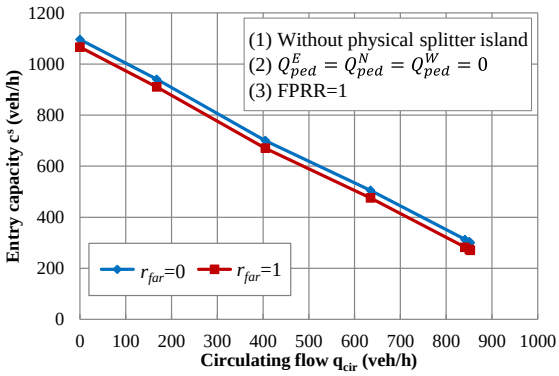

(a) Pedestrian demand at Entry S: 50ped/h

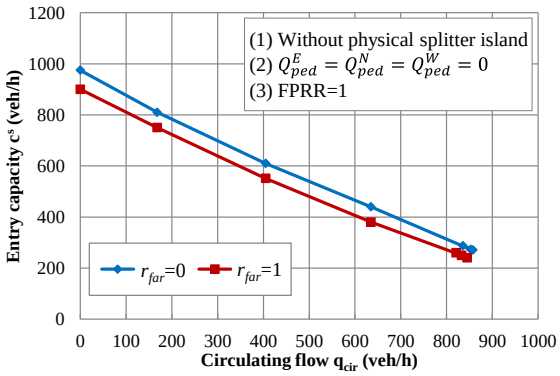

(b) Pedestrian demand at Entry S: 100ped/h

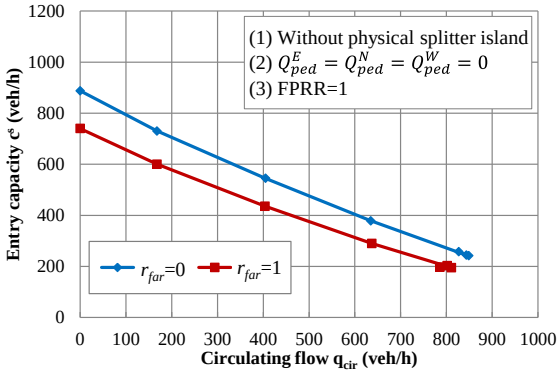

(c) Pedestrian demand at Entry S: 200ped/h

Figure 3.38 Entry capacity varies as pedestrian approaching side under various pedestrian demand under the condition without physical splitter island

It was found that under the condition without physical splitter island, entry capacity is reduced more when all pedestrians are from far-side than that under the condition all pedestrians from near-side. This is because the waiting time which is shown in Figure 3.39for pedestrians from far-side is longer than that for pedestrians from near-side under the assumption that all entry vehicles stopped at the moment when pedestrians are about to cross at the curb of crosswalk and wait until pedestrians complete crossing the conflict area. It implies that entry capacity will be reduced more at the entrance when more pedestrians

are from far-side, especially under the condition without physical splitter island.

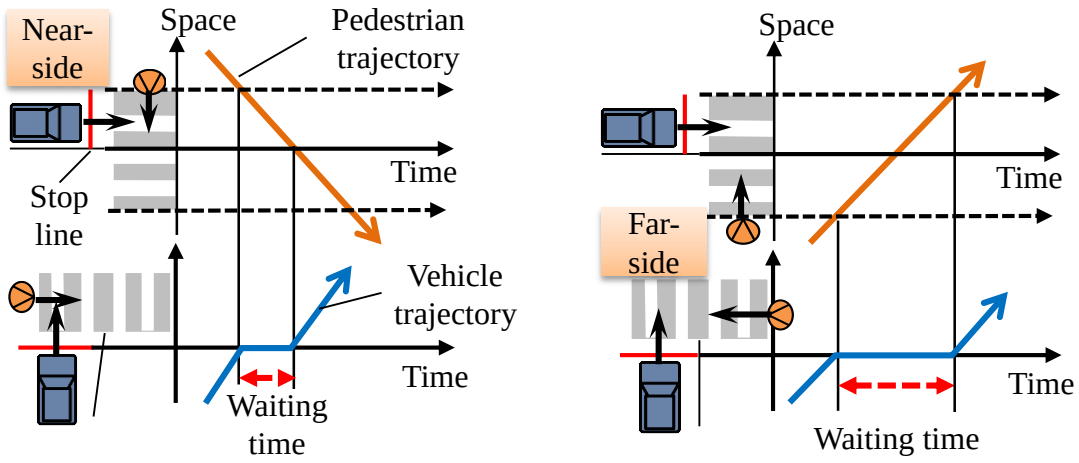

(a) Pedestrians from near-side (b) Pedestrians from far-side

Figure 3.39 Illustration of waiting time of pedestrians from different sides

3.4.4 Far-side Pedestrian Recognition Rate FPRR

In the analysis of pedestrian approaching side, all entry vehicles are assumed to react to far-side pedestrians at the moment when pedestrians are about to cross the far-side curb of crosswalk. However, in the real world, not all drivers exactly behave in the same way to recognize pedestrians under the same condition. Therefore, FPRR is utilized to represent this uncertainty. Figure 3.40 represents the estimated entry capacity regarding FPRR under the conditions (1) without physical splitter island; (2) no pedestrians across other entries and (3) r_{far}=1 at Entry S. The results under the pedestrian demands of 50ped/h, 100ped/h and 200ped/h were selected as the examples and show in Figure 3.40 (a), (b) and (c), respectively.

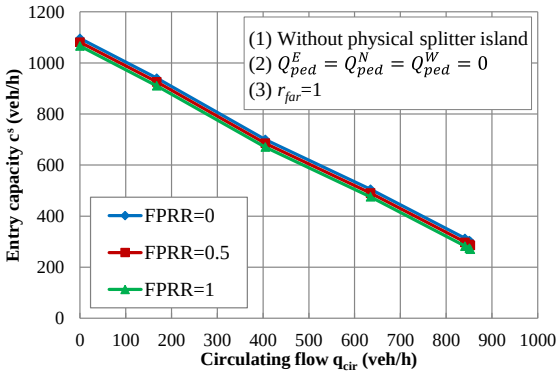

(a) Pedestrian demand at Entry S: 50ped/h

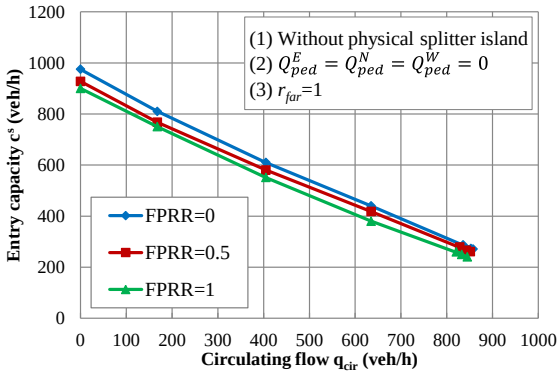

(b) Pedestrian demand at Entry S: 100ped/h

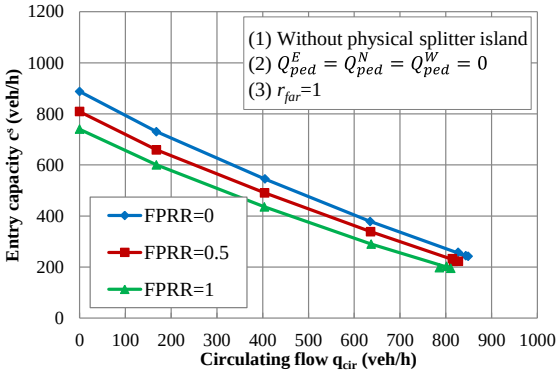

(c) Pedestrian demand at Entry S: 200ped/h

Figure 3.40 Estimated entry capacity changing with FPRR considering pedestrians from far-side

It was found that under the same level of pedestrian demand and a certain level of circulating flow in each figure, entry capacity is reduced with the increase of FPRR. Entry capacity performs the lowest and highest value under the rate of 100% and 0, respectively.

FPRR in the range of (0, 100%) reflects the real world situation, which implies that when only assuming FPRR equals 100% impact of pedestrian will be overestimated further underestimating entry capacity. It can be suggested that a realistic FPRR should be considered with pedestrian approaching side in entry capacity estimation so that the real world situation can be appropriately reflected.

3.4.5 Physical Splitter Island

The results of estimated entry capacity considering with/without physical splitter island and under the conditions (1) no pedestrians across other entries; (2) r_{far}=1 at Entry S and (3) FPRR=1 are shown in Figure 3.41. All pedestrians are assigned from far-side and recognized by entry vehicles. The results under the pedestrian demands of 50ped/h, 100ped/h and 200ped/h were selected as the examples and show in Figure 3.41(a), (b), (c), respectively.

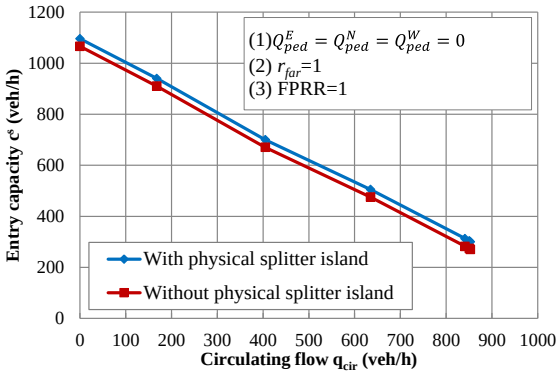

(a) Pedestrian demand at Entry S: 50ped/h

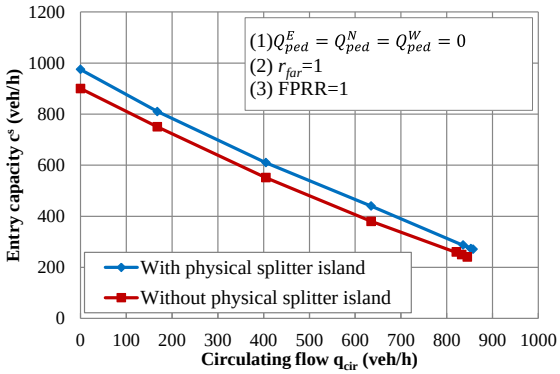

(b) Pedestrian demand at Entry S: 100ped/h

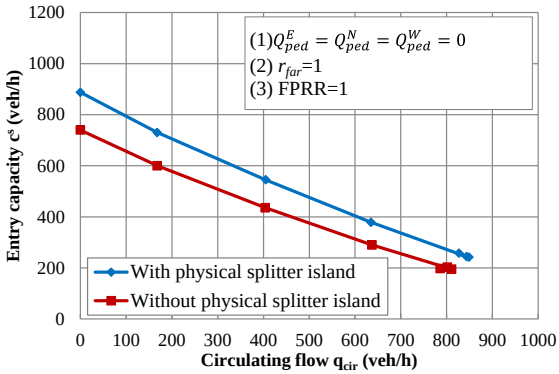

(a) Pedestrian demand at Entry S: 200ped/h

Figure 3.41 Estimated entry capacity under the condition with/without physical splitter island considering pedestrians from far-side

From the simulation output, it was found that under certain pedestrian demand, entry capacity performs higher value under the condition with physical splitter island since more vehicles can pass and waiting time is shortened under this condition as shown in Figure 3.42. In addition, the difference of entry capacity at a certain level of circulating flow between with and without physical splitter island becomes larger when pedestrian demand

increases due to increase in total waiting time.

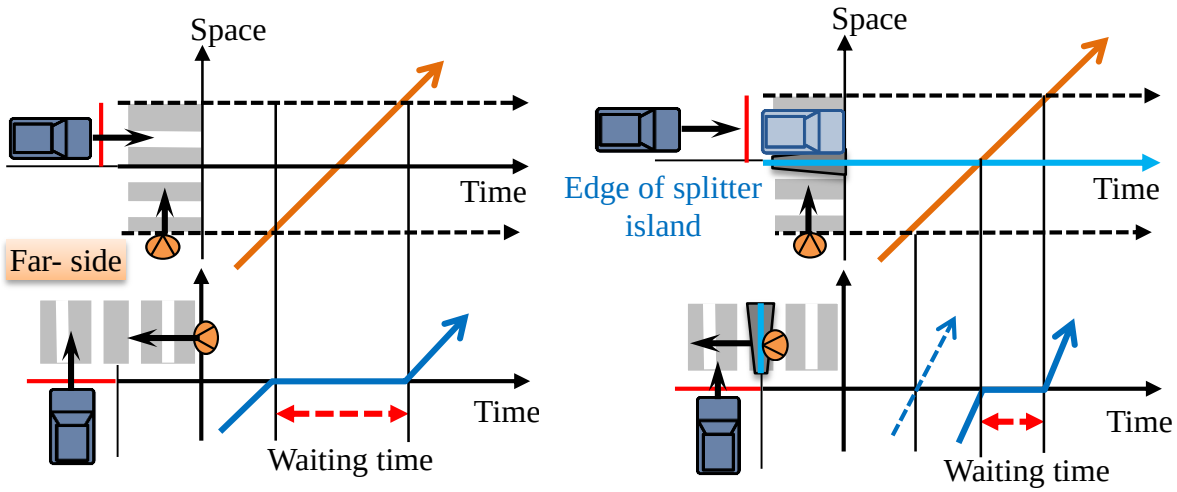

(a) With splitter island (b) Without splitter island

Figure 3.42 Waiting time under the condition with/without physical splitter island

However, in real world, the function of physical splitter island will be not as significant as simulation showing when pedestrian demand is at the high level. Pedestrians will cross as platoon due to high demand so that drivers have to choose to take stopping behavior, no matter physical splitter island existing or not. On the other hand, when pedestrian demand is at low level, although entry capacity varies slightly under the condition with physical splitter island based on simulation output, physical splitter island plays an important role from the safety consideration in real world. Under this condition, most of drivers will pass the crosswalk without giving priority to pedestrians due to low pedestrian demand. Moreover, pedestrians have to mind both of the entry and exit vehicle flows at same time during crossing when physical splitter island is uninstalled. These cause pedestrians having to wait and increasing the risk during crossing. Therefore, physical splitter island is strongly recommended to be installed at the entrance of roundabouts from the considerations of mobility and safety.

3.4.6 Distance between crosswalk and yield line

The results of estimated entry capacity considering the distance between crosswalk and yield line and under the conditions (1) no pedestrians across other entries and (2) r_{far}=0.5 are shown in Figure 3.43. This examination is conducted under the condition with/without physical splitter island and under the condition without splitter island FPRR=0.5 is set. All pedestrians are assigned from far-side and recognized by entry vehicles. The results under the pedestrian demands of 50ped/h, 100ped/h and 200ped/h were selected as the examples and show in Figure 3.43(a), (b), (c), respectively.

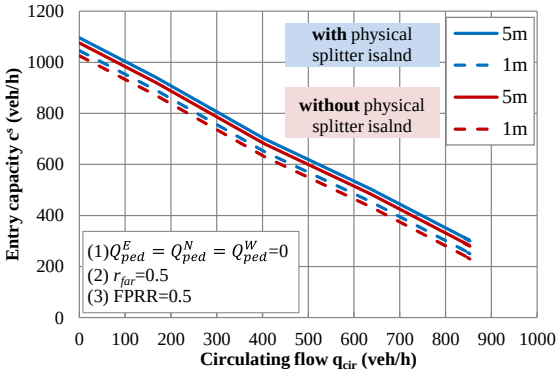

(a) Pedestrian demand at Entry S: 50ped/h

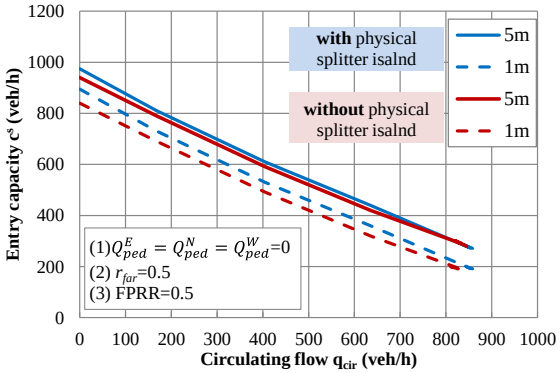

(b) Pedestrian demand at Entry S: 100ped/h

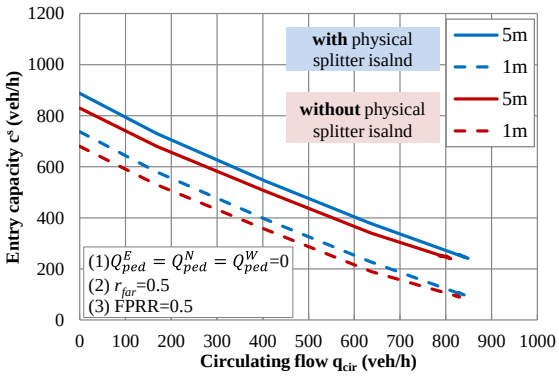

(a) Pedestrian demand at Entry S: 200ped/h

Figure 3.43 Estimated entry capacity under the different conditions of distance between crosswalk and yield line

It was found that at the same level of pedestrian and circulating flow, either with or without physical splitter island estimated entry capacity is reduced more under the condition the space is shorter than one-vehicle length comparing to the condition that one vehicle can be accommodated in this space. In addition, this difference between two cases is enlarged

when pedestrian flow increases. These findings can be contributed that under the condition the space is shorter than one-vehicle length entry vehicles have to wait until both pedestrians and circulating vehicles providing available gaps. This results in available gaps of circulating vehicles will be neglected and decrease entry capacity. The probability of available gaps of pedestrians is reduced with the increase of pedestrian flow so that the difference between two cases is enlarged when pedestrians at Entry S increases.

This result demonstrated the function of the space between crosswalk and yield from the approach of operational performance which is the space accommodating one vehicle is necessary for entry capacity, since it provides the space for entry vehicles to separately judge pedestrians and circulating vehicles.

3.4.7 Pedestrians across at other entries

Figure 3.44 represents the estimated entry capacity regarding pedestrians across other entries under the conditions (1) with physical splitter island; (2) identical pedestrians demand at other entries and (3) no pedestrians across Entry S.

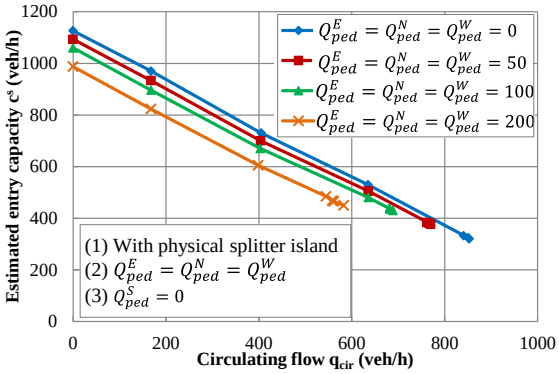

Figure 3.44 Estimated entry capacity changing with pedestrians across other entries

It was found that entry capacity is reduced with the increase of pedestrian demand, which is similar as the result in section 3.4.2.

Through these output it is found that influencing factors. i.e. pedestrian approaching sides, physical splitter island, far-side pedestrian rate and pedestrians at other entries have significant impact on entry capacity. Based on these results, a regression model is developed as follows.

3.5 Regression model based on simulation analysis

3.5.1 Assumptions of regression model

The estimation formula used in Germany which is shown in Equation 2.25 can be expressed by Equation 3.8.

$$c_e = \frac{3600}{t_f}\exp\left[-\frac{q_{cir}}{3600}\left(t_c - \frac{t_f}{2} - \tau\right)\right] - \frac{\tau}{t_f}q_{cir}\exp\left[-\frac{q_{cir}}{3600}\left(t_c - \frac{t_f}{2} - \tau\right)\right] \quad (3.8)$$

This estimation method is developed based on gap acceptance theory. Since entry vehicles crossing pedestrian flow by available gaps as well, the maximum entry flow considering pedestrians can also be estimated dependent on gap acceptance theory. Thus, considering entry capacity c_{RAB} (c^s in simulation) and circulating flow q_{cir} as the dependent and independent variables, respectively, the entry capacity under the impact of both pedestrian and circulating flows is assumed to follow Equation 3.9 based on Equation 3.8.

$$c_{RAB} = A\exp(-Bq_{cir}) - Cq_{cir}\exp(-Bq_{cir}) \quad (3.9)$$

A, B and C are parameters considering influencing factors. They are shown by Equations 3.10~3.12.

$$A = f(x_1, x_2, \cdots, x_n) \quad (3.10)$$

$$B = g(x_1, x_2, \cdots, x_n) \quad (3.11)$$

$$C = h(x_1, x_2, \cdots, x_n) \quad (3.12)$$

Based on the simulation output, pedestrian demand at Entry S (subject entry), pedestrian demand at Entry E, N, W, physical splitter island, distance between crosswalk and yield line and pedestrian approaching sides are considered as the variables to estimate parameters of *A*, *B* and *C*. The definitions and values of variables are shown in Table 3.10.

Table 3.10 Definitions and values of variables in regression model

Variables	Definition	Value in simulation
x_1	Pedestrian demand across Entry S (ped/h)	0, 50, 100, 200
x_2	Pedestrian demand across other entries (ped/h)	0, 50, 100, 200

x_3	Far-side pedestrian directional ratio r_{far}	0, 0.5, 1
x_4	Far-side pedestrian recognition rate FPRR	0, 0.5, 1

Since entry drivers behaves significantly different under the condition with/without physical splitter island, the estimations of parameters *A*, *B* and *C* is separated to two situations, with and without physical splitter island. One curve of entry capacity changing with circulating flow can obtain one group of parameters of *A*, *B* and *C*. Thus, for each situation (with/without physical splitter island), each parameter has 45 samples.

Parameters *A*, *B* and *C* are first fitted based on simulation outputs. Then, correlation analysis is conducted between each two variables to make sure the variables are independent each other by SPSS. The relationship of parameters *A*, *B* and *C* and the variables are identified by correlation analysis as well. After tests several types of regressions, e.g. linear regression, exponential regression and logic regression, it is shown that the linear regression gives best result of fit. According to this, variables including in each parameter are determined and the linear regression functions of *A*, *B* and *C* are shown in Equations 3.13~3.15.

$$A = a_0 + a_1x_1 + a_2x_2 + a_3x_3 + a_4x_4 \tag{3.13}$$

$$B = b_0 + b_1x_1 + b_2x_2 + b_3x_3 + b_4x_4 \tag{3.14}$$

$$C = c_0 + c_1x_1 + c_2x_2 + c_3x_3 + c_4x_4 \tag{3.15}$$

3.5.2 Results of regression model

Through simulation output it is found that the performance of estimated entry capacity can be divided into two independent cases, “with physical splitter island” and “without physical splitter island”. Thus, the models are explained under the condition with/without physical splitter island in Table 3.11.

In each estimated model, t-value at 95% confidence level shows that the variables of pedestrian demand across Entry S and other entries have significant impact on each parameter. While, under the condition with physical splitter island, the impact of r_{far} and FPRR in each model is not significant. R^2 values show that all models are well fitted by considering there variables.

Table 3.11 Results of regression model

Parameters	Variables	With physical splitter island	Without physical splitter island
		Result(t-value)	Result(t-value)
A	Coefficient (a_0)	1046 (50.50)	997.8 (38.26)
	Pedestrian demand across Entry S (a_1)	-1.154 (-23.64)	-1.213 (-19.04)
	Pedestrian demand across other entries (a_2)	-0.3272 (-9.086)	-0.3210 (-6.330)
	r_{far} (a_3)	-0.004625 (-0.3093)	-119.3 (-4.788)
	FPRR (a_4)	-0.003724 (-0.4117)	-85.26 (-5.2352)
	R^2	0.9001	0.9129
B	Coefficient (b_0)	4.659×10^{-5} (1.907)	1.423×10^{-4} (1.926)
	Pedestrian demand across Entry S (b_1)	2.312×10^{-7} (4.928)	6.987×10^{-7} (3.485)
	Pedestrian demand across other entries (b_2)	2.210×10^{-7} (4.068)	2.445×10^{-7} (2.513)
	r_{far} (b_3)	4.169×10^{-7} (0.01759)	2.755×10^{-4} (2.980)
	FPRR (b_4)	3.244×10^{-7} (0.0523)	2.920×10^{-4} (3.006)
	R^2	0.6256	0.6589
C	Coefficient (c_0)	0.7895 (83.95)	0.9263 (28.78)
	Pedestrian demand across Entry S (c_1)	-0.002369 (-49.78)	-0.001642 (-20.75)
	Pedestrian demand across other entries (c_2)	8.259×10^{-4} (31.56)	7.010×10^{-4} (11.78)
	r_{far} (c_3)	-0.003899 (-0.2938)	-0.2011 (-6.492)
	FPRR (c_4)	-0.004012 (-0.3026)	-0.2137 (-7.522)
	R^2	0.9784	0.9622

The positive and negative of each coefficient shows that entry capacity is reduced when pedestrian demand is increased regardless entries. Either with/without physical splitter

island, entry capacity is reduced more when the distance between crosswalk and yield line is enough to accommodate one vehicle. In addition, under the condition without physical splitter island, entry capacity is reduced more when more pedestrians are from far-side and FPRR increases. These results follow the simulation output.

Dependent on the t-test values of variables, r_{far} and FPRR shows great significance under the condition without physical splitter island however they are not significance under the condition with physical splitter island. This is because r_{far} and FPRR has no impact on entry capacity under the condition with physical splitter island which follows the assumption of pedestrian approaching sides regarding the waiting time under the condition with/without physical splitter island.

3.5.3 Validation

The regression model is validated under the input conditions (1) pedestrian demand at Entry S is 80ped/h; (2) pedestrian demand at other entries is identical and equal to 80ped/h; (3) r_{far}=0.6 and (4) FPRR=0.6. The results of regression model and simulation output under the condition with/without physical splitter island are shown in Figure 3.45.

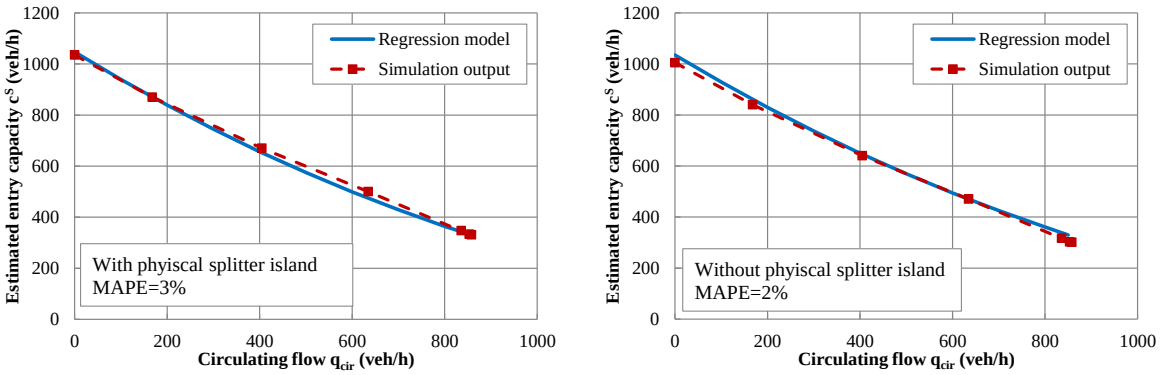

(a) With physical splitter island (b) Without physical splitter island

Figure 3.45 Validation of regression model under the condition with/without physical splitter island

The MAPE value is calculated by Equation 3.16.

$$MAPE_i = \left(\frac{1}{N} \sum_{i=1}^{N} \frac{| x_i - \hat{x}_i |}{x_i} \right) \cdot 100\% \tag{3.16}$$

where x_i = the estimated results of proposed regression model

$\hat{x}_i$ = the estimate results from simulation analysis

Thus, it can be concluded that under the condition either with or without physical splitter island, the regression model well matched the simulation output based on the result of MAPE value (MAPE< 5%).

3.6 Summary

The impacts of several influencing factors on entry capacity from the view point of Japanese situation were examined based on simulation VISSIM 5.40. It was found that entry capacity was reduced more significantly when more pedestrians are from far-side under the condition without physical splitter island and the assumption that all entry vehicles stopped at the moment when pedestrians are about to cross the curb. Moreover, FPRR was added to make the situation more realistic and entry capacity was found to be improved as decreasing FPRR. After assuming the condition with physical splitter island, entry capacity under the condition of pedestrians from far-side was relatively increased due to the shorter waiting time.

This analysis in this chapter demonstrated the function of physical splitter islands that it plays an important role of improving the entry capacity. Therefore, also from the view point of operational performance, the physical splitter island is recommended to be installed at entrance, e.g., under the condition of high pedestrian demand and high FPRR.

Based on simulation analysis, a theoretical model considering these influencing factors is developed in next chapter.

4 Chapter 4

DEVELOPING A THEORETICAL MODEL FOR ESTIMATION OF ROUNDABOUT ENTRY CAPACITY

4.1 Framework of the proposed model

A standard single-lane roundabout with four legs under the left-hand traffic control is assumed, which includes crosswalk, physical splitter island and the space of one-vehicle length between crosswalk and yield line at every leg. The capacity of Entry S c^S is estimated considering two cases of circulating flow in front of Entry S. Circulating vehicles are assumed to be flowing in case (a) whereas they are assumed to be queuing in circulating roadway in case (b). Illustration of cases (a) and (b) is shown in Figure 4.1(a) and (b), respectively.

case (a)

Under the condition of flowing circulating vehicles, entry capacity c_a is determined by pedestrians across Entry S, circulating flow passing in front of Entry S and several influencing factors, i.e. physical splitter island, pedestrian approaching side and distance between crosswalk and yield line.

case (b)

On the other hand, the vehicles exiting to Exit N, E or W which are blocked by pedestrians

across at these exits may lead to a queue in circulating roadway. When the queuing vehicles reaches up to front of Entry S, vehicles at Entry S are prevented from entering roundabout due to these queuing vehicles. Thus, entry capacity c_b is equal to zero under this condition since vehicles cannot enter roundabout at all.

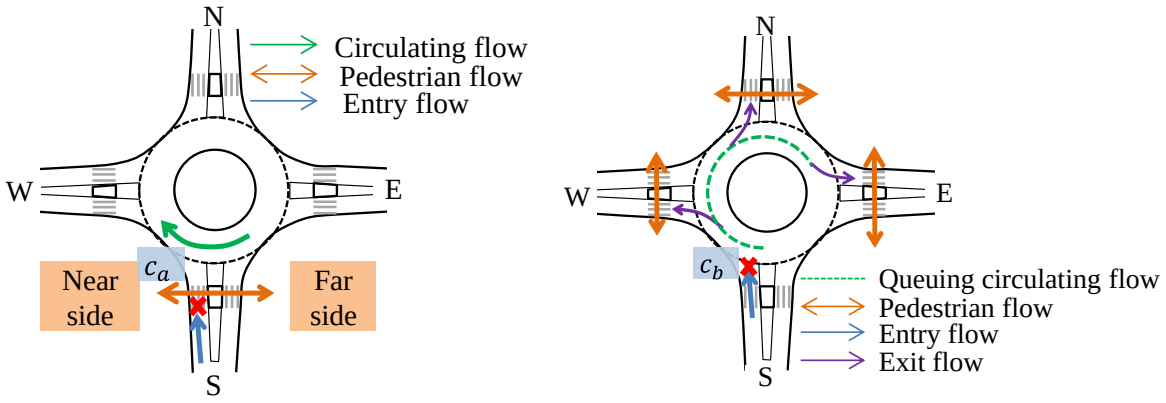

(a) Entry capacity c_a under the condition of flowing circulating vehicles

(b) Entry capacity c_b under the condition of queuing circulating vehicles

Figure 4.1 The capacity of Entry S considering two cases regarding the situations of circulating flow

$P_{flowing}$ is defined as the probability of circulating vehicles flowing in front of Entry S in case (a), and P_{queue} is defined as the probability of queuing vehicles reaching up to front of Entry S in case (b). Accordingly, entry capacity c^S considering cases (a) and (b) is estimated by Equation 4.1.

$$c^S = P_{flowing} \cdot c_a + P_{queue} \cdot c_b \tag{4.1}$$

Since the situations of circulating flow in case (a) and (b) are independent, $P_{flowing}+P_{queue}=1$. In addition, c_b is equal to zero as described in case (b). Thus, Equation (2) is changed to Equation 4.2.

$$c^S = (1 - P_{queue}) \cdot c_a \tag{4.2}$$

The framework of the proposed model is shown in Figure 4.2.

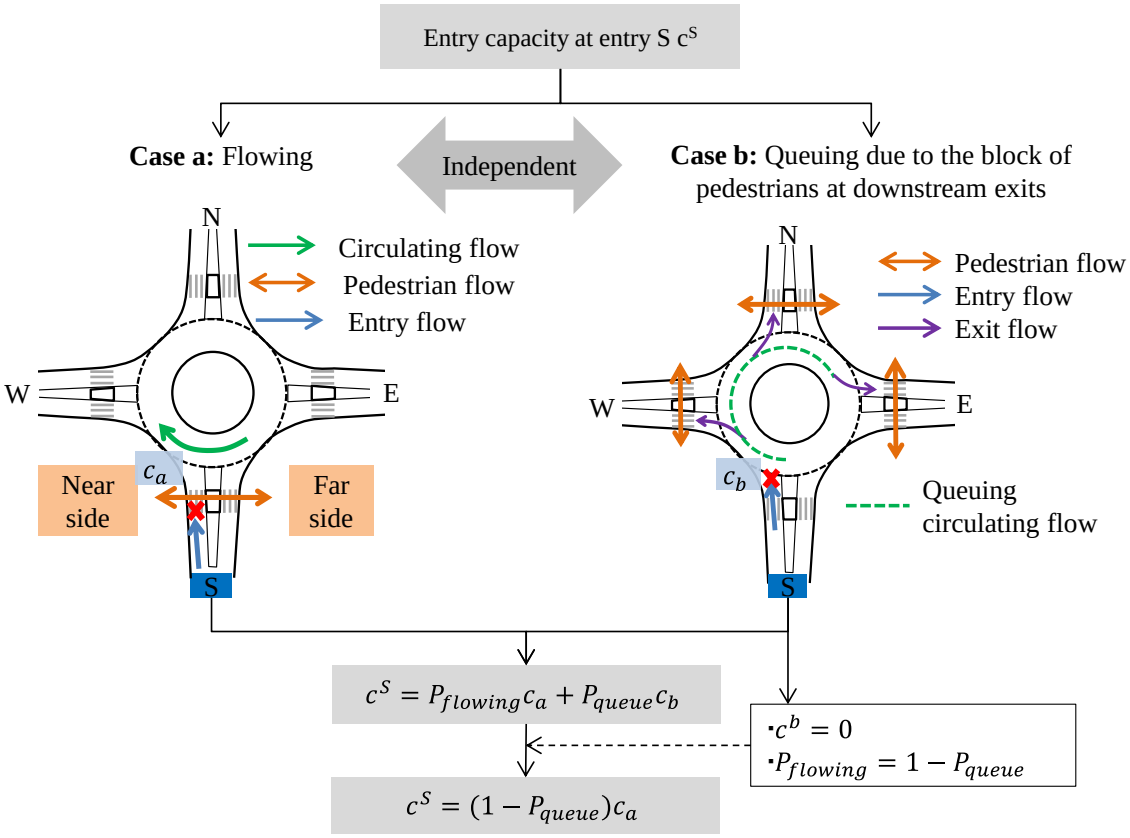

Figure 4.2 Framework of the proposed theoretical model

4.2 Estimation of c_a

4.2.1 Introduction of applied theory

Based on HBS (2001) and HCM (2010), a standard roundabout is generally designed with the space of one-vehicle length between downstream edge of crosswalk and yield line. For entry vehicles, this space has a function of storage to wait for an available gap of circulating vehicles before entering roundabout. Thus, entering procedure is divided into two separate parts due to this storage space, first crossing pedestrian flow and then circulating flow. Such kind of separate crossing also occurs at two-stage unsignalized intersection, which major road is divided into two separate parts by some storage space. Brilon et al (1996) developed a model for estimating capacity of minor road traffic at the two-stage unsignalized intersection. The application of this theory on roundabout is explained as follows.

Entry capacity is determined by circulating flow passing in front Entry A and how many

vehicles waiting at the yield line. These waiting entry vehicles are from entry vehicles which cross pedestrian flow. Thus, the number of vehicles can wait at yield line is determined by pedestrian flow and the maximum number of vehicles which can be stored between crosswalk and yield. As shown in Figure 4.3(a), n_a is defined as the maximum number of vehicles which can be stored between crosswalk and yield line and n is defined as the number of vehicles which are queuing in the storage space in certain period T_a.

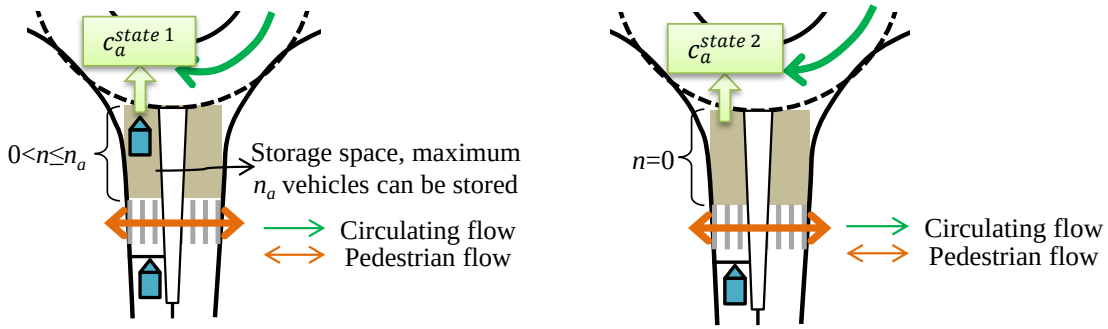

(a) Entry capacity c_a^{state1} under the condition $0<n\leq n_a$

(b) Entry capacity c_a^{state2} under the condition $n=0$

Figure 4.3 Entry capacity c_a under different situations of storage space

P_n is defined as the probability of number of n vehicles queuing in the storage space. Sum of the probabilities P_n for all of the possible number of queuing vehicles n must be equal to 1 when the condition is $0\leq n\leq n_a$, as shown in Equation 4.3.

$$\sum_{n=0}^{n_a} P_n = 1, n_a \in N = \{1,2,\cdots,n\}, n \in I = \{1,2,\cdots,n_a\} \tag{4.3}$$

Dependent on the value of n_a, the entering procedure can be classified into two states which the illustrations of these two states are shown in Figures 4.2(a) and (b).

***State* 1, $0<n\leq n_a$**

The illustration of this state is shown in Figure 4.2(a). Under this condition, n ($0\leq n\leq n_a$) vehicles queue in the space and the maximum number of vehicles which can enter roundabout is determined by the circulating flow q_{cir}. This maximum number of entering vehicles can be described by a function of $f(q_{cir})$Thus, entry capacity of state 1 $c_a^{state\ 1}$ is calculated by the function $f(q_{cir})$ with the probability of P_n as shown in Equation 4.4.

$$c_a^{state1} = P_1 f(q_{cir}) + P_2 f(q_{cir}) + \cdots + P_{n_a} f(q_{cir}) = \left(\sum_{n=1}^{n_a} P_n \right) f(q_{cir})$$
$$= (1 - P_0) f(q_{cir}) \quad (4.4)$$

***State* 2, *n*=0**

n=0 represents the situation of no vehicle queuing in storage space. Under this situation, entry vehicle should cross pedestrian flow and circulating flow simultaneously without stopping in the storage space. Thus, entry capacity of state 2 $c_a^{state\,2}$ is calculated by a function of circulating flow q_{cir} and pedestrian flow q_{ped}, $g(q_{ped}, q_{cir})$ with the probability of P_0 as shown in Equation 4.5.

$$c_a^{state2} = P_0 g(q_{ped}, q_{cir}) \quad (4.5)$$

Therefore, entry capacity c_a is calculated by the sum of entry capacity in these two states as shown in Equation 4.6.

$$c_a = c_a^{state1} + c_a^{state2} = (1 - P_0) f(q_{cir}) + P_0 g(q_{ped}, q_{cir}) \quad (4.6)$$

P_0 is calculated as follows.

Considering the real situation at roundabout, n_a cannot be an infinite value. Thus, it is assumed that $n_a \leq 2$ based on the real situation of roundabout. Follow-up time is defined as the headway between two vehicles queuing in minor road to cross an available gap of major flow. At roundabout, circulating and pedestrian flow are two major flows whereas entry flow is minor flow. Dependent on the definition of follow-up time, regarding a given available gap of minor flow, the follow-up time will not change with different subjects of major flows. Thus, the follow-up times crossing pedestrian flow and merging into circulating flow are assumed to be identical, noted as t_f. According to this, A continuous period, e.g. 1 hour, can be divided into *n* intervals of duration t_f, as 1h=3600sec=n*t_f. Therefore, the situation of the storage space will change at the end of each t_f. In one interval of t_f, the end of this interval is noted as time t. At time t, the situation of queuing vehicle in the storage space has (n_a+1) possibilities (0, 1, 2, … , n_a). Since at time t only one situation of queuing vehicles occurs, (n_a+1) possibilities are independent and the

probability of each possibility is the same, which is equal to $1/(n_a+1)$ as shown in Equation 4.7.

$$P_0(t) = P_1(t) = \cdots = P_i(t) = \cdots = P_{n_a}(t) = \frac{1}{n_a + 1} \tag{4.7}$$

Accordingly, the entry capacity in a certain interval of t_f is described in Equation 4.8 based on Equations 4.6 and 4.7.

$$c_a(t_f) = [1 - P_0(t)] f[q_{cir}(t_f)] + P_0(t) g[q_{ped}(t_f), q_{cir}(t_f)] \tag{4.8}$$

Here, $f[q_{cir}(t_f)]$ and $g[q_{ped}(t_f), q_{cir}(t_f)]$ are denoted as the maximum entry flow considering circulating flow only and both circulating and pedestrian flows in duration t_f.

Thus, the entry capacity in 1h can be expressed by $(n^*c_a(t_f))$ as shown in Equations 4.9 and 4.10.

$$c_a = nc_a(t_f), \qquad n = \frac{3600}{t_f} \tag{4.9}$$

$$c_a = [1 - P_0(t)]\left\{ f[q_{cir}(t_f)\frac{3600}{t_f}\right\} + P_0(t)\left\{ g[q_{ped}(t_f), q_{cir}(t_f)]\frac{3600}{t_f}\right\} \tag{4.10}$$

Here, $\{f[q_{cir}(t_f)]^*3600/t_f\}$ is equal to the 1h maximum entry flow considering circulating flow only within the duration of 1h, and $\{g[q_{ped}(t_f), q_{cir}(t_f)]^*3600/t_f\}$ is equal to the 1h maximum entry flow considering both pedestrian and circulating flows within the duration of 1h. Therefore, the Equation 4.10 can be transferred to Equation 4.11.

$$c_a = [1 - P_0(t)] f(q_{cir}) + P_0(t) g(q_{ped}, q_{cir}) \tag{4.11}$$

Therefore, the entry capacity c_a is calculated by Equation 4.12 dependent on Equations 4.7 and 4.11.

$$c_a = \frac{n_a}{n_a + 1} f(q_{cir}) + \frac{1}{n_a + 1} g(q_{ped}, q_{cir}) \quad (4.12)$$

$f(q_{cir})$ is estimated by existing methods referring to c_{cir} which are introduced in Chapter 2.; $g(q_{ped}, q_{cir})$ is estimated based on Wu's theory (2001) as follows.

Wu (2001) developed a model for estimating capacity of minor road traffic in a certain period T through classifying situation of major road traffic into four items, "queuing", "bunching", "single vehicle" and "free space". Period T is assumed to have the probability of 1. Headway distribution of the single flow in major road is assumed to follow Cowan's M3 model. "Queuing" happens under the congested situation; headway of vehicles in "bunching" and "single vehicle" item is assumed to be equal to minimum headway τ and the intercept gap size t_0 in $E(t)$, respectively and "free space" is denoted as the situation of no vehicle. According to gap acceptance theory and Siegloch's model (1973), minor road traffic can only cross major road traffic under the condition of "free space". In period T, many short periods of items will occur and each of them has a probability. Since each item is independent, summing up all small periods of one item to a large period, four large periods are finally included in period T. Dependent on definition of the conditioned probabilities, probability of "free space" P_F is calculated under the condition of {"no single vehicle $P_{0,Q}$"|("no bunching vehicle $P_{0,B}$"|"no queuing vehicle $P_{0,S}$")}. P_F is expressed by Equation (14).

$$P_F = P_{0,S} \cdot P_{0,B} \cdot P_{0,Q} \quad (4.13)$$

Capacity of minor road traffic c^{minor} is estimated by probability of free space P_F multiplying saturation capacity of minor road c_{max} which is calculated by follow-up time of minor road traffic t_f^{minor}.

Probability of queue P_Q is calculated by degree of saturation x of the flow, then $P_{0,Q}$ is calculated by Equation 4.14.

$$P_{0,Q} = 1 - P_Q = 1 - x \quad (4.14)$$

Probability of bunching P_B is calculated dependent on average minimum headway $\bar{\tau}$ and flow demand q (veh/s). Thus, probability of no bunching $P_{0,B}$ is calculated by in Equation

4.15.

$$P_{0,B} = 1 - P_B = 1 - q\bar{\tau} \tag{4.15}$$

$P_{0,S}$ is the probability of headway t in the major road traffic larger than t_0 under the condition that headway t is larger than minimum headway τ, which is calculated by Equation 4.16.

$$P_{0,S} = P(t > t_0 \mid t > \tau) = \frac{P(t > t_0)}{P(t > \tau)} = \frac{1 - F(t = t_0)}{1 - F(t = \tau)} \tag{4.16}$$

where F(t) =the distribution function of headway t in major road traffic

Since headway of major road traffic is assumed to follow the shifted-negative exponential distribution, $F(t)$ regarding t_0 and τ is calculated by Equations 4.17 and 4.18.

$$F(t = t_0) = e^{-q(t_0 - \tau)} \tag{4.17}$$

$$F(t = \tau) = 0 \tag{4.18}$$

When m major streams which are independent each other exist, e.g., major streams from two directions, total free space probability P_F^m becomes the product result of the probabilities of free space of all flows as shown in Equation 4.19.

$$P_F^m = \prod_{k=1}^{m} P_F^k = \prod_{k=1}^{m} P_{0,S}^k \prod_{k=1}^{m} P_{0,B}^k \prod_{k=1}^{m} P_{0,Q}^k \qquad m \in \mathrm{N} = \{1,2,3,\cdots,n\} \tag{4.19}$$

Accordingly, capacity of minor road traffic c^{minor} crossing m independent major streams is estimated by Equation 4.20.

$$c^{\min or} = c_{\max} P_F = c_{\max} \prod_{k=1}^{m} P_F^k \tag{4.20}$$

4.2.2 Assumptions

Entry vehicles pass pedestrian flow through available gaps of pedestrians, which is similar

as merging into circulating flow. Thus, impact of pedestrians in this study is estimated based on gap acceptance theory. In order to calculate this impact, several assumptions are needed as follows.

- Pedestrians walk on crosswalk as the straight line parallel to the crosswalk;
- Pedestrians from different directions walk in different lines;
- Pedestrians in one walking line is independent to ones in another line;
- Pedestrians do not change the line during walking;
- Overtaking behavior does not occur in each pedestrian walking line on crosswalk;
- Headway of pedestrians in each walking line is assumed to follow shifted-negative exponential distribution.

Based on these assumptions, pedestrians are assigned to cross as different walking lines, which are independent each other. n_{Wl} is defined as the maximum number of walking lines in crosswalk, which is determined by the width of crosswalk w_c and social distance between pedestrians. s_R, s_L is defined as right and left distance when a pedestrian keeps to another, which is assumed to be 0.5m in this study. Thus, n_l is calculated by Equation 4.21. The illustration of social distance is shown in Figure 4.4.

$$n_{Wl} = [\frac{w_c}{s_L} + 1] \in I = \{2,3,\cdots,n\} \tag{4.21}$$

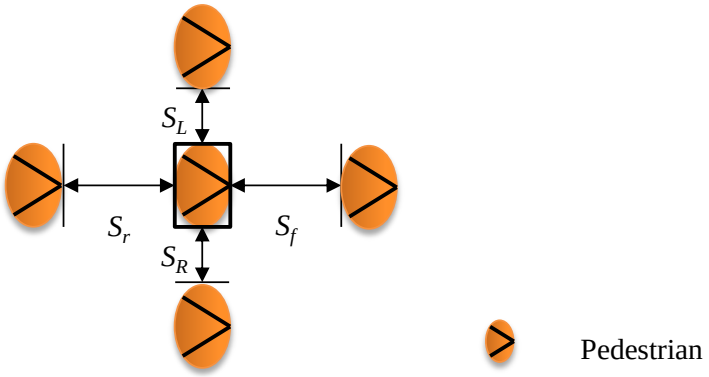

Figure 4.4 The illustration of social distance

Pedestrian approaching side is classified into near-side and far-side based on direction of

entry flow. The parameter of r_{far} is utilized here to calculate the number of walking lines for pedestrians from each direction. Thus, number of walking lines for near-side and far-side pedestrian n_{Wl}^{N} and n_{Wl}^{F} is calculated by the proportion (1-r_{far}) and r_{far} as shown in Equations 4.22 and 4.23.

$$n_{Wl}^{N} = [(1 - r_{far}) n_{Wl}] \in I = \{0,1,2,\cdots, n_{Wl}\} \tag{4.22}$$

$$n_{Wl}^{F} = [r_{far} n_{Wl}] \in I = \{0,1,2,\cdots, n_{Wl}\} \tag{4.23}$$

Pedestrian demand in each walking line is assigned by α_i or α_j, which is defined as the proportion of pedestrian demand in walking line i (j) in total near-side (far-side) pedestrian demand. The illustration is shown in Figure 4.5. Regarding these lines of pedestrians, it is assumed that entry drivers judge all the lines simultaneously. Accordingly, in view of mathematical derivation process, the assumption regarding the left/right social distance (S_L=S_R=0.5m) will actually not have impact on the result of the proposed model.

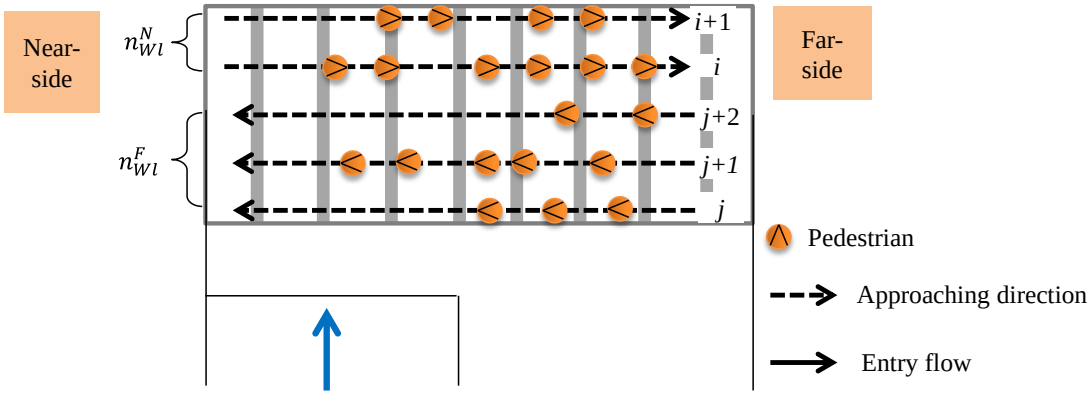

Figure 4.5 The illustration of pedestrian walking lines

Here, far-side pedestrian recognition rate FPRR can be realized by multiplying the parameter FPRR on α_j (on α_i for exit vehicles) since FPRR actually is a parameter reflecting the percentage of far-side pedestrians who are recognized by entry vehicles (exit vehicles for near-side pedestrians).

At roundabout, pedestrian and circulating flows are major streams. Thus, an entry vehicle will at most cross n_{Wl}^{N} near-side pedestrian flows, n_{Wl}^{F} far-side pedestrian flows and one circulating flow before entering roundabout and all flows are assumed to be independent.

Dependent on Wu's theory (2001), $g(q_{ped}, q_{cir})$ can be estimated by Equation 4.24.

$$g(q_{ped},q_{cir}) = c_{\max}\left(\prod_{i=1}^{n_{Wl}^{N}} P_{0,S}^{i}\prod_{i=1}^{n_{Wl}^{N}} P_{0,B}^{i}\prod_{i=1}^{n_{Wl}^{N}} P_{0,Q}^{i}\prod_{j=1}^{n_{Wl}^{F}} P_{0,S}^{j}\prod_{j=1}^{n_{Wl}^{F}} P_{0,B}^{j}\prod_{j=1}^{n_{Wl}^{F}} P_{0,Q}^{i}\right) P_{0,S}^{cir} P_{0,B}^{cir} P_{0,Q}^{cir} \quad (4.24)$$

4.3 Estimation of P_{queue}

At downstream Exit X (referring to N, E or W), exit vehicles have conflict with pedestrians and cross pedestrian flow by available gaps of pedestrians. Thus, a queue of exit vehicles may be generated when there is no available gap in pedestrian flow. Exit vehicles and pedestrians form a queuing system, which pedestrian flow plays a role of service centre. Both headway distributions of exit vehicles and pedestrians are assumed to follow shifted-negative exponential distribution. P_{queue} is the probability of the queue in circulating roadway reaching up to front of Entry S. For Exit X, n_b^{XS} is defined as the maximum number of vehicles which can be stored between downstream Exit X and Entry S. $P_{nb}{}^{XS}$ is defined as probability of n_b^{XS} vehicles queuing in circulating roadway. P_{queue} is calculated as the maximum value of $P_{nb}{}^{XS}$ in all downstream exits as shown in Equation 4.25.

$$P_{queue} = \max\left(P_{n_b}^{XS}\right) \quad (4.25)$$

According to queue theory, $P_{nb}{}^{XA}$ can be calculated by Equation 4.26.

$$P_{n_b}^{XS} = \left(1-\frac{\lambda_X}{\mu_{ped}^{X}}\right)\left(\frac{\lambda_X}{\mu_{ped}^{X}}\right)^{n_b^{XS}} \quad (4.26)$$

where λ_X =arrival rate of vehicles exiting from the downstream Exit X

μ_{ped}^{X} =service rate which is the reciprocal value of the average service time

λ_X is related to the circulating flow passing in front of Entry S. α_D^X is defined as the proportion of demand of vehicles exiting from the downstream Exit X in circulating flow q_{cir} passing in front of Entry S. It is calculated by Equation 4.27.

$$\lambda_X = \frac{\alpha_D^X q_{cir}}{3600} \tag{4.27}$$

Since pedestrian flow plays a role of service center and exit vehicles cross pedestrian flow dependent on available gaps of pedestrians, service time is defined as the total time of rejected gaps between two acceptable gaps. Dependent on Siegloch's model (1975), exit vehicles cannot cross pedestrian flow when headway *t* of pedestrians is shorter than t_0^X. Service rate μ_{ped}^X is calculated by the probability of headway *t* under the condition $t < t_0^X$. The same assumptions regarding pedestrians across Entry S (setting of walking lines for pedestrians from different sides which is defined as $n_{Wl}^{N\_X}$ and $n_{Wl}^{F\_X}$ for pedestrians from near-side and far-side, respectively) are given to pedestrians across Exit X as well and dependent on Wu's theory (2001), μ_{ped}^X is calculated based on probability of free space P_F^X as shown in Equation 4.28.

$$\mu_{ped}^X = 1 - P_F^X = 1 - \prod_{i=1}^{n_{Wl}^{N\_X}} P_{0,S}^i \prod_{i=1}^{n_{Wl}^{N\_X}} P_{0,B}^i \prod_{i=1}^{n_{Wl}^{N\_X}} P_{0,Q}^i \prod_{i=1}^{n_{Wl}^{F\_X}} P_{0,S}^i \prod_{i=1}^{n_{Wl}^{F\_X}} P_{0,B}^i \prod_{i=1}^{n_{Wl}^{F\_X}} P_{0,Q}^i \tag{4.28}$$

Finally, based on Equations 4.3, 4.14 and 4.25, roundabout entry capacity c^S including cases (a) and (b) can be estimated.

4.4 Examination of proposed theoretical model

4.4.1 Assumptions and input conditions

The proposed theoretical model is examined under the following assumptions.

- Physical splitter islands are assumed to install at Entries N, E, W;
- Two conditions of physical splitter island are assumed at Entry S: with/without;
- Pedestrians from different sides are assumed to walk on different lines and lane changing behavior and overtaking behavior regarding pedestrians are not allowed during crossing;
- Since gap acceptance theory is applied on pedestrians, it is assumed that the values of t_f of entry vehicles crossing pedestrian flow and merging into circulating flow are

identical and equal to the value which is input in simulation, t_f=3.2sec. In addition, this value is applied for each pedestrian walking line. On the other hand, the value of t_c of pedestrians is calculated by the simulation input values based on the relationship of gaps which is shown in Figure 3.21 and the values in Table 3.8. Thus, under the condition with physical splitter island, t_c^{Near}=t_c^{Far}=6.2 sec for both sides pedestrians whereas under the condition without physical splitter island, t_c^{Near} =6.2 and t_c^{Far}=10.5 for the near-side and far-side pedestrians.

- Regarding the queue event in circulating roadway, it is assumed that entry vehicles cannot enter roundabout when the number of queuing vehicle in circulating roadway reaches the maximum value and the vehicles at Entry S can enter roundabout again immediately after the queuing vehicles find an accepted gap of pedestrians to cross at downstream exit;
- Circulating flow: 0~1200veh/h with interval of 100veh/h;
- Pedestrian flow at Entry S: 0~200ped/h with interval of 50ped/h.
- $r_{far}^{N} = r_{far}^{E} = r_{far}^{W} = 0.5$
- $FPRR^{N}$=$FPRR^{E}$=$FPRR^{W}$=0.5
- The percentage of pedestrian demand in each walking line is identical at any entry, i.e. α_i=α_{i+1}, α_j=α_{j+1};
- Minimum headway between pedestrians τ_{ped} is set based on front/rear social distance which is assumed to be 2m in this research and pedestrian walking speed which is input in simulation (3.6km/h). Thus, τ_{ped}=2sec.
- German formula (Equation 2.25) is applied for $f(q_{cir})$

The detailed input values are shown in Table 4.1.

Table 4.1 Parameters setting for examining theoretical model

Parameter	Value	Parameter	Value

n_a	1 vehicle	$n_b^{WA} = n_b^{NA} = n_b^{EA}$	3/5/7 vehicles
$w_c^S = w_c^W = w_c^N = w_c^E$ (m)	2.00	t_f (sec)	3.20
t_c^{Near} (with) (sec)	6.20	t_c^{Far} (without) (sec)	10.5
t_c^{Near} (with/without) (sec)	6.20	t_{c_cir}	4.50
τ_{cir} (sec)	2.20	τ_{ped} (sec)	2.00

4.4.2 Results and discussions

Figure 4.6 shows the estimation result of entry capacity under the conditions (1) no pedestrians across other entries (2) with physical splitter island at Entry S; (3) r_{far}=0.5 and (4) FPRR=0.5. It is found that estimated entry capacity is reduced with increase of circulating flow and pedestrian flow, which follows the results described in other existing methods (e.g., HCM, 2010).

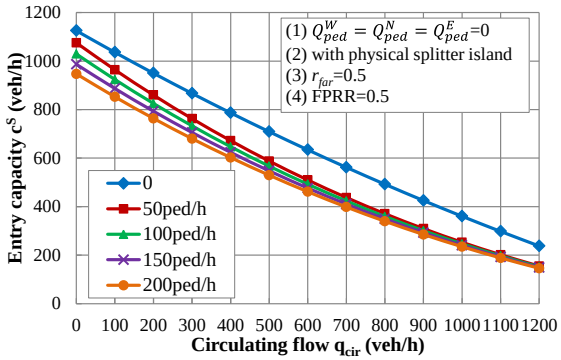

Figure 4.6 Estimated entry capacity changing with circulating and pedestrian flows under the fixed condition and input values

Examination of pedestrian approaching side

Figure 4.7 plots the estimated entry capacity considering pedestrian approaching side under the conditions (1) without physical splitter island; (2) no pedestrians across other entries and (3) FPRR=1. The results under the pedestrian demands of 50ped/h, 100ped/h and 200ped/h were selected as the examples shown in Figure 4.7(a), (b) and (c), respectively.

It is found that under the condition without physical splitter island, entry capacity is reduced more significantly when all pedestrians are from far-side in each level of pedestrian demand. The results follow the simulation output which is shown in Chapter 3.

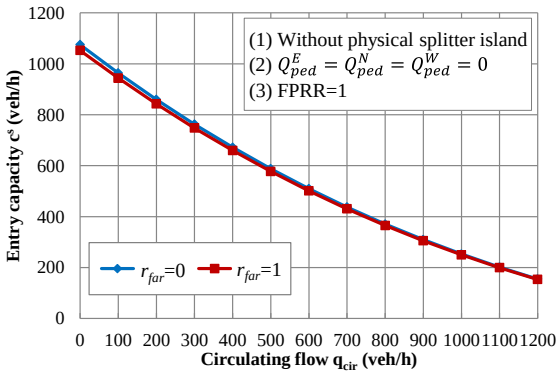

(a) Pedestrian demand at Entry S: 50ped/h

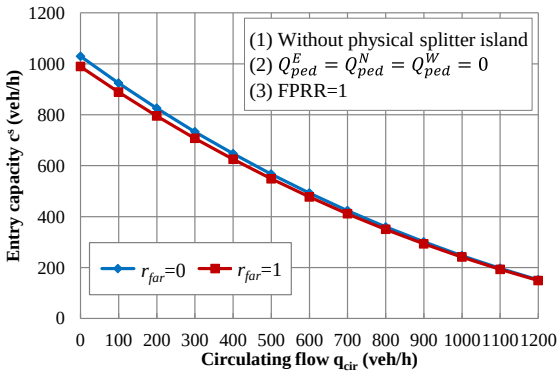

(b) Pedestrian demand at Entry S: 100ped/h

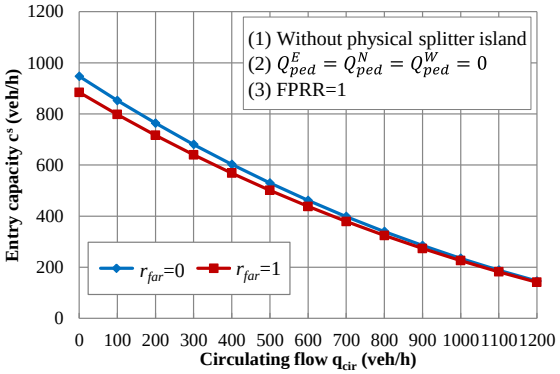

(c) Pedestrian demand at Entry S: 200ped/h

Figure 4.7 Examination of pedestrian approaching sides from the proposed model under the condition without physical splitter island

Examination of far-side pedestrian recognition rate FPRR (%)

Figure 4.8 represents the estimated entry capacity regarding FPRR under the conditions (1) without physical splitter island; (2) no pedestrians across other entries and (3) r_{far}=1 at Entry S. The results under the pedestrian demands of 50ped/h, 100ped/h and 200ped/h were selected as the examples and show in Figure 4.8(a), (b) and (c), respectively. It was found that under a certain level of pedestrian demand, entry capacity is reduced with the increase of FPRR. Entry capacity performs the lowest and highest value under the rate of 100% and 0, respectively.

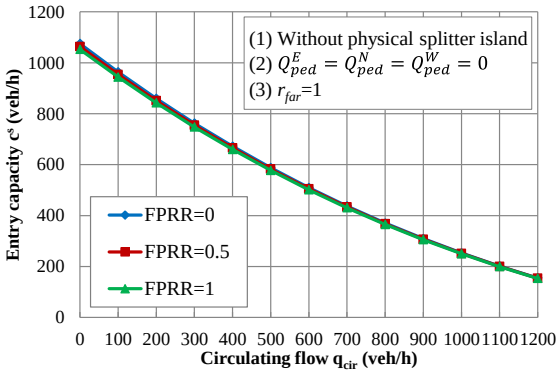

(a) Pedestrian demand at Entry S: 50ped/h

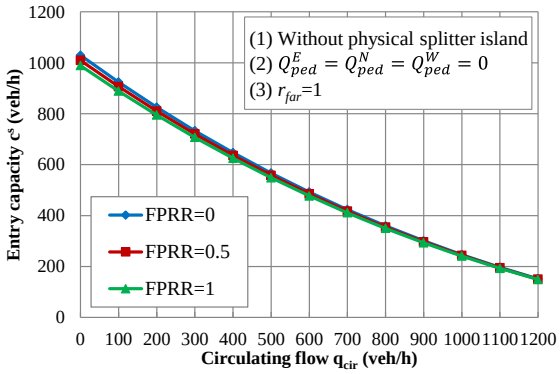

(b) Pedestrian demand at Entry S: 100ped/h

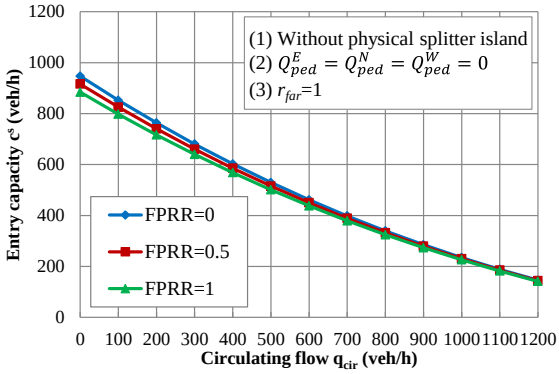

(c) Pedestrian demand at Entry S: 200ped/h

Figure 4.8 Examination of FPRR considering pedestrians from far-side

It is found that estimated entry capacity from the proposed model is reduced when FPRR increases. These results also follow the simulation output.

Examination of physical splitter island

The results of estimated entry capacity considering with/without physical splitter island and under the conditions (1) no pedestrians across other entries; (2) r_{far}=1 at Entry S and (3) FPRR=1 are shown in Figure 4.9. All pedestrians are assigned from far-side and recognized by entry vehicles. The results under the pedestrian demands of 50ped/h, 100ped/h and 200ped/h were selected as the examples and show in Figure 4.9(a), (b), (c), respectively.

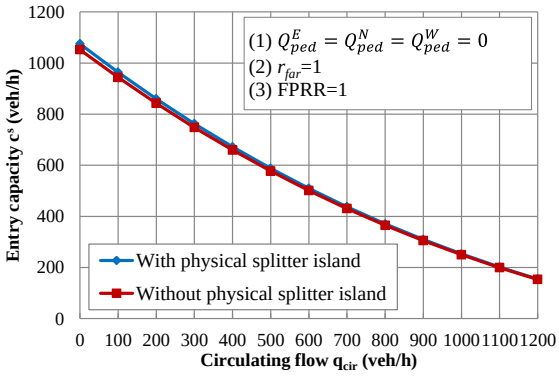

(a) Pedestrian demand at Entry S: 50ped/h

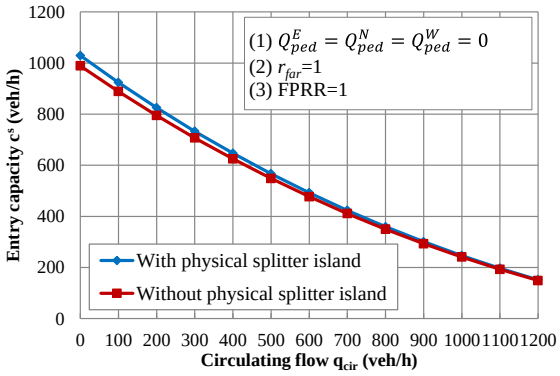

(b) Pedestrian demand at Entry S: 100ped/h

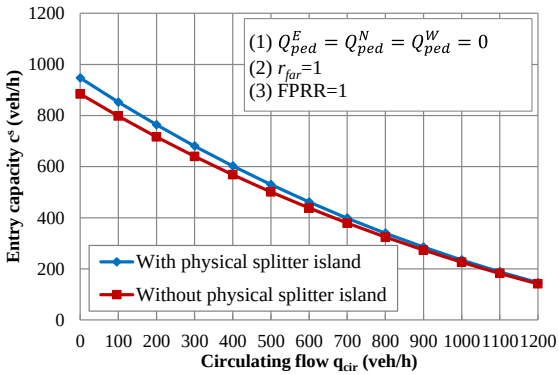

(a) Pedestrian demand at Entry S: 200ped/h

Figure 4.9 Examination of physical splitter island considering pedestrians from far-side

From the sensitivity examination, it is found that the estimated entry capacity reduced more under the condition without physical splitter island. This tendency was also observed in simulation analysis.

Examination of distance between crosswalk and yield line

In the proposed model, the distance between crosswalk and yield line is controlled by the parameter n_a which is the maximum number of vehicles can be stored in the space between crosswalk and yield line. The examination of n_a is conducted under the condition with/without physical splitter island. When physical splitter island is assumed to be installed, several conditions, i.e. (1) no pedestrians are set at Entries N, W and E and (2) r_{far}=0.5 at Entry S are required. When physical splitter island is assumed not to be installed, an additional condition, i.e. FPRR=0.5 at Entry S is set based on the conditions which are set for the situation without physical splitter island.

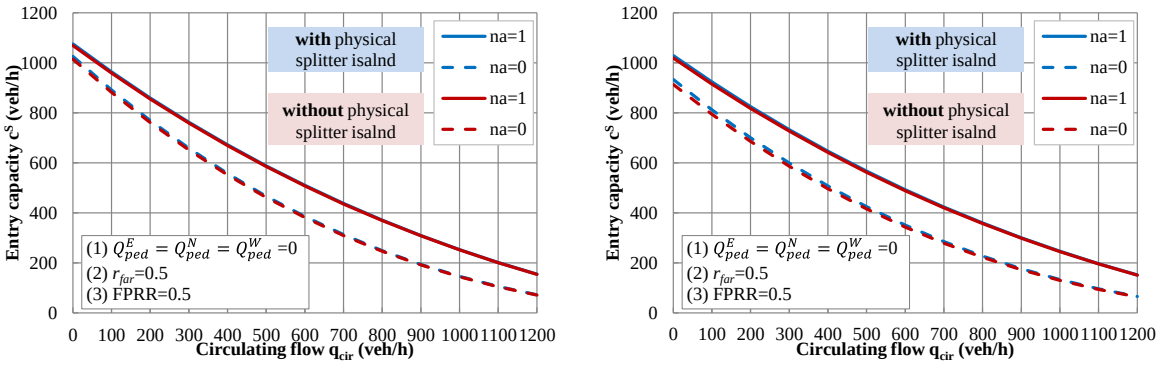

(a) Pedestrian demand at Entry S: 50ped/h (b) Pedestrian demand at Entry S: 100ped/h

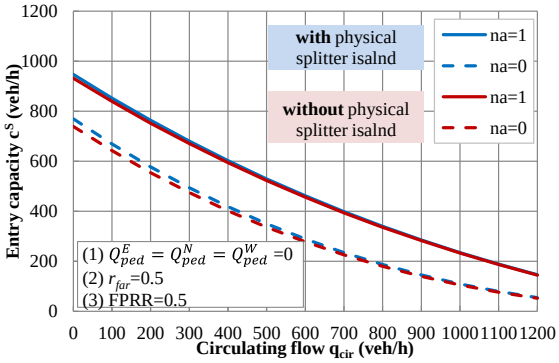

(a) Pedestrian demand at Entry S: 200ped/h

Figure 4.10 Examination of physical splitter island considering pedestrians from far-side

Figure 4.10 shows the results of estimated entry capacity regarding the cases n_a=0 and n_a=1. The results under the pedestrian demands of 50ped/h, 100ped/h and 200ped/h were selected as the examples and show in Figure 4.10(a), (b), (c), respectively. It was found

that under the condition either with or without physical splitter island, estimated entry capacity is reduced more when n_a=0 comparing to the situation n_a=1. In addition, the difference between two cases becomes larger when pedestrian demand at Entry S increases. The results from the proposed model follow the ones from simulation study.

Examination of pedestrians across at other entries

Figure 4.11 represents the estimated entry capacity regarding pedestrians across other entries under the conditions (1) with physical splitter island; (2) identical pedestrians demand at other entries and (3) no pedestrians across Entry S. (3). Based on the input conditions, the highest probability of queuing vehicle P_{queue} in circulating roadway is always observed at the adjacent downstream exit Exit W due to the smaller space to Entry S comparing to other exits. From the result of examination, it is found that entry capacity is reduced with the increase of pedestrian demand. The similar results were obtained in simulation analysis

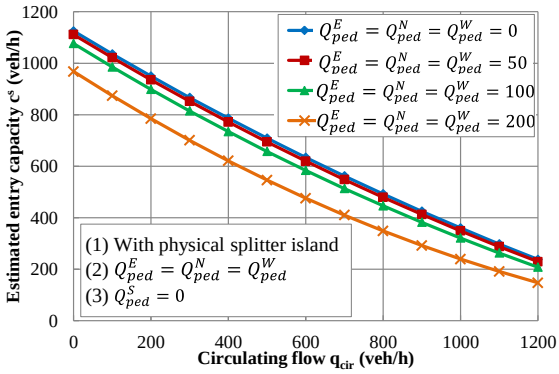

Figure 4.11 Estimated entry capacity changing with pedestrians across other entries

4.5 Summary

In this chapter, a theoretical model was developed for estimating roundabout entry capacity considering the influencing factors, i.e., physical splitter island, pedestrian approaching side, far-side pedestrian recognition rate, distance between crosswalk and yield line and queuing vehicles blocked by pedestrians across downstream exits. The impact of these influencing factors has been examined in the previous chapter. In this proposed model, impact of pedestrian is considered based on gap acceptance theory, instead of an adjustment factor, since in real world entry drivers cross pedestrian flow by available gaps

of pedestrians which is similar to merging into circulating flow. The impacts of all influencing factors are realized through inputting parameters, e.g. t_c^{Nar}, t_c^{Far} and so on. Through sensitivity analyses it was found that the changing tendency of estimated entry capacity follows the results which were obtained by simulation analysis. Thus, it can be concluded that the impacts of influencing factors which are considered in simulation are successfully reflected in this proposed theoretical model.

5 Chapter 5

COMPARISON OF PROPOSED ESTIMATION METHODS AND THEIR APPLICATION IN PRACTICE

5.1 Comparison of the results from simulation and theoretical model

Considering one curve of entry capacity changing with circulating flow as one case, in the simulation analysis, totally 49 cases were conducted in Chapter 3 considering the influencing factors, i.e. physical splitter island, far-side pedestrian directional ratio, far-side pedestrian recognition rata and pedestrians across other entries. The information of all cases is shown in Table 5.1. The cases under the condition with/without physical splitter island are shown in Table 5.1(a) and (b), respectively. Since pedestrian approaching sides and far-side pedestrian recognition rate do not have impact on entry capacity under the condition with physical splitter island, the cases are only classified by pedestrian demand at other entries.

Table 5.1 All examined cases with information in simulation analysis

(a) With physical splitter island			
1	$Q_{ped}^{N} = Q_{ped}^{E} = Q_{ped}^{W} = 0$ D_{cy}=1m	2	$Q_{ped}^{N} = Q_{ped}^{E} = Q_{ped}^{W} = 0$ D_{cy}=5m

3	$Q_{ped}^{N} = Q_{ped}^{E} = Q_{ped}^{W} = 50$ D_{cy}=5m		4	$Q_{ped}^{N} = Q_{ped}^{E} = Q_{ped}^{W} = 100$ D_{cy}=5m	
5	$Q_{ped}^{N} = Q_{ped}^{E} = Q_{ped}^{W} = 150$ D_{cy}=5m		6	$Q_{ped}^{N} = Q_{ped}^{E} = Q_{ped}^{W} = 200$ D_{cy}=5m	
(b) Without physical splitter island					
7	$Q_{ped}^{N} = Q_{ped}^{E} = Q_{ped}^{W} = 0$ r_{far}=0, FPRR=0 D_{cy}=5m		8	$Q_{ped}^{N} = Q_{ped}^{E} = Q_{ped}^{W} = 0$ r_{far}=0, FPRR=0.5 D_{cy}=5m	9	$Q_{ped}^{N} = Q_{ped}^{E} = Q_{ped}^{W} = 0$ r_{far}=0, FPRR=1 D_{cy}=5m
10	$Q_{ped}^{N} = Q_{ped}^{E} = Q_{ped}^{W} = 0$ r_{far}=0.5, FPRR=0 D_{cy}=5m		11	$Q_{ped}^{N} = Q_{ped}^{E} = Q_{ped}^{W} = 0$ r_{far}=0.5, FPRR=0.5 D_{cy}=5m	12	$Q_{ped}^{N} = Q_{ped}^{E} = Q_{ped}^{W} = 0$ r_{far}=0.5, FPRR=1 D_{cy}=5m
13	$Q_{ped}^{N} = Q_{ped}^{E} = Q_{ped}^{W} = 0$ r_{far}=1, FPRR=0 D_{cy}=5m		14	$Q_{ped}^{N} = Q_{ped}^{E} = Q_{ped}^{W} = 0$ r_{far}=1, FPRR=0.5 D_{cy}=5m	15	$Q_{ped}^{N} = Q_{ped}^{E} = Q_{ped}^{W} = 0$ r_{far}=1, FPRR=1 D_{cy}=5m
16	$Q_{ped}^{N} = Q_{ped}^{E} = Q_{ped}^{W} = 50$ r_{far}=0, FPRR=0 D_{cy}=5m		17	$Q_{ped}^{N} = Q_{ped}^{E} = Q_{ped}^{W} = 50$ r_{far}=0, FPRR=0.5 D_{cy}=5m	18	$Q_{ped}^{N} = Q_{ped}^{E} = Q_{ped}^{W} = 50$ r_{far}=0, FPRR=1 D_{cy}=5m
19	$Q_{ped}^{N} = Q_{ped}^{E} = Q_{ped}^{W} = 50$ r_{far}=0.5, FPRR=0 D_{cy}=5m		20	$Q_{ped}^{N} = Q_{ped}^{E} = Q_{ped}^{W} = 50$ r_{far}=0.5, FPRR=0.5 D_{cy}=5m	21	$Q_{ped}^{N} = Q_{ped}^{E} = Q_{ped}^{W} = 50$ r_{far}=0.5, FPRR=1 D_{cy}=5m
22	$Q_{ped}^{N} = Q_{ped}^{E} = Q_{ped}^{W} = 50$ r_{far}=1, FPRR=0 D_{cy}=5m		23	$Q_{ped}^{N} = Q_{ped}^{E} = Q_{ped}^{W} = 50$ r_{far}=1, FPRR=0.5 D_{cy}=5m	24	$Q_{ped}^{N} = Q_{ped}^{E} = Q_{ped}^{W} = 50$ r_{far}=1, FPRR=1 D_{cy}=5m
25	$Q_{ped}^{N} = Q_{ped}^{E} = Q_{ped}^{W} = 100$ r_{far}=0, FPRR=0 D_{cy}=5m		26	$Q_{ped}^{N} = Q_{ped}^{E} = Q_{ped}^{W} = 100$ r_{far}=0, FPRR=0.5 D_{cy}=5m	27	$Q_{ped}^{N} = Q_{ped}^{E} = Q_{ped}^{W} = 100$ r_{far}=0, FPRR=1 D_{cy}=5m
28	$Q_{ped}^{N} = Q_{ped}^{E} = Q_{ped}^{W} = 100$ r_{far}=0.5, FPRR=0 D_{cy}=5m		29	$Q_{ped}^{N} = Q_{ped}^{E} = Q_{ped}^{W} = 100$ r_{far}=0.5, FPRR=0.5 D_{cy}=5m	30	$Q_{ped}^{N} = Q_{ped}^{E} = Q_{ped}^{W} = 100$ r_{far}=0.5, FPRR=1 D_{cy}=5m
31	$Q_{ped}^{N} = Q_{ped}^{E} = Q_{ped}^{W} = 100$ r_{far}=1, FPRR=0 D_{cy}=5m		32	$Q_{ped}^{N} = Q_{ped}^{E} = Q_{ped}^{W} = 100$ r_{far}=1, FPRR=0.5 D_{cy}=5m	33	$Q_{ped}^{N} = Q_{ped}^{E} = Q_{ped}^{W} = 100$ r_{far}=1, FPRR=1 D_{cy}=5m

34	$Q_{ped}^{N}=Q_{ped}^{E}=Q_{ped}^{W}=150$ r_{far}=0, FPRR=0 D_{cy}=5m	35	$Q_{ped}^{N}=Q_{ped}^{E}=Q_{ped}^{W}=150$ r_{far}=0, FPRR=0.5 D_{cy}=5m	36	$Q_{ped}^{N}=Q_{ped}^{E}=Q_{ped}^{W}=150$ r_{far}=0, FPRR=1 D_{cy}=5m
37	$Q_{ped}^{N}=Q_{ped}^{E}=Q_{ped}^{W}=150$ r_{far}=0.5, FPRR=0 D_{cy}=5m	38	$Q_{ped}^{N}=Q_{ped}^{E}=Q_{ped}^{W}=150$ r_{far}=0.5, FPRR=0.5 D_{cy}=5m	39	$Q_{ped}^{N}=Q_{ped}^{E}=Q_{ped}^{W}=150$ r_{far}=0.5, FPRR=1 D_{cy}=5m
40	$Q_{ped}^{N}=Q_{ped}^{E}=Q_{ped}^{W}=150$ r_{far}=1, FPRR=0 D_{cy}=5m	41	$Q_{ped}^{N}=Q_{ped}^{E}=Q_{ped}^{W}=150$ r_{far}=1, FPRR=0.5 D_{cy}=5m	42	$Q_{ped}^{N}=Q_{ped}^{E}=Q_{ped}^{W}=150$ r_{far}=1, FPRR=1 D_{cy}=5m
43	$Q_{ped}^{N}=Q_{ped}^{E}=Q_{ped}^{W}=200$ r_{far}=0, FPRR=0 D_{cy}=5m	44	$Q_{ped}^{N}=Q_{ped}^{E}=Q_{ped}^{W}=200$ r_{far}=0, FPRR=0.5 D_{cy}=5m	45	$Q_{ped}^{N}=Q_{ped}^{E}=Q_{ped}^{W}=200$ r_{far}=0, FPRR=1 D_{cy}=5m
46	$Q_{ped}^{N}=Q_{ped}^{E}=Q_{ped}^{W}=200$ r_{far}=0.5, FPRR=0 D_{cy}=5m	47	$Q_{ped}^{N}=Q_{ped}^{E}=Q_{ped}^{W}=200$ r_{far}=0.5, FPRR=0.5 D_{cy}=5m	48	$Q_{ped}^{N}=Q_{ped}^{E}=Q_{ped}^{W}=200$ r_{far}=0.5, FPRR=1 D_{cy}=5m
49	$Q_{ped}^{N}=Q_{ped}^{E}=Q_{ped}^{W}=200$ r_{far}=1, FPRR=0 D_{cy}=5m	50	$Q_{ped}^{N}=Q_{ped}^{E}=Q_{ped}^{W}=200$ r_{far}=1, FPRR=0.5 D_{cy}=5m	51	$Q_{ped}^{N}=Q_{ped}^{E}=Q_{ped}^{W}=200$ r_{far}=1, FPRR=1 D_{cy}=5m
52	$Q_{ped}^{N}=Q_{ped}^{E}=Q_{ped}^{W}=0$ r_{far}=0.5, FPRR=0.5 D_{cy}=1m				

Considering the real situation, the cases 3 and 20 are selected for the comparison of the entry capacity which is estimated by simulation analysis and proposed theoretical model. Figure 5.1 and Figure 5.2 show the comparison of each case and pedestrian demand of 0, 50ped/h, 100ped/h and 200ped/h at Entry S are chosen as the examples and shown in (a)~(d) in each figure. In order to evaluate the relative margin of estimation errors, one statistic is applied: *Mean Absolute Percentage Error* (*MAPE*). *MAPE* returns the absolute percentage difference in both values. The equation is provided below.

$$MAPE_i = \left(\frac{1}{N} \sum_{i=1}^{N} \frac{| x_i - \hat{x}_i |}{x_i} \right) \cdot 100\% \tag{5.1}$$

where x_i = the estimated results of proposed theoretical model

$\hat{x}_i$ = the estimate results from simulation analysis

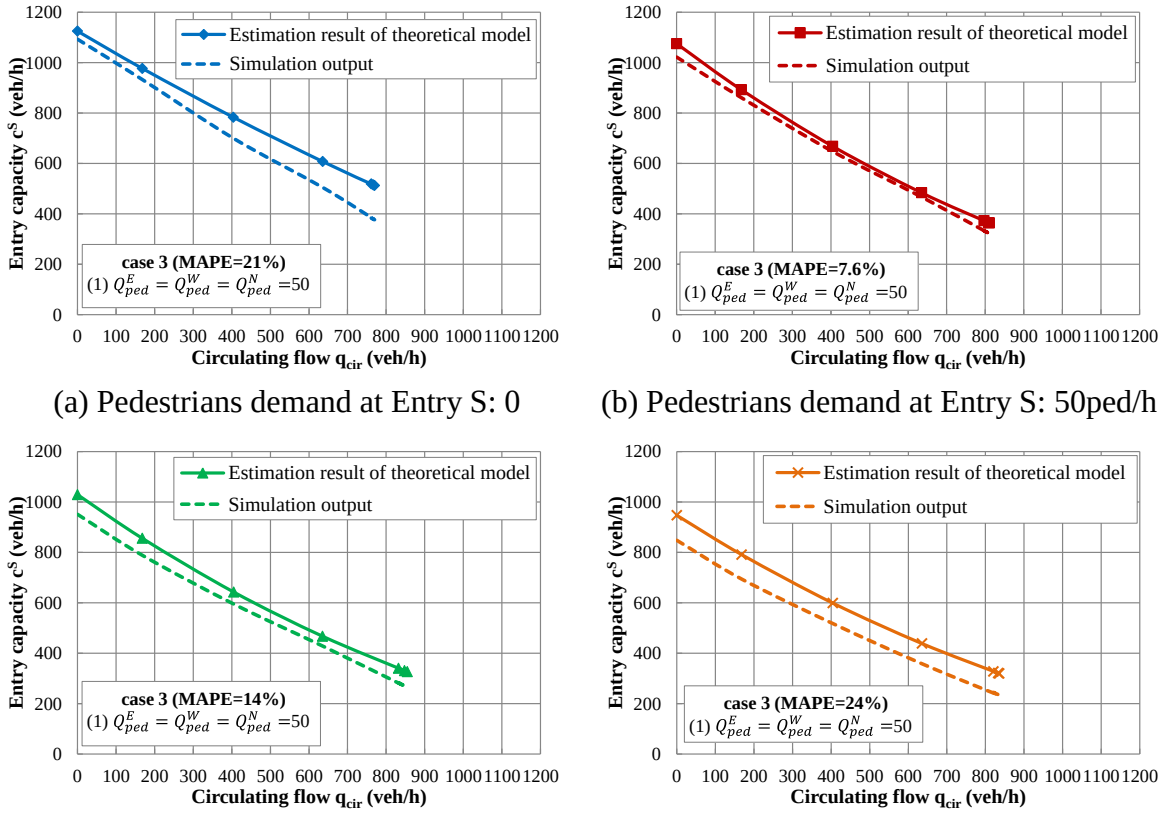

(a) Pedestrians demand at Entry S: 0

(b) Pedestrians demand at Entry S: 50ped/h

(c) Pedestrians demand at Entry S: 100ped/h

(d) Pedestrians demand at Entry S: 200ped/h

Figure 5.1 Comparison of the estimated entry capacity regarding case 3

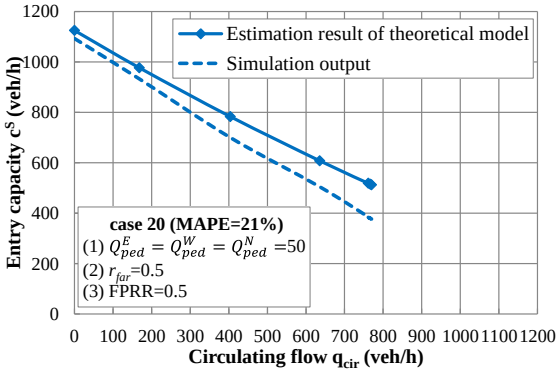

(a) Pedestrians demand at Entry S: 0

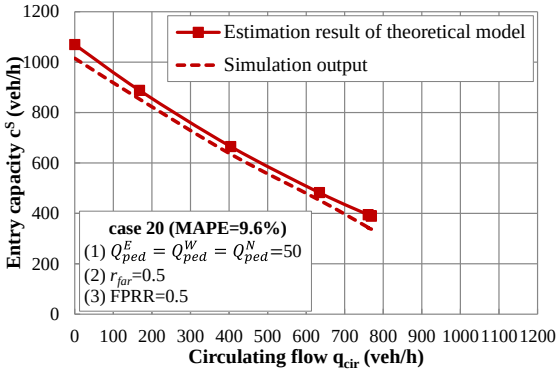

(b) Pedestrians demand at Entry S: 50ped/h

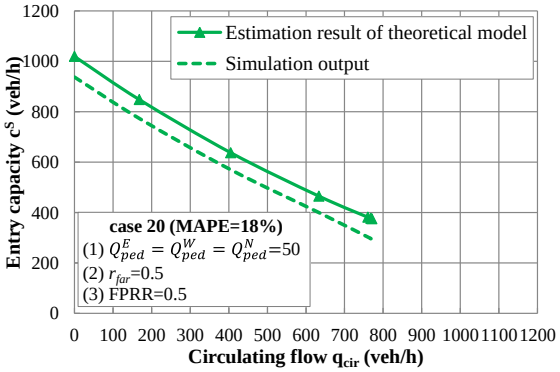

(c) Pedestrians demand at Entry S: 100ped/h

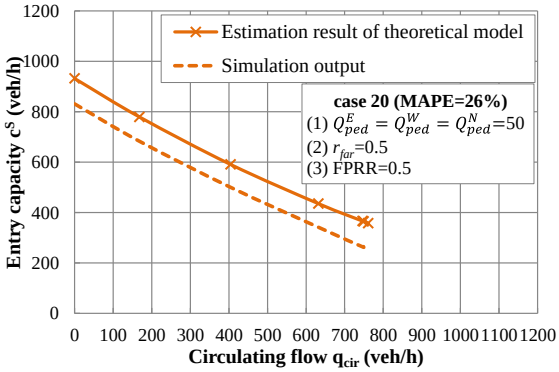

(d) Pedestrians demand at Entry S: 200ped/h

Figure 5.2 Comparison of the estimated entry capacity regarding case 20

From the comparison it is found that circulating flow in simulation output is lower than that assumed in theoretical model. Actually, this can be observed in all cases. The reason has been explained in Chapter 3 section 3.4.1. Circulating flow passing in front of Entry S is formed by the vehicles from other entries which are also affected by circulating vehicles. Heavy entry flow makes high level of circulating flow which prevents entry vehicle entering roundabout. Thus, circulating flow will not unlimited increase.

Then, the difference between simulation output and the results of theoretical model is observed from the two figures. The results from simulation are lower than that from proposed theoretical model in the two cases at each level of pedestrian demand. In addition, the difference becomes larger when pedestrian demand at Entry S increases. In both cases, the maximum MAPE is observed when pedestrian demand is 200ped/h.

The difference between the two methods is supposed to generate by the limitations of the

methods.

In the theoretical model, regarding blocking event in circulating roadway due to the pedestrians across downstream exits, it is assumed that entry vehicles cannot enter roundabout when the number of queuing vehicle in circulating roadway reaches the maximum value and the vehicles at Entry S can enter roundabout again immediately after the queuing vehicles find an accepted gap of pedestrians to cross at downstream exit. This assumption does not consider the discharge time of queuing vehicles. While, this discharge time can be directly reflected in simulation as shown in Figure 5.3. This assumption may result in overestimation result of theoretical model.

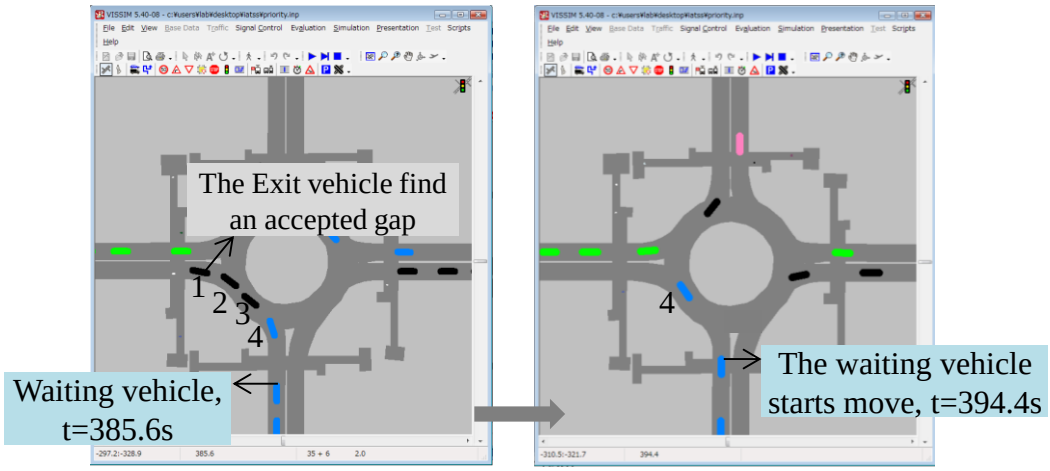

Figure 5.3 Discharge time of queue in simulation

Another possible reason is related to the headway distribution function $h(t)$ which is utilized in theoretical model. In the function of $h(t)$, free flow form upstream is assumed and then a negative exponential function was obtained. Under this assumption, the cross of the entry and the circulating roadway in front of this entry is likely to be considered as T-intersection as shown in Figure 5.4(a). However, in reality, circulating flow is not a free flow. It is significantly influenced by the geometry of the circulating roadway. Moreover, since circulating flow is composed by vehicles from other entries as shown in Figure 5.4(b), it is also affected by the traffic situations, e.g. priority of the road (major/minor) and turning ratio at other upstream entries. These impacts on circulating flow can be directly reflected in simulation but not included in the theoretical model.

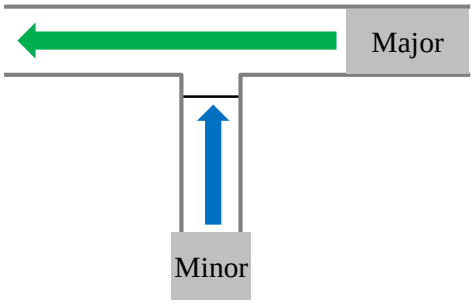

(a) Development environment of $h(t)$ in existing theoretical model

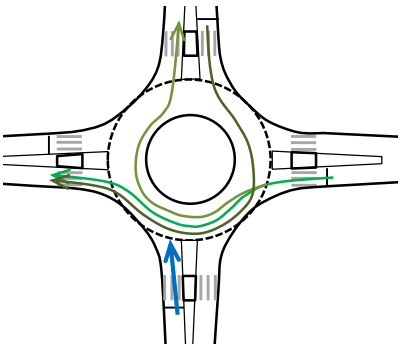

(b) Real situation of circulating flow at roundabout

Figure 5.4 Considerations of circulating flow in theoretical model and simulation

Moreover, blocking events of exit vehicles at the same lag and pedestrians also have impact on the arrival pattern of circulating vehicles which is not considered in the proposed model. Thus, headway distribution of circulating vehicles may not follow the negative exponential function. In simulation, entry capacity is directly collected and all the impacts of priority of roads, turning ratio and impact from upstream entries have been included. Thus, entry capacity may be overestimated by theoretical model due to these non-considerations on the impact of upstream entries.

On the other hand, the pedestrian behavior in simulation cannot be calibrated due to limited number of samples. This limitation of simulation analysis is also the possible reason to cause difference between two methods.

The limitations of each method are described in Table 5.2.

Table 5.2 Limitations of simulation and theoretical model

Simulation	Theoretical model
1. Calibration of pedestrian behavior is necessary	1.The discharge time of queue in circulating roadway is necessary to be considered
	2. Several influencing factors, i.e. priority of roads, turning ratio, queuing exit vehicles at the lag which have impact on headway distribution of circulating vehicles should be considered

5.2 Comparison of the proposed methods and the existing model f_{pedSB}

The adjustment factor f_{pedSB} is the one which is applied in HCM 2010 for considering pedestrian impact on entry capacity. In this section, both two proposed methods are compared to this f_{pedSB}. The estimated result from f_{pedSB} is calculated based on the Equation 2.30. In order to focus on identifying the effect of f_{pedSB}, c_{cir} in this equation is input by the German formula which is utilized in theoretical model or the simulation output under the condition only with circulating vehicles. f_{pedSB} is calculated by Equations 2.37~2.39 dependent on the demand of circulating vehicles and pedestrians. Since f_{pedSB} model was developed for the roundabout with physical splitter island, the cases 1 in simulation and the results from theoretical model under the same input conditions are selected.

Estimation results from f_{pedSB} model and two proposed methods are shown in Figure 5.5 and Figure 5.6. The results under pedestrian demands of 100ped/h and 200ped/h are selected as the examples. It is found that, at each level of circulating flow, the estimation result from f_{pedSB} model is higher than that in both two methods in all situations. It is implied that f_{pedSB} model may overestimate entry capacity.

MAPE is utilized for identifying the difference of the estimated results from f_{pedSB} model and proposed models. The MAPE value is calculated by Equation 5.2.

$$MAPE_{i(j)} = \left(\frac{1}{N} \sum_{i(j)=1}^{N} \frac{| x_{i(j)} - \hat{x}_{i(j)} |}{x_{i(j)}} \right) \cdot 100\% \tag{5.2}$$

where x_i = simulation output

x_j =estimated results from theoretical model

$\hat{x}_{i(j)}$ = estimation result from f_{pedSB} model in each comparison.

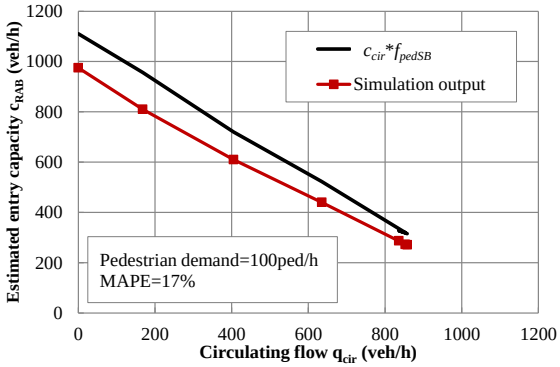

(a) Pedestrian demand=100ped/h

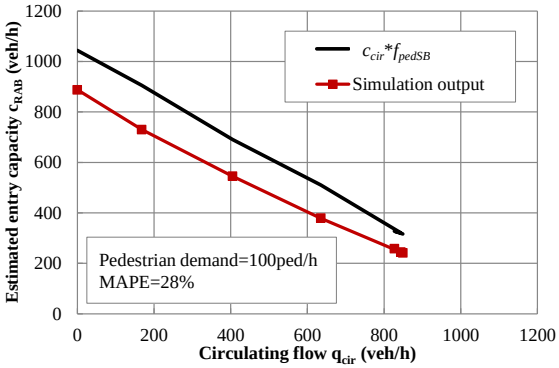

(b) Pedestrian demand=200ped/h

Figure 5.5 Comparison of results from f_{pedSB} model and simulation output

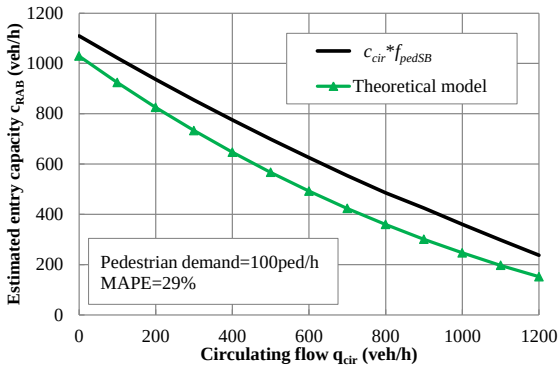

(a) Pedestrian demand=100ped/h

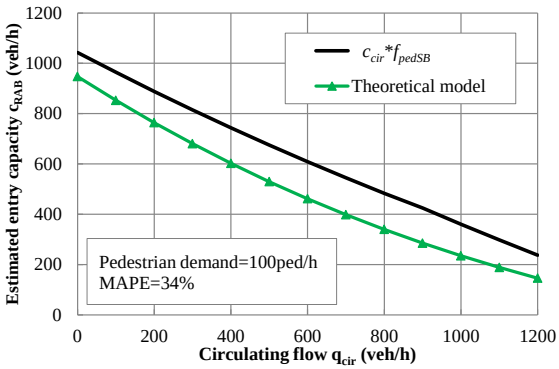

(b) Pedestrian demand=200ped/h

Figure 5.6 Comparison of the results from f_{pedSB} model and theoretical model

It is found that although the same conditions are input to the proposed methods based on the development environment of f_{pedSB}, the results from the f_{pedSB} model are different from those which are calculated by the proposed methods. *MAPE* of all samples either comparing to simulation output or the results from theoretical model reveal the estimation error higher than 17% and the value of *MAPE* is increased when pedestrian demand increases. As mentioned in Chapter 2, from the microscopic view point, entry capacity is the output of driver behavior. The f_{pedSB} model was developed based on the empirical data in Germany which reflects the German driver behavior. While, the parameters in both simulation analysis and theoretical model are calibrated and considered based on Japanese situation. Thus, it is implied that the f_{pedSb} model is not appropriate to apply on Japanese situations.

Thus, the simulation analysis is selected as the proposed methodology for practice since theoretical model and f_{pedSB} model may overestimate entry. While, simulation has the

inconvenience on application, the regression model is applies since it is developed based on simulation output and provides reliable results.

5.3 Application of the estimation methods in practice considering Japanese situations

The regression model was developed based on the fixed conditions which are shown in Table 5.3. Based on the existing methods, entry capacity will be affected by roundabout geometry, pedestrian demand and gap judgment et al. Thus, entry capacity recently can be only estimated at the roundabout with these conditions.

Table 5.3 Applying conditions based on the developing condition of regression model

1.	Four-leg roundabout with the angle of 90 degree between two adjacent approaches	
2.	Diameter of 27m	
3.	Space of one-vehicle length between crosswalk and yield line at any entry/exit	
4.	With physical splitter island at each entry (the subject entry is not included)	
5.	Fixed gap parameters:	Vehicles: t_c=4.5sec, t_f=3.2sec, τ=2.2sec
		Pedestrians:, t_c=6.5sec/10.2sec, t_f=3.2s, τ=2.0sec
6.	Range of pedestrian demand: [0, 200ped/h/approach]	
7.	No significant difference on the pedestrian demand at all entries (exclude the subject entry	

And the input necessary parameters are shown in Table 5.4.

Table 5.4 Necessary input parameters for application

1.	Circulating demand (veh/h)
2.	Pedestrian demand at subject entry (ped/h)
3.	Pedestrian demand at other entries (ped/h)
4.	With/without physical splitter island at subject entry
5.	Far-side pedestrian directional ratio r_{far}
6.	Far-side pedestrian recognition rate FPRR

After inputting these input parameters, the output for certain condition can be obtained. The expected output is a series of curves and one example is shown in Figure 5.7. One

curve represents the result of entry capacity changing with circulating flow under the certain level of pedestrian demand at the subject. Different curves show the changing of pedestrian demand at the subject entry.

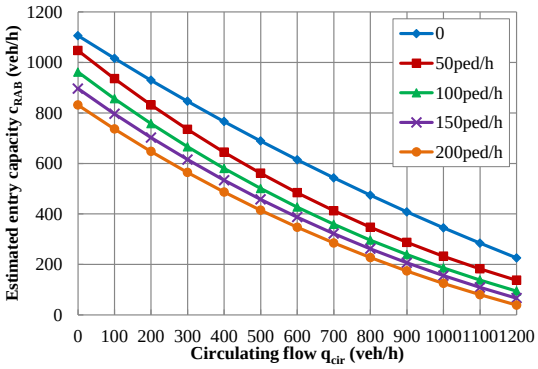

Input parameters into regression model (with physical splitter island)	
Pedestrian demand on other entries (ped/h)	60
r_{far}	/
FPRR	/

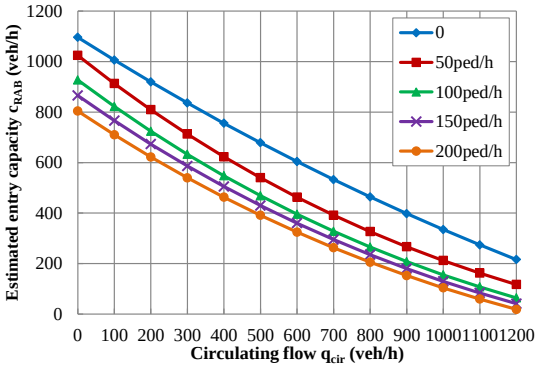

Input parameters into regression model (without physical splitter island)	
Pedestrian demand on other entries (ped/h)	60
r_{far}	0.4
FPRR	0.3

Figure 5.7 Example of expected output in application

5.4 Summary

Two comparative analyses were conducted in this chapter. First is between the simulation and theoretical model for interpreting the limitation of each method and then the existing method f_{pedSB} model was compared to the two proposed methods in order to examine the existing model. The theoretical model gives a little higher result of entry capacity comparing to that from simulation since queue discharge time and several influencing factors, i.e. priority of roads, turning ratios and offside vehicles which have impact on headway distribution are not considered in the model. The result from simulation analysis is the reference for the estimation results since entry capacity is difficult to be observed in reality. Based on the results of t-value in the comparison, theoretical model can be concluded to be reasonable. Considering the safety edge for operational performance, the simulation analysis is selected to apply in practice. Since simulation has inconvenience on

application, the regression which is developed based on the simulation output is finally utilized. The simulation is built based on the fixed conditions, e.g. diameter of 27m, thus, currently it can only be applied for the certain conditions.

6 Chapter 6

CONCLUSIONS AND FUTURE WORK

6.1 Conclusions

Entry capacity is one of the most important indices for performance evaluation of roundabout. In addition to circulating vehicles, pedestrian flow is another key conflicting stream having significant impact on entry capacity. In Japan, due to the space limitation, roundabouts cannot be always installed by standard design with physical splitter island, crosswalk and distance of one-vehicle length between crosswalk and yield line. Based on these limitations, the existing methods of entry capacity estimation considering pedestrian impact which were developed based on standard design may be not appropriate to apply in Japanese situations. Moreover, several influencing factors, i.e. pedestrian approaching sides, far-side pedestrian recognition rate and pedestrians across downstream exits which have impact on entry capacity have not been considered in existing estimation methods. In view of that, an estimation methodology of entry capacity considering pedestrian impact and various influencing factors was developed that enable authorities to reasonably check the performance of roundabout at planning stage and accordingly better design roundabout by adopting appropriate strategies under Japanese situations. Conclusions and results of the study are briefly described in the following sections.

The estimation methodology of roundabout entry capacity is established from two aspects, simulation analysis and theoretical model. Simulation is applied for identifying and examining influencing factors. And then, a theoretical model is developed including all the influencing factors which have been examined in the simulation analysis.

6.1.1 Conclusions from the simulation analysis

The simulation study utilizing VISSIM 5.40 is calibrated based on empirical data which is observed in Japanese roundabouts. Then, a series of simulation experiments are conducted to identify influencing factors. It is found through simulation analysis that, entry capacity was reduced more significantly when more pedestrians are from far-side under the condition without physical splitter island and the assumption that all entry vehicles stopped at the moment when pedestrians are about to cross the curb. Moreover, FPRR was added to make the situation more realistic and entry capacity was found to be improved as decreasing FPRR. After assuming the condition with physical splitter island, entry capacity under the condition of pedestrians from far-side was relatively increased due to the shorter waiting time.

Although the function of physical splitter island, space between crosswalk and yield line and far-side pedestrian recognition rate is realized in simulation study, the application of these elements in real world should be carefully considered and discussed.

Physical splitter island

Through simulation output, estimated entry capacity showed different performance under the condition with/without physical splitter island when pedestrian demand is in the high level. However, in real world, the improvement of entry capacity under the condition with physical splitter island may not be as significant as simulation showing when pedestrian demand is in the high level. This is because pedestrians will cross as platoon due to high demand so that drivers have to choose to take stopping behavior, no matter physical splitter island existing or not. Accordingly, in the places where pedestrian platoon has high probability to happen, e.g. the area near to school or working places, the simulation study may give overestimated results. An adjustment factor which can represent the percentage of time duration of pedestrian platoon is expected to reflect the impact of this behavior if necessary.

On the other hand, when pedestrian demand is in the low level, the improvement of entry capacity is not significant when physical splitter island is assumed to be installed. However, the function of physical splitter island is reflected on safety performance more than operational performance. Under the condition of low pedestrian demand, most of drivers

will pass the crosswalk without giving priority to pedestrians. In the view of pedestrians, they have to mind both of the entry and exit vehicle flows at same time during crossing when physical splitter island is not installed. These cause pedestrians having to wait and increasing the risk during crossing. Physical splitter island provides the space for pedestrians to realize two-stage crossing which will reduce the possibility of risk and relatively improves entry capacity Therefore, physical splitter island is strongly recommended to be installed at the entrance of roundabouts from the considerations of mobility and safety.

Distance between crosswalk and yield line

Regarding the examination of the case of 1m, all entry vehicles are assigned to stop at the stop line in simulation since there is no waiting space between crosswalk and yield line. However, in real world, not all vehicles will follow this rule and vehicles will stop at the yield line even occupying crosswalk, especially when entry flow is in the high level or pedestrians demand is in the low level. This occupying behavior may relatively improve the reduction of entry capacity due to small space between crosswalk and yield line. Accordingly, simulation may give underestimated results comparing to the reality.

On the other hand, for the case of 5m, all vehicles assigned to stop in the space between crosswalk and yield line since the space can accommodate one vehicle. While in reality, it also does not definitely happen at any time. Some drivers may stop at the stop line in the view of caring about circulating vehicles no matter pedestrians exist or not. This will reduce entry capacity more comparing to the simulation output. In the places where these kinds of behavior (opposite behavior to the geometry condition) are often observed, the impact of the behavior should be considered in application. The impact is expected to be reflected by an adjustment factor which represents the ratio of opposite behavior in total cases.

Moreover, in simulation analysis, it is assumed that when the distance between crosswalk and yield line is shorter 5m (one-vehicle length), all the cases will have the same results. That means the estimated results under the condition of 1m are the same as that under the condition of 4m. However, in reality, the entry capacity under the condition of 4m may be higher than that under the condition of 1m. This is because from the view of the entry

drivers who prefer to choose to stop at the yield line, the case of 4m is the better condition than 1m for stopping although the space is not enough for accommodating one vehicle. This suppose should be confirmed by observation.

Far-side pedestrian recognition rate FPRR

FPRR is applied under the condition without physical splitter island and it is assumed that under the condition with physical splitter island, all pedestrians from far-side will be unrecognized. In real world, it can be observed that even under the condition with physical splitter island, pedestrians from far-side are recognized at the moment when they are about to cross due to concern about pedestrians. Under the situation that pedestrians and drivers are not so familiar with two-stage cross, this phenomena will be often observed, e.g. Japan. Moreover, in this research, based on the consideration of safety, it is assumed that for near-side pedestrians FPRR is equal to 1. While in some cases, e.g. entry vehicles travel as high speed, these vehicles cannot stop at the stop line at the moment when near-side pedestrians are about to cross the curb. Under this condition, near-side pedestrian may not be recognized. Therefore, the recognition rate should also be applied under the condition with physical splitter island and on near-side pedestrians.

6.1.2 Conclusions from the theoretical model

In this proposed model, impact of pedestrian is considered based on gap acceptance theory, instead of an adjustment factor, since in real world entry drivers cross pedestrian flow by available gaps of pedestrians which is similar to merging into circulating flow. Two conditions of circulating flow, i.e. flowing circulating flow and queuing circulating flow are considered as the basic concept. The impacts of all influencing factors are realized through inputting parameters, e.g. t_c^{Nar}, t_c^{Far}. Through sensitivity analyses it was found that the changing tendency of estimated entry capacity follows the results which were obtained by simulation analysis. Thus, it can be concluded that the impacts of influencing factors which are considered in simulation are successfully reflected in this proposed theoretical model.

In order to establish the structure of the theoretical model, several strict assumptions are given: (1) overtaking behavior does not happen in pedestrians during walking; (2) pedestrian trajectory is parallel to crosswalk; (3) all lanes of pedestrians are judged by

entry drivers at the same time and (4) regarding the queue in circulating roadway, entry drivers are assumed to reenter roundabout immediately after the queue in circulating roadway find available gap of pedestrians at downstream exits.

Pedestrian behavior on the crosswalk is fixed by the assumptions of overtaking behavior and pedestrian trajectory. While as the most simple case of pedestrian behavior, these assumptions are effective for establishing the structure of the theoretical model. Pedestrian crossing behavior can be considered as the improvement of the model in future. Based on these two assumptions, drivers are assumed to be given an easy situation for judgment and theoretical model may provide overestimated results.

Regarding the assumption that all lanes of pedestrians are judged by entry drivers at the same time, this assumption also provides an easy environment of judgment for entry drivers which may obtain overestimated results from theoretical model. In addition, based on this assumption, the number of lanes of pedestrians does not have impact on final results of entry capacity. The relationship between the number of lanes of pedestrians and entry capacity should be examined in reality for the improvement of the proposed model.

Through the assumption regarding queue in circulating roadway, the discharge time of queue is considered to be zero. Due to this assumption, the theoretical model will relatively overestimate entry capacity. The discharge time should be included in the proposed model.

6.1.3 Conclusions from the comparison of estimation methods

Two comparative analyses were conducted regarding three estimation methods, proposed simulation analysis and theoretical model in this research and the existing method f_{pedSB} model which was developed by Germany (Brilon et al. 1993).

Through the comparison of the simulation and theoretical model it is found that the theoretical model gives a little higher result of entry capacity comparing to that from simulation. The possible reasons regarding this difference were considered from the limitations of each proposed method, e.g. queue discharge time is not considered in the model.

Another important possible reason is related to the headway distribution function $h(t)$ which is utilized in theoretical model. In the function of $h(t)$, free flow form upstream is

assumed and then a negative exponential function was obtained. Under this assumption, the cross of the entry and the circulating roadway in front of this entry is likely to be considered as T-intersection. However, in reality, circulating flow is not a free flow. It is significantly influenced by the geometry of the circulating roadway. Moreover, since circulating flow is composed by vehicles from other entries, it is also affected by the traffic situations, e.g. priority of the road (major/minor) and turning ratio at other upstream entries. These impacts on circulating flow can be directly reflected in simulation but not included in the theoretical model. The result which is shown in Figure 3.36 actually reflects this difference. Through this result it was also found that the circulating flow in simulation cannot be larger than 850veh/h while in the theoretical model circulating flow is assumed to achieve to be 1200veh/h. This is because in simulation the circulating vehicles which are generated by entry vehicles from other entries will also be blocked by circulating vehicles passing in front of other entries. However, this phenomenon cannot be reflected in the theoretical model. The characteristics of circulating flow at roundabout are expected to be reflected by adding the impact of priority of the road and turning ratios in the headway distribution model.

Regarding the expression of simulation, the exit flow at the same lag is another influencing factor which is reflected in simulation while not considered in theoretical model. The exit flow at the same lag is also considered to have impact on headway distribution of circulating flow.

The result from simulation analysis is the reference for the estimation results since entry capacity is difficult to be observed in reality. Based on the results of t-value in the comparison, theoretical model can be concluded to be reasonable. On the other hand, the comparison between the proposed models and existing model shows that the f_{pedSB} model may overestimate entry capacity under the Japanese situations since the model was developed based on Germany environment. Thus, the simulation analysis is selected to apply in practice. In addition, due to the inconvenience applicability of simulation, the regression which is developed based on the simulation output is finally utilized. The simulation is built based on the fixed conditions, e.g. diameter of 27m, thus, currently it can only be applied for the certain conditions.

In view of the limited land use and driver behavior in Japan, it is necessary to consider

characteristics of roundabouts, e.g. without physical splitter island, and the impact from pedestrians, i.e. pedestrian approaching sides and far-side pedestrian recognized rate on estimation of entry capacity. These results provide valuable insights into decision making at planning stage and enable a better design of roundabout considering pedestrian and space issues in Japan.

6.2 Future works

This study was achieved based on several assumptions which may be improved. In addition, the scope of this study could be further expanded to enable a wider usage of the methodology. Based on the primary conclusions summarized in the previous section, some directions for future applications are addressed in the following sections.

6.2.1 Effect of discharge time of the queue in circulating roadway in theoretical model

The impact of downstream exits on entry capacity is considered in this research. Vehicles exiting to downstream exit may be blocked by pedestrians and a queue is generated even extending to the circulating roadway which prevents entry vehicles entering roundabout. Regarding this queue, the proposed theoretical model assumes the waiting entry vehicles will restart to enter roundabout immediately after the first exit in the queue finding an accepted gap of pedestrians to cross. This assumption does not consider discharge time of the queue which causes overestimation of entry capacity by the theoretical model. Toward this, the sub-model which is used to estimate the probability queue in circulating roadway is needed to improve by considering the discharge time of queue.

6.2.2 Effect of offside vehicles exiting to the subject lag

Suzuki et al (2013) examined that headway distribution of circulating flow passing in front of the subject entry will be affected by the offside exit vehicles further influencing entry capacity. In this research, this impact has not been considered in the theoretical model which also results the overestimation of entry capacity by the model. In future, the impact of offside exit vehicles will be considered either in headway distribution or a separate part in the model.

6.2.3 Effect of the impact from upstream entries on headway distribution of circulating flow

In existing methods, headway distribution was developed based on the assumption of free flow. The circulating vehicles passing in front of the subject entry will be affected by the situations of upstream entries, e.g. priority of road of the lag and turning ratio of each entry since circulating flow is composed by the vehicles from upstream entries and the distance between the subject entry and upstream entry is limited. Headway distribution function is the main part of the model since it is established based on gap acceptance theory. Thus, headway distribution is needed to improve considering situations of upstream entries.

6.2.4 Calibration of pedestrian behavior in simulation

Due to the limited number of samples regarding pedestrians, the parameters which are utilized to reflect pedestrian behavior in the function of "conflict area" could not be calibrated. Toward this, data collection on the sites with relatively higher pedestrian demand should be conducted in future.

6.2.5 Considerations of pedestrian behavior in simulation and proposed theoretical model

In simulation and proposed theoretical model, pedestrian behavior on the curb is not considered. It is assumed pedestrian behavior, e.g. travelling direction on the curb, the direction approaching to entry vehicles or the same direction with entry vehicles will has impact on driver' judgment to pedestrians further influencing entry capacity since the visibility of drivers regarding pedestrians. Thus, pedestrian behavior on the curb should be carefully considered in future.

In addition, although physical splitter island is considered as an influencing factor in this research, the width of physical splitter island is not considered in this research. The value of width has impact on pedestrian travelling time in the island which will be related to the gap judgment to pedestrians further have influence on entry capacity. Thus, the width of splitter island should be considered in future.

6.2.6 Considerations of setting of pedestrian recognition rate based on empirical data

The pedestrian recognition rate should also be considered for near-side pedestrians and the case under the condition with physical splitter island. The setting of the value should be corresponding to the real situation by empirical data.

Reference

AustRoads (1993). Guide to Traffic Engineering Practice Part 6—Roundabouts, Sydney, Australia.

Akcelik, R. and M. Besley (1996). SIDRA 5: User Guide. ARRB Transport Research, Vermont South, Victoria, Australia.

AIMSUN Vission 6.1Users Manual (2010)

Bovy, H., K. Dietrich, and A. Harmann. (1991). Guide Suisse des Giratoires. Lausanne, Switzerland, p. 75 (cf. summary: Straße und Verkehr (Road and traffic), No. 3, p. 137–139, March 1991).

Breiman, L. (1963). The Poisson Tendency in Traffic Distribution. Ann. Math. States. No. 34, p. 308-311

Breiman L., Gafarian A. V., Lawrence R. L. and Murthy V. K. (1968). An Experimental Analysis of Single-lane Time Headways in Freely Flowing Traffic. 4th Int. Sympos. Traffic, Karlsruhe.

Brilon, W. (1988). Recent Developments in Calculation Methods for Unsignalized Intersections in West Germany. In: Intersections without Traffic Signals (Ed.: W. Brilon). Springer publications, Berlin.

Brilon, W. and Grossmann, M. (1991). The New German Guideline for Capacity of Unsignalized Intersections. Intersections without Traffic Signals Ⅱ (Ed.: Brilon, W.). Springer Publications, Berlin.

Brilon, W. and Stuwe, B. (1991). Kreisverkehrsplaetze-Leistungsfaehigkeit, Sicherheit und verkehrstechnische Gestaltung. (Roundabouts-Capacity, safety, and design), Strassenverkehrstechnik, Vol. 6.

Brilon, W., Stuwe, B. and Drews., O. (1993). Sicherheit und Leistungsfähigkeit von

Kreisverkehrsplätzen (Safety and Capacity of Roundabouts). Research Report. Ruhr-University Bochum, Germany.

Brilon, W., Wu, N., & Lemke, K. (1996). Capacity at unsignalized two-stage priority intersections. Transportation Research Record 1555.

Brilon, W. (2005): Roundabouts: A State of the Art in Germany. Presented at the 1st National Roundabout Conference, Vail, Colorado.

Brown M. (1972). Low Density Traffic Streams. Adv. Appl. Prob. 4, p. 177-192.

Buckley, D.J. (1962). Road Traffic Headway Distribution, Proceedings, 1st ARRB Conf., No. 1(1) , p. 153-186.

Cox, D.R. and Lewis, P.A.W. (1966). The Statistical Analysis of Series of Events.

Cowan, R. J. (1975). Useful Headway Models. Transportation Research, 9(6), p. 371-375.

Duran, C. and Cheu, R.L. (2011). Effect of crosswalk location and pedestrian volume on entry capacity of roundabouts. Proceedings of the 90th Transportation Research Board Annual Meeting, Washington, D.C.

Forschungsgesellschaft für Straßen-und Verkehrswesen (Hrsg.) FGSV Verlag GmbH (2001). Handbuch für die Bemessung von Straßenverkehrsanlagen (German Highway Capacity Manual). No. 299. Köln, Germany.

FHWA (2007). National Cooperative Highway Research Program, NCHRP Report 572, Roundabout: An Information Guide, U.S.

Griffiths, J. D. (1981). A mathematical model of a non signalized pedestrian crossing. Transportation Science, Vol. 15, No. 3, p. 223–232.

Harders, J. (1976). Grenz- und Folgezeitlücken als Grundlage für die Leistungsfähigkeit von Landstrassen (Critical Gaps and Move-Up Times as the Basis of Capacity Calculations for Rural Roads). Schriftenreihe Strassenbau und Strassenverkehrstechnik, Vol. 216.

Justel, A., Peña, D. and Zamar, R. (1997). A Multivariate Kolmogorov-Smirnov Test of Goodness of Fit. Statistics & Probability Letters 35(3), 251–259.

Kang, N., Nakamura, H. and Asano, M. (2012). An Empirical Analysis on Critical Gap and Follow-up Time at Roundabout Considering Geometry Effect. Proceedings of Infrastructure Planning, No. 46, 8 pages, CD-ROM, Sayitama, Japan.

Kimber, R.M. and Semmens, M.C. (1977). A Track Experiment on the Entry Capacities of Offside Priority Roundabouts. TRRL Supplementary Report 334. Transport and Road Research Laboratory, Crowthorne, Berkshire, U.K.

Kimber, R.M. (1980). The Traffic Capacity of Roundabouts, TRRL Laboratory Report 942. Transport and Road Research Laboratory, Crowthorne, Berkshire, U.K.

Kolmogorov, A. (1933). Sulla Determinazione Dmpirica di Una Legge di Distribuzione.G. Ist. Ital, Attuari 4: 83–91.

Louah, G. (1992). Panorama Critique des Modeles Francais de Capacite des Carrefours Giratoires. Proc., Roundabouts 92, Nantes, France.

Lu, G. X. Lu, Guan, F. and Noyce, D. A. (2011). Simulation Study of Access Management at Modern Roundabouts: Pedestrian Crosswalk Treatments, Proceedings of the 90th Transportation Research Board Annual Meeting, Washington, D.C.

McDonald, M. and Armitage, D. J. (1978). The Capacity of Roundabouts. Traffic Engineering & Control. Vol. 19(10), p. 447-450.

Marlow, M., and G. Maycock (1982). The effect of zebra crossing on junction entry capacities. Special Report SR 724. Transport and Road Research Laboratory, Crowthorne, Berkshire, United Kingdom.

Ourston, L. (2001): Roundabout Design Guidelines. Ourston Roundabout Engineering, U.S.

Robinson, B. W., L. Rodegerdts, W. Scarbrough, W. Kittelson, R. Troutbeck, W. Brilon, L. Bondzio, K. Courage, M. Kyte, J. Mason, A. Flannery, E. Myers, J. Bunker, and G. Jacquemart (2000). Roundabouts: An Informational Guide. Report FHWA-RD-00-067. FHWA, U. S. Department of Transportation.

Rodegerdts, L.A. and Blackwelder, G.E. (2005). Analytical Analysis of Pedestrian

Effects on Roundabout Exit Capacity, National Roundabout Conference, Colorado, U.S.

Salamati, K. (2014), A Cross-Cultural Study of Driver Yielding Behavior to Pedestrians at Roundabouts: An American-Portuguese Comparison, Presented on the 4th International Roundabout Conference, Seattle, Washington, U.S.

Schuhl, A. (1955). The Probability Theory Applied to the Distribution of Vehicles on Two-Lane Highways. Poisson and Traffic. The Eno Foundation for Highway Traffic Control. Sangatuck, CT.

Siegloch, W. (1973). Die Leistungsermittlung an Knotenpunkten Ohne Lichtsignalsteuerung (Capacity Calculations for Unsignalized Intersections). Schriftenreihe Strassenbau und Strassenverkehrstechnik, Vol. 154.

Semmens, M.C., Fairweather, P.J., and Harrison, I.B. (1980). Roundabout Capacity: Public Road Experiment at Wincheap, Canterbury. TRRL Supplementary Report 554, Transport and Road Research Laboratory, Crowthorne, Berkshire, U.K.

Smirnov, N. (1948). Table for Estimating the Goodness of Fit of Empirical Distributions. Annals of Mathematical Statistics 19, 279–281.

Stuwe, B. (formerly Hartz, B.) (1992). Untersuchung der Leistungsfähigkeit und Verkehrssicherheit an deutschen Kreisverkehrsplätzen. Schriftenreihe des lehrstuhls für Verkehrswesen der Ruhr-universität Bochum, Heft 10, Ruhr-University Bochum, Bochum, Germany.

Sullivan, D. and Troutbeck, R. J. (1993). Relationship Between the Proportion of Free Vehicles and Flow Rate on Arterial Roads. Physical Infrastructure Centre Report, 92- 21, Queensland University of Technology, Brisbane.

Suzuki, K. and Nakamura, H. (2006). TrafficAnalyzer-The Integrated Video Image Processing System for Traffic Flow Analysis, 13th World Congress on Intelligent Transportation System, London

Suzuki J., Kuwahara, M. and Hara, Y. (2013).歩行者を考慮したラウンドアバウトの交通容量推定に関する研究. Proceedings of Infrastructure Planning, No. 47, 5 pages,

CD-ROM, Hiroshima, Japan.

Tanner, J. C. (1962). A Theoretical Analysis of Delays At An Uncontrolled Intersection. Biometrica 49(1 and 2), p. 163-70.

Thedeen T. (1964). A Note on the Poisson Tendency in Traffic Distribution. Ann. Math. Slats. No. 35, p. 1823-1824.

Transport Research Laboratory Supplementary Report 554 (1980): Roundabout Capacity: Public Road Experiment at Wincheap, Canterbury. U.K.

Transport Research Laboratory Report LR 942 (1980). The Traffic Capacity of Roundabouts. U.K.

Troutbeck. R. J. (1986). A verage Delay at an Unsignalized Intersection with Two Major Streams Each Having a Dichotomized Headway Distribution. Transportation Science, 20(4), p. 272-286.

Transportation Research Board (2000). Highway Capacity Manual. Washington D.C.

Transportation Research Board (2010). Highway Capacity Manual. Washington D.C.

Tollazzi T., Lerher T. and Sraml M. (2007). Simulation of the Pedestrians' Influence to the Capacity of Motorised Vehicles in a Roundabout, American Journal of Applied Sciences 5(1): 34-41.

VISSIM Vision 5.40 Users Manual (2012)

Weiss G. and Herman R. (1962). Statistical Properties of Low Density Traffic. Quart. Appl. Math. No. 20, p. 121-130.

Wu, N. (2001). A Universal Procedure for Capacity Determination at Unsignalized (priority-controlled) Intersections. Trasportation Research B, No. 35, Issue 6, p. 593-623.

国土交通省道路省 (2014)，ラウンドアバウトの計画・設計に必要な知見に関する検討，第2回ラウンドアバウト検討委員会配布資料，2014.